APPLICATION OF ABANDONED MINE DRAINAGE FOR REUSE OF MARCELLUS SHALE FLOWBACK WATER: WASTEWATER AND SOLID WASTE MANAGEMENT

by

Can He

Bachelor of Engineering, Harbin Institute of Technology, 2011

Master of Science, Carnegie Mellon University, 2012

Submitted to the Graduate Faculty of

Swanson School of Engineering in partial fulfillment

of the requirements for the degree of

Doctor of Philosophy

University of Pittsburgh

2015

UNIVERSITY OF PITTSBURGH

SWANSON SCHOOL OF ENGINEERING

This dissertation was presented

by

Can He

It was defended on

November 19, 2015

and approved by

Radisav D. Vidic, Ph.D., Professor, Department of Civil and Environmental Engineering

Gregory V. Lowry, Ph.D., Professor, Department of Civil and Environmental Engineering at Carnegie Mellon University

Leonard W. Casson, Ph.D., Associate Professor, Department of Civil and Environmental Engineering

Leanne M. Gilbertson, Ph.D., Assistant Professor, Department of Civil and Environmental Engineering

Dissertation Director: Radisav D. Vidic, Ph.D., Professor, Department of Civil and Environmental Engineering

APPLICATION OF ABANDONED MINE DRAINAGE FOR REUSE OF MARCELLUS SHALE FLOWBACK WATER: WASTEWATER AND SOLID WASTE MANAGEMENT

Can He, Ph.D.

University of Pittsburgh, 2015

Marcellus Shale play, underlying 70% of Pennsylvania, is the largest onshore shale gas reservoir in United States. Recent advancements in horizontal drilling and multi-stage hydraulic fracturing technologies enabled economical recovery of unconventional (shale) natural gas resource and greatly expanded natural gas production in the United States. Flowback water generated during shale gas extraction in Pennsylvania typically contains high concentrations of total dissolved solids (TDS), heavy metals (e.g., Ba and Sr), and naturally occurring radioactive materials (NORMs), which raises significant public concerns and environmental challenges related to wastewater management. Due to limited capacity for wastewater disposal by deep well injection in Pennsylvania, flowback water is generally reused for hydraulic fracturing. As only 10-30% of hydraulic fracturing fluid is recovered, large volume of make-up water is required to support hydraulic fracturing of new wells. Abandoned mine drainage (AMD) is an environmental legacy from coal mining industry and one of the most serious threats to water quality in Pennsylvania.

Application of AMD for reuse of Marcellus Shale flowback water has never been tried by the unconventional gas industry before. Key technical barriers include compatibility of the treated water with fracturing chemicals and management of radioactive solid waste generated

from this practice. This study employs laboratory and pilot-scale systems to demonstrate the feasibility of this approach for flowback water reuse and to elucidate the underlying fundamental mechanisms as well as develop engineering solutions to implement this management strategy.

Laboratory studies evaluated the kinetics and equilibrium of precipitation reactions that occur when flowback water and AMD are mixed. Sulfate removal through mixing flowback water and AMD is governed by barite ($BaSO_4$) precipitation and chemical equilibrium can be predicted thermodynamic models with Pitzer's equation for activity corrections. An empirical model was developed to predict the kinetics of barite precipitation. Celestite ($SrSO_4$) precipitation requires over 10 hours to reach equilibrium and does not contribute significantly to the control of sulfate concentration in the finished water due to kinetic limitations in the treatment plant.

The feasibility of using microfiltration to separate particulate matter that is originally present in the wastewaters or that is created through mixing flowback water and AMD, was studied using both dead-end and cross-flow filtration systems. Early flowback water can cause severe membrane fouling due to the presence of stable submicron colloidal particles. Floc breakage is a key factor that may cause severe permeate flux decline during filtration of the flowback water that does not contain such colloidal particles.

A pilot-scale system was used to demonstrate the feasibility of co-treatment of flowback water and AMD. The finished water from this treatment process can be adjusted to meet the criteria for unrestricted use in hydraulic fracturing operations. The barite particles generated in this process have high radium content due to coprecipitation of radium with barium sulfate. The pilot-scale study revealed that sludge recycling could enable the use of Ra-enriched barite particles recovered from this process as a weighting agent in drilling mud formulation.

Impact of antiscalants on the fate of barium sulfate that may be formed in unconventional gas wells was also evaluated in this study. Antiscalants are unlikely to prevent formation of barite particles because of high supersaturation levels that are typical in unconventional gas extraction. When the fracturing fluid is rich in sulfate, barite particles will inevitably form in the subsurface and may be transported through the proppant pack during the flowback period. While most common antiscalants cannot act as threshold inhibitors for barite formation, they can enhance the mobility of barite particles through proppant pack by limiting the size of barite particle and providing steric repulsion at high ionic strength condition.

The key finings of this study indicate that it is feasible to utilize AMD as a make-up water source for flowback water reuse. The co-treatment process demonstrated in this study offers an alternatively approach for the management of flowback water generated in Pennsylvania.

TABLE OF CONTENTS

LIST OF TABLES

LIST OF FIGURES

ACKNOWLEDGEMENT

I am deeply grateful to my advisor and mentor, Professor Radisav Vidic, for giving me the opportunity to work on this exciting and profoundly important research project that is of both fundamental and applied importance. I thank him for his guidance, patience, encouragement and support throughout my doctoral studies. His enthusiasm, innovative ideas and profound knowledge provided the foundation of this research. His encouragement and advices as a great mentor will be invaluable assets for my professional career and personal life in the future.

I would also like to thank my Ph.D. committee members: Professor Leonard W. Casson, Gregory Lowry, and Leanne Gilbertson, who shared their precious knowledge and insights regarding the academic research and personal professional development. Professor Leonard W. Casson shared his knowledge and experience on engineering application. Professor Gregory Lowry and Leanne Gilbertson provided advises on the fate and transport of particles through porous media. Their profound knowledge and experiences of surface electrochemistry were remarkably useful.

I want to thank my inspired and diligent colleagues: Dr. Wenshi Liu, Dr. Tieyuan Zhang, Dr. Shi-Hsisang Chien, Yang Li, Li Chen, Xin Zhao, Xuan Zheng, Omkar Lokare. I will never forget the days and nights we spent together to pursue the truth.

I want to give special thanks to my friends Erke Huang, Lei Yang, Chao Shi, Xiaoyue Zhao, Lina Xu, Hui Wang, Haifeng Yu, Yu-ming Kuo, Xiaoyu Guo, Qiuyan Li, Jiyong Huang,

Jiaming Wu, Yipei Wen and Fei Lan. The valuable time that we spent together will always be a great memory in my life.

I would also like to thank the U.S. Department of Energy (DOE) for funding this study (Grant Number DE-FE0000975).

Finally, I want to thank my girlfriend, Lin Li, who stand beside me silently and assist me through countless discouragement. I greatly appreciate my family members, particularly my parents Yulin He and Ruijuan Chang. They stand by my side silently and assist me through countless difficulties. I sincerely thank for the encouragement and support from my family. Their unconditional love, care and support are the most important asset to me.

To Them I dedicate

My Parents, Yulin He and Ruijuan Chang

1.0 INTRODUCTION

Natural gas that exists in both conventional and unconventional geological formations offers more environmental benefits over coal in terms of combustion byproducts and pollutant emissions [1, 2]. Based on the prediction of U.S. Energy Information Administration (EIA), natural gas will become the nation's largest source of energy for electricity generation [3]. Due to recent advances in horizontal drilling and multi-stage hydraulic fracturing technologies, extraction of continental shale gas reservoirs recently became economically viable [4, 5]. Marcellus Shale of the Appalachian Basin that underlies most of Northern and Western Pennsylvania is the largest on shore reservoir of shale gas in the U.S. [6] and is estimated to contain between 262-500 Tcf (trillion cubic feet) of natural gas [7]. U.S. Energy Information Administration (EIA) projects that shale gas production will increase from 9.7 Tcf in 2012 to 16.6 Tcf in 2040 [3].

While shale gas is a promising energy source that has the potential to reduce the reliance on energy imports for U.S. and many other countries around the world, it raises significant environmental challenges in terms of water resources and wastewater management [2, 8]. Key technologies for economical recovery of natural gas from shale formation are horizontal drilling and hydraulic fracturing (Figure 1.1). Large volume of water (2-5 million gallons/well) are injected in subsurface at high pressure to widen the pre-existing natural fractures and create new fractures, which increases the permeability of the shale formation. More than 1,000 tons of

proppant sands is pumped downhole together with the injection fluid to keep the fractures open and enhance transport of trapped natural gas into the production casing. After hydraulic fracturing is complete, the fracturing fluid is allowed to flow back to surface enabling recovery of natural gas. Flowback water generally refers to fracturing fluid that is recovered in the first 2-3 weeks following well completion, while produced water refers to the fluid that is generated together with natural gas once the well is placed in production.

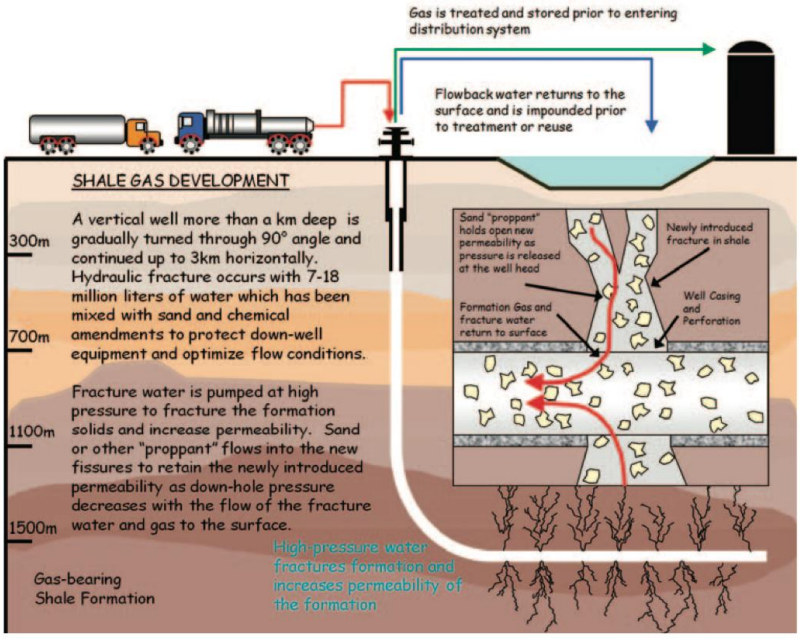

Figure 1.1 Overview of unconventional shale gas extraction process [8].

Marcellus Shale flowback water is characterized by high concentration of total dissolved solids, dissolved metals (e.g., Ba and Sr), radioactive elements (e.g., Ra) and organic matter [9]. The most common management approach for this wastewater is the disposal in Class II Underground Injection Control (UIC) wells [8]. However, this is not a viable option in Pennsylvania because of the lack of Class II UIC wells [2]. Due to the high salinity of the Marcellus Shale flowback water, treatment is required prior to discharge. Reverse osmosis is the

conventional desalination process, but the high salinity of flowback waters prohibits its use. Therefore, energy-intensive thermal processes (e.g., distillation, crystallization) are required to meet the total dissolved solids (TDS) limits (i.e., 500 mg/L) prescribed by the Pennsylvania Department of Environmental Protection (PA DEP) for discharge to the environment [10] making this option not economically advanatages. Reuse of Marcellus Shale flowback water for hydraulic fracturing is therefore the dominant management practice in PA (the reuse rate is about 90% based on PA DEP data) [2]. As only a portion of the fracturing fluid is recovered, an alternative make-up water source is required to supplement the flowback water for hydraulic fracturing operations.

Abandoned mine drainage (AMD), an environmental legacy pollutant from coal mining industry, generally contains elevated concentration of metals, especially Al, Mn and Fe. It was estimated that AMD affected the water quality of over 3,000 miles of surface streams in Pennsylvania [11]. AMD affects living conditions of the organisms that comprise the community structure of ecosystem, which poses significant threats to the ecological stability [12]. Approximately 6.1×10^{11} gallons of AMD is discharged annually to Pennsylvania waterways, while extraction of unconventional natural gas from Marcellus Shale produces about 8.2×10^{8} gallon flowback water per year [13]. As AMD sources are abundant in the vicinity of permitted shale gas extraction sites in Pennsylvania, they can potentially serve as a source of make-up water for flowback water reuse. The proposed approach simultaneously alleviates environmental impacts by i) reducing discharge of a hazardous pollutant (AMD) into natural waterways and ii) displacing fresh water sources currently used as make-up water [1].

Given the interests in the application of AMD for flowback water reuse, advancing the understanding of kinetics and thermodynamics of chemical reactions that occur when flowback

water and AMD are mixed, evaluating feasible solid separation processes, and demonstrating the feasibility of the co-treatment process with a pilot-scale system, are critical for advancing management option for flowback water during hydraulic fracturing of Marcellus Shale for unconventional natural gas extraction.

1.1 RESEARCH OBJECTIVES

The overall goal of this study is to evaluate the feasibility of using AMD to assist the reuse of Marcellus Shale flowback water for hydraulic fracturing. Co-treatment of AMD and flowback involves solids precipitation, separation of suspended solids and management of solid waste. This study aims to elucidate and solve underlying fundamental and engineering problems associated with co-treatment of flowback water and AMD. The questions that are addressed in this study include:

- What are the environmental challenges associated with AMD and flowback water?
- What are potential technical and regulatory concerns for the co-treatment of flowback water and AMD?
- What is the kinetics of solid precipitation when flowback water and AMD are mixed?
- Can chemical equilibrium be predicted using thermodynamic model?
- Can precipitated barite particles be used for drilling mud formulation?
- Can membrane microfiltration be used to separate the suspended solids from the mixture of flowback water and AMD?
- When sulfate-rich fracturing fluid is used, what is the fate of barium sulfate that is likely to form in unconventional gas wells.

Motivated by these questions, experimental investigation were conducted to achieve the following interconnected objectives:

1) Conduct laboratory tests to examine the kinetics and thermodynamics of solids that form by mixing flowback water and AMD.

2) Examine the feasibility of membrane microfiltration to separate solids that are originally presents in AMD and flowback water and those that are formed by mixing these waters.

3) Employ a pilot-scale system to demonstrate the feasibility of utilizing AMD for flowback water reuse for hydraulic fracturing.

4) Evaluate the feasibility of recovering barite from this process that meets specifications for use in drilling mud formulation.

5) Understand the fate of barite in the subsurface when sulfate-rich fracturing fluid is used with emphasis on the impact of antiscalants on scale inhibition and transport of barite through the proppant pack.

1.2 SCOPE OF THE DISSERTATION

Following this chapter that introduces the scope and objectives of this study, Chapters 2-8 are organized as individual manuscripts for journal publication. Chapter 2 provides a general overview of the environmental challenges associated with the flowback water generated by unconventional natural gas extraction from Marcellus Shale and the potential for using of AMD as a make-up water source for flowback water reuse. Technical and regulatory concerns

associated with the use of AMD in hydraulic fracturing are discussed in this chapter. As AMD sites in Pennsylvania are often located in the vicinity of planned shale gas extraction sites, it would be beneficial to use AMD as source water for hydraulic fracturing operations to alleviate pressure on fresh water sources while at the same time helping to reduce environmental impact of AMD.

Current strategies and perspectives for the management of Marcellus Shale flowback water are reviewed in Chapter 3. The schematic of a treatment system that would be suitable for the co-treatment of flowback water and AMD is proposed. The proposed system consists of a rapid mix reactor followed by coagulation/flocculation and sedimentation process. Preliminary analysis of radium co-precipitation with barium sulfate reveals that the solid waste generated by mixing flowback water and AMD will probably exceed technically enhanced naturally occurring radioactive material (TENORM) limit for unrestricted disposal in municipal landfills. Therefore, the solid waste needs to be carefully managed and alternative approaches for managing such radioactive solids are needed.

Chapter 4 examines the kinetics and equilibrium of precipitation reaction that occur when mixing flowback water and AMD. Laboratory tests indicate that barite ($BaSO_4$) precipitation is the main reaction that governs sulfate removal from the liquid phase. Because of the requirement to minimize the size of the treatment system, slow celestite ($SrSO_4$) precipitation should not be considered for the control of sulfate in treated water. A semi-empirical model was developed to predict the kinetics of barium sulfate precipitation.

Chapters 5 and 6 evaluate feasibility of membrane microfiltration for the removal of suspended solids that are originally present in both wastewaters and those that are formed after mixing flowback water and AMD.

Chapter 7 demonstrates co-treatment of flowback water and AMD produced in northeastern Pennsylvania in a pilot-scale system. A novel approach for the management of Ra-enriched solid waste was proposed and tested in the pilot-scale treatment system.

Chapter 8 investigates the fate of barium sulfate in unconventional natural gas wells when sulfate-rich hydraulic fracturing fluid is injected in to the shale formation. Impact of antiscalants on the formation of barium sulfate and subsequent transport of these particles through proppant pack were evaluated.

Chapter 9 summarizes the main contributions, key findings and conclusions of this study. Specific future work that is based on the results of this work is provided at the end of this chapter.

2.0 USE OF ABANDONED MINE DRAINAGE FOR THE DEVELOPMENT OF UNCONVENTIONAL SHALE GAS RESOURCES

This work has been published as:

He, C.; Zhang, T.; Vidic, R. D., Use of abandoned mine drainage for the development of unconventional gas resources. *Disruptive Science and Technology* (2013), *1*(4), 169-176.

Wastewater generated by natural gas extraction from Marcellus Shale activities and abandoned mine drainage (AMD) are the two most significant environmental concerns in Pennsylvania for their potential impacts on surface and groundwater. Reuse of Marcellus Shale wastewater for hydraulic fracturing represent an innovative solution that reduces potential environmental impacts of this industry. Because abundant AMD sources exist in the vicinity of shale gas extraction sites, it would be beneficial to utilize AMD as make-up water for hydraulic fracturing operation and reduce the impacts of this legacy issue from another energy-related industry in the region.

This approach would alleviate demand for fresh water by the gas industry, reduce environmental impact of AMD, reduce the cost of water transportion for hydraulic fracturing, reduce the greenhouse gas emissions by the gas industry and reduce the cost of wastewater

treatment prior to reuse for hydraulic fracturing. However, this approach has never before been tried by the unconventional gas industry and barriers to implementation range from technical issues to regulatory concerns. Technical issues include compatibility with fracturing chemicals, excessive scaling and biological growth in the well, and management of solid waste that would be generated by mixing these water sources. Regulatory issues include liability for perpetual AMD treatment that is implied by current regulations. These issues are discussed together with potential solutions based on original studies and review of the literature.

2.1 INTRODUCTION

Recent advances in horizontal drilling and hydraulic fracturing technologies made it economically viable to develop unconventional (shale) gas resources in the United States [1]. Natural gas is a more environmentally benign fossil energy source compared with coal in terms of combustion byproducts and pollutant emissions. Based on the U.S. Energy Information Administration (EIA) projections, shale gas production will grow to 16.6 trillion cubic feet in 2040, which will account for 50 % of total U.S. natural gas production [2].

While shale gas is an attractive energy source that may reduce the reliance on energy imports for a number of regions in the world, it comes with its own environmental challenges in terms of water resources and flowback water management. Extraction of natural gas from the shale rock requires large amounts of water for hydraulic fracturing (2-5 million gallons/well) and generates significant quantities of wastewater during the flowback period. The most dominant management approach for this wastewater is the disposal in Class II Underground Injection Control (UIC) wells [3]. However, this is not a viable option in Pennsylvania that sits on top of

one of the largest shale gas reservoirs in the world, Marcellus Shale, while it only has five Class II UIC wells [4]. Moreover, high salinity of the flowback water from Marcellus Shale precludes the use of conventional desalination processes (e.g., reverse osmosis) and would require energy-demanding thermal processes (e.g., distillation, crystallization) to meet the total dissolved solids (TDS) limits (i.e., 500 mg/L) prescribed by the Pennsylvania Department of Environmental Protection (DEP) for discharge to the environment.

Abandoned mine drainage (AMD) is an environmental legacy from another energy-related industry (i.e., coal mining) and is one of the most serious threats to water quality in Pennsylvania. Considering that AMD sites in Pennsylvania are often located in the vicinity of shale gas extraction sites, it would be truly beneficial to use AMD as source water for hydraulic fracturing operations to alleviate pressure on fresh water sources while at the same time helping to reduce environmental impact of AMD.

This study points to the synergy in solving environmental problems associated with unconventional shale gas extraction technology and abandoned mine drainage in Marcellus Shale region as archetypical example of rapidly growing shale gas development in the United States. Opportunities and concerns with direct use of AMD water for hydraulic fracturing are discussed together with potential process for co-treatment of AMD and flowback water to reuse in shale gas development.

2.2 UNCONVENTIONAL SHALE GAS EXTRACTION

Gas shale has extremely low permeability (< 0.1 microDarcy), which limits the flow of gas to a wellbore [5, 6]. With recent innovations in drilling and hydraulic fracturing (fracking), shale gas

production that was originally considered not to be economical has now become quite viable [1]. The success in gas extraction from Barnett Shale served to promote natural gas development in United States.

Advancements in horizontal drilling make it feasible to drill multiple wells from a single pad with each horizontal leg being even more than a mile long. This allows access to as much as 1 square mile of shale located more than a mile deep from a single well pad. Once horizontal drilling is completed, the production casing is placed into a wellbore and is sealed with cement to ensure that produced water and natural gas do not contaminate other subsurface layers, including groundwater. Hydraulic fracturing fluid is then pumped downhole at high pressure to widen the pre-existing fractures and creates new fractures that increases the permeability of shale formation. Together with the fracturing fluid, more than 1,000 t of proppant (most commonly silica sand) is pumped into these fractures to prevent them from closing once water is evacuated from the wellbore and pressure is relieved.

Once the hydraulic fracturing is completed, the valve on the wellhead is opened and fracturing fluid is allowed to flow back to the surface. The fluid recovered during this period is called “flowback water”. As illustrated in Figure 2.1, the flow rate during this period experiences a sharp decline and stabilizes after about two weeks. Typically, 10% - 30% of the injected fracturing fluid returns to the surface during this period. Water that continues to flow to surface during the life of a well is referred to as “produced water” [7].

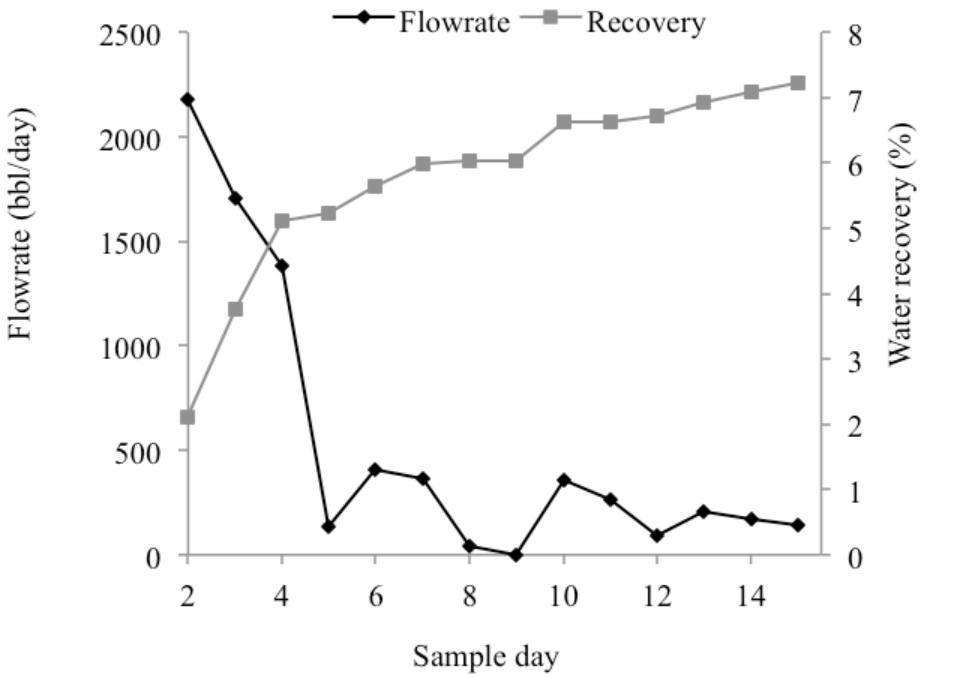

Figure 2.1 Variation of flowrate and water recovery during the flowback period

The key characteristics of flowback water result from mixing of the injected fluid and the formation brine [8]. Management of flowback and produced water from Marcellus Shale formation causes growing public concern due to its high total dissolved solids (TDS), radioactive elements and organic matter. Table 2.1 lists typical flowback water characteristics [8]. It is important to note that the flowback water from Marcellus Shale has much higher barium and much lower sulfate concentration compared with that from Barnett Shale, which is likely due to profound differences in geochemical characteristics of the two formations [9]. High TDS concentrations and the lack of Class II underground injection control wells in Pennsylvania pose a great challenge for flowback water management [10, 11].

Table 2.1 Typical water characteristics flowback water from Marcellus Shale

	minimum	maximum	average	number of samples
TDS (mg/L)	680	345,000	106,390	129
TSS (mg/L)	4	7,600	352	156
oil and grease (mg/L)	4.6	802	74	62
COD (mg/L)	195	36,600	15,358	89
TOC (mg/L)	1.2	1530	160	55
pH	5.1	8.42	6.56	156
Alkalinity (mg/L as CaCO3)	7.5	577	165	144
SO4 (mg/L)	0	763	71	113
Cl (mg/L)	64.2	196,000	57,447	154
Br (mg/L)	0.2	1,990	511	95
Na (mg/L)	69.2	117,000	24,123	157
Ca (mg/L)	37.8	41,000	7,220	159
Mg (mg/L)	17.3	2,550	632	157
Ba (mg/L)	0.24	13,800	2,224	159
Sr (mg/L)	0.59	8,460	1,695	151
Fe dissolved (mg/L)	0.1	222	40.8	134
Fe total (mg/L)	2.6	321	76	141
gross alpha (pCi/L)	37.7	9,551	1,509	32
gross betaa (pCi/L)	75.2	597,600	43,415	32
Ra228 (pCi/L)	0	1,360	120	46
Ra226 (pCi/L)	2.75	9,280	623	46
U235 (pCi/L)	0	20	1	14
U238 (pCi/L)	0	497	42	14

Data for Northeast Pennsylvania only [8]
COD, chemical oxygen demand; TDS, total dissolved solids; TOC, total organic carbon; TSS total suspended solid.

The flowback water management options include water reuse with or without treatment as well as desalination and disposal. Because of the high salinity (average salt content in Marcellus Shale flowback water is 10 wt.%), desalination by reverse osmosis is not technically feasible. Although distillation and crystallization could remove salts from this water and produce effluent suitable for discharge, they are not the best options for dealing with large quantities of flowback water due to their high energy costs. The best option for wastewater generated during gas extraction in Pennsylvania would be to reuse it for fracking subsequent gas wells. Concerns

with the reuse of this water range from its compatibility with chemicals that are added to the fracturing fluid (e.g., friction reducers) to potential scaling downhole due to the presence of divalent cations (e.g., Ba, Sr, Ca). Because only 10 - 30% of the injected fluid returns to the surface during the flowback period, there is likely a need to find other sources of make-up water to meet the production schedule.

2.3 ABANDONED MINE DRAINAGE

Environmental concerns with AMD come from elevated concentration of metals and metalloids, high sulfate content and potentially acidic nature of the discharge which all have adverse impacts on surface and groundwater quality in the coal mining region [12, 13]. AMD typically has orange color which is due to the precipitation of ferric hydroxide ($Fe(OH)_{3(s)}$) when pH is above 3.5.

Abandoned mine drainage or coal mine drainage is sourced from mine waste rock, tailings, and mine structures, and its quality depends on the mineralogy of rock material and availability of water and oxygen [14]. When pyrite or other sulfidic minerals are exposed to both oxygen and water, oxidation of these minerals (mainly pyrite) would govern the quality of AMD. The mechanism of pyrite oxidation has been widely studied [12, 15-17]:

$$FeS_2 + \frac{7}{2}O_2 + H_2O \rightarrow Fe^{2+} + 2SO_4^{2-} + 2H^+ \quad (2\text{-}1)$$

$$Fe^{2+} + \frac{1}{4}O_2 + H^+ \rightarrow Fe^{3+} + \frac{1}{2}H_2O \quad (2\text{-}2)$$

$$Fe^{3+} + 3H_2O \rightarrow Fe(OH)_3 + 3H^+ \quad (2\text{-}3)$$

$$FeS_2 + 7Fe_2(SO_4)_3 + 8H_2O \rightarrow 15FeSO_4 + 8H_2SO_4 \quad (2\text{-}4)$$

As shown by Equations (2-1) - (2-4), ferric iron and oxygen both serve as pyrite oxidants. Oxidation by ferric iron is the dominant process at pH below 4.5, while O_2 is the primary pyrite oxidant at neutral or alkaline pH [12, 17].

AMD from coal and mineral mining operations represent difficult and costly environmental problems in the U.S [14]. In Pennsylvania, AMD influences the quality of more than 3,000 miles of streams and associated ground water and is demonstrated to be the most critical source of water contamination [18]. Remediation of AMD in Pennsylvania is estimated to cost up to 15 billion dollars [19].

2.4 CO-TREATMENT OF FLOWBACK WATER AND AMD

Currently, many operators are practicing flowback water reuse for hydraulic fracturing of adjacent wells (latest review of PA DEP data reveals that about 90% of flowback water generated in Pennsylvania is reused). The flowback water is generally pretreated to remove suspended solids and, occasionally, metals (calcium, barium, strontium) that have the potential to create mineral scales (e.g., sulfates, carbonates) and is stored before reuse. Pretreated flowback water is then mixed with fresh water to make up for the fraction of the fracturing fluid that is not recovered during the flowback period and to control the salinity of this mixture for subsequent operations.

The advantage of using AMD as makeup water is that it is located in the vicinity of shale gas extraction site, which reduces the overall water transportation costs and reduces the total greenhouse gas emissions of the unconventional gas industry (i.e., reduces the CO_2 emissions generated by water transport). Figure 2.2 depicts the locations of permitted Marcellus Shale gas

extraction wells in 2010 and known AMD sites in Pennsylvania. As illustrated by this figure, there is an abundance of AMD sources near permitted gas wells, especially in Western Pennsylvania. AMD can not only serve as makeup water for hydraulic fracturing operations and reduce the demand on high quality water resources but it also provides a source of chemicals that can be used to treat the flowback water and remove divalent cations that could form mineral scales and reduce permeability of gas wells. Sulfate ions that are often present in AMD at elevated levels will react with Ba^{2+}, Sr^{2+}, and Ca^{2+} in the flowback water to precipitate them as their insoluble sulfate forms. In addition, some AMD sources are net alkaline, which would lead to additional precipitation of metal carbonates. The removal of divalent cations depends on the concentrations of species of interest (i.e., Ba^{2+}, Sr^{2+}, Ca^{2+} and SO_4^{2-}) that are related to flowback time, quality of AMD and blending ratio. The blending ratio can be adjusted to achieve the desired final hydraulic fracturing fluid quality. After mixing of these two waters, a simple gravity separation process is needed to remove the suspended solids created by chemical reactions so that the quality of the finished water would be suitable for hydraulic fracturing. Although AMD and flowback water co-treatment is certainly beneficial, there are still some concerns and barriers for the use of AMD in unconventional gas extraction.

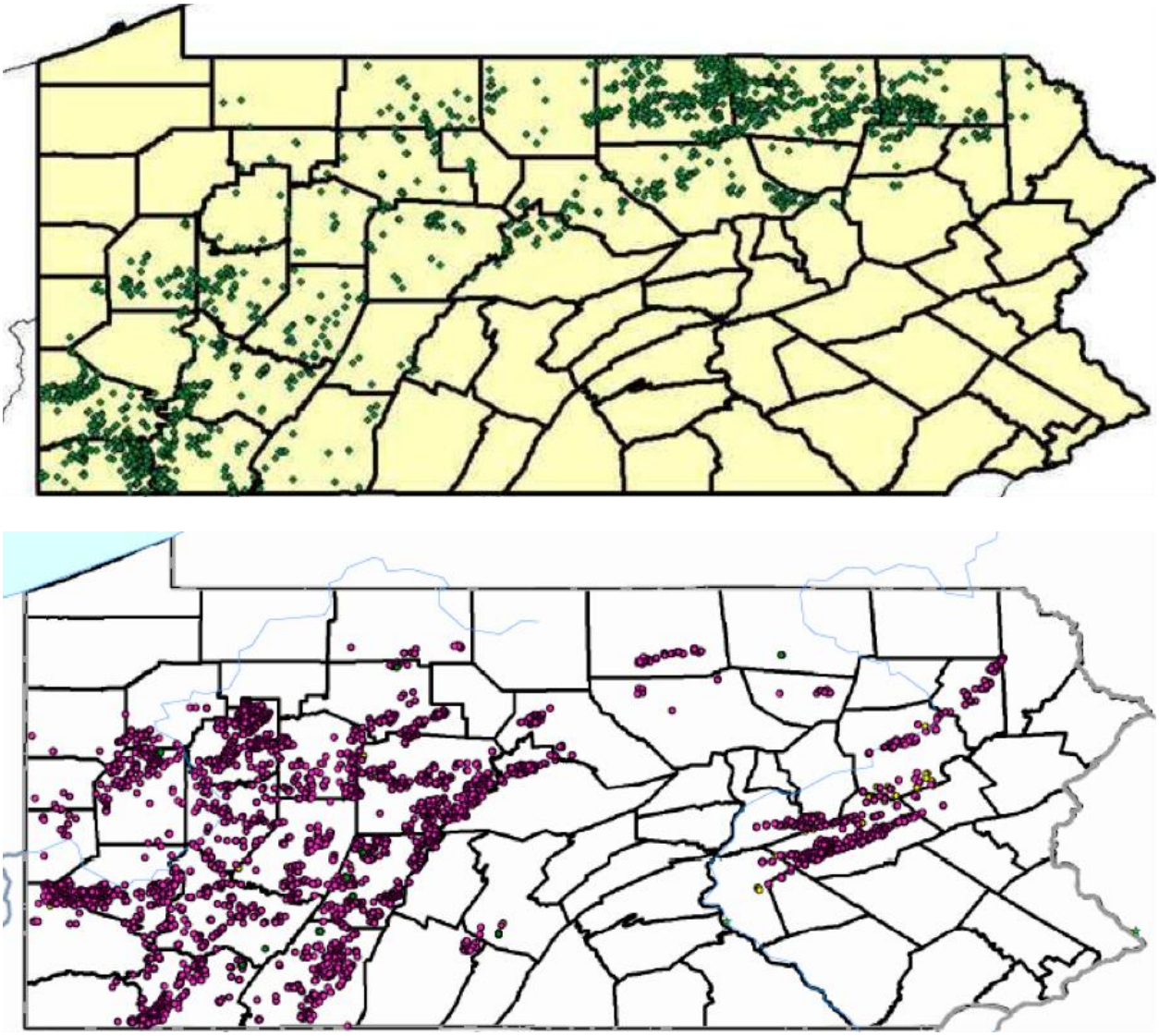

Figure 2.2 Locations of permitted shale gas wells (top) and AMD (bottom) in Pennsylvania in 2010

2.5 CONCERNS REGARDING AMD USE IN UNCONVENTIONAL GAS EXTRACTION

2.5.1 Compatibility with hydraulic fracturing chemical additives

Quality of AMD varies with locations and is influenced by underlying geology of coal formation and environmental conditions in the abandoned mine. Analysis of 140 AMD samples demonstrated that pH varies in a wide range (2.7 - 7.3) with a bimodal distribution in the acidic pH (2.5 - 4) and near-neutral pH (6 - 7) range [20]. Low pH of AMD would exacerbate corrosion of production casing and will prevent its use in hydraulic fracturing operations. However, low-pH AMD are often equipped with active (e.g., lime addition) or passive (e.g., limestone ponds ort channels) treatment systems to neutralize acidity.

Friction reducers are high molecular weight polymers added to the fracturing fluid to reduce the pumping losses during hydraulic fracturing operations, which in turn reduces the operating costs. Several studies have demonstrated that high TDS of fracturing fluid can impair the effectiveness of polyacrylamide-based friction reducers [21, 22]. As the TDS concentration of AMD is between 1,000 - 2,000 mg/L, it is not expected that the use of AMD as make up water will add to the concerns about the effectiveness of friction reducers because the flowback water normally has 2 orders of magnitude higher salt content than AMD. In addition, high salinity tolerant frication reducers have been developed to overcome these problems and it is currently feasible to use water with TDS as high as 100,000 mg/L without compromising the effectiveness of friction reducers [23].

Additional concern regarding AMD quality for use in hydraulic fracturing is the dissolved iron content that may interfere with gel cross-linking if gel systems are used to

increase the viscosity of fracturing fluid and enhance its ability to carry proppant into deeper fractures. Commonly acceptable iron concentration in cross-linked systems is 10 - 20 mg/L. Because AMD could have several hundred mg/L of dissolved iron, it may be necessary to implement iron removal (e.g., aeration and sedimentation) to address this concern. In the case of slickwater fracturing, which is typically used in Marcellus shale, the concern about the iron presence is not as pronounced and much higher concentrations can be tolerated (total divalent cation concentration as high as 15,000 mg/L is acceptable).

2.5.2 Impact on well productivity

One of the key issues related to AMD use in hydraulic fracturing is its sulfate concentration because of the scaling potential that exists in barium-rich Marcellus Shale formation [8, 24]. Dissolved sulfate in the fracturing fluid will inevitably react with barium in the subsurface to precipitate barium sulfate (barite), which could potentially cause the scaling of production casing, proppant pack or the shale itself and reduce production of natural gas from the well. Strontium and calcium sulfate are less likely to precipitate because barite has much lower solubility product compared to celestite or gypsum. Barite scale is very tenacious (not soluble in concentrated hydrochloric acid) and difficult to remove. This is of particular concern in situation with continuous supply of scale forming ions as the growth of barite scale can lead to complete plugging of pipes or fractures. However, this is not the case in Marcellus Shale formation where sulfate concentration in the flowback water ranges from non-detect to several mg/L [8]. The most likely fate of barite particles that would form downhole is that they would be captured in the proppant pack that would serve as a granular filter media (typical proppant sand is 40/70 U.S.

Mesh) during the flowback period. This means that the key concern with high levels of sulfate in the frack fluid would be permeability reduction of the proppant pack due to plugging with freshly precipitated barite.

The volume of freshly precipitated barite that would form in a well can be estimated assuming that there is sufficient barium in the shale to facilitate complete sulfate removal. Assuming that a total of 3 million gallons of fracturing fluid containing 800 mg/L of sulfate is injected together with 9 wt.% of proppant, the maximum volume of barite that can potentially precipitate downhole would be 4.9 m^3. This volume of barite is less than 0.5% of the total volume of proppant injected in the well. Hence, it can be concluded that the total volume of barite solids formed downhole is negligible compared to the volume of proppant remaining downhole and that the well-plugging due to high sulfate in the fracturing fluid may be very limited.

2.5.3 Potential for bacterial activity

Sulfate reducing bacteria (SRB) use simple organic acids or molecular H_2 as energy source while reducing sulfate to hydrogen sulfide. Typically, the temperature in Marcellus Shale formation is between 35°C to 51 °C, which is optimal for certain SRB species [11, 25]. Any sulfate that is present in the fracturing fluid as free ion would promote growth of SRB under anaerobic conditions that are prevalent in Marcellus Shale formation. Hydrogen sulfide that would form as a result of SRB activity can contaminate (sour) natural gas and increase the cost of gas preparation and purification. Hydrogen sulfate would also promote precipitation of ferrous sulfide that could lead to plugging of the production casing, propant pack and/or shale fractures and would accelerate corrosion of iron and steel pipes [26].

As indicated earlier, any sulfate that is present in the fracturing fluid will likely be precipitated as barium sulfate due to fairly high concentration of barium in Marcellus Shale. Therefore, the availability of free sulfate ions in solution to promote SRB activity will likely be very limited. However, several studies found that *Desulfovibrio desulfuricans* can utilize barite solids as electron acceptor and dissolve Ba and Ra that co-precipitated with barite [27, 28]. It is then important to ensure that the biocides that are typically added with the fracturing fluid remain active in the subsurface as long as possible to prevent proliferation of *Desulfovibrio desulfuricans.* If not, excessive biological growth would not only reduce the quality of gas produced from this well but could also reduce well productivity.

2.5.4 Management of solid wastes

Radium is a naturally occurring radioactive material (NORM) that is often present in Marcellus Shale flowback water at levels ranging from several hundred to several thousand pCi/L. Ra-226 with a half-life of 1622 years is one of the major radium isotopes and it dominates radioactivity in the flowback water. When flowback water is mixed with AMD in above-surface treatment process, radium and barium sulfate will co-precipitate despite the fact that the solubility product of $RaSO_4$ ($K_{sp,RaSO_4} = 10^{-10.38}$) is almost never exceeded under typical process conditions [29]. Solids generated as a result of adding AMD to flowback water could have appreciable radioactivity and even exceed the RCRA-D (Resource Conservation and Recovery Act, Subtitle D) non-hazardous landfill disposal limit of 25 pCi/g that is stipulated in Pennsylvania [30]. Since AMD and flowback water mixture is a dilute solution, the extent of Ra that would be incorporated into the barite solids can be estimated by Nernst-Berthelot Equation [31]:

$$\frac{RaSO_4}{BaSO_4} = K_d \frac{Ra^{2+}}{Ba^{2+}}$$

where, K_d is the equilibrium distribution coefficient, $BaSO_4$ and $RaSO_4$ are the concentrations of barium and radium carriers in the solid solution, and Ba^{2+} and Ra^{2+} are dissolved ion concentrations in the liquid phase.

Figure 2.3 depicts relationship between Ra and Ba removal during co-precipitation of barium and radium sulfate as predicted by Nernst-Berthelot Equation and verified by experimental studies. In the case of excess sulfate in solution, barium removal by precipitation would be almost complete because of low barite solubility and all theoretical calculations indicate that all Ra in solution will also be incorporated into the solids that would precipitate. Figure 2.4 shows Ra concentration in solids (pCi/g) that would precipitate after mixing high-sulfate AMD with flowback water as a function of Ra and Ba concentration in the flowback water. As can be seen in Figure 2.4, it is very likely that the Ra concentration in solid waste generated by this process would exceed the landfill disposal limit, which could be a major concern for managing solid waste that would be created by this process.

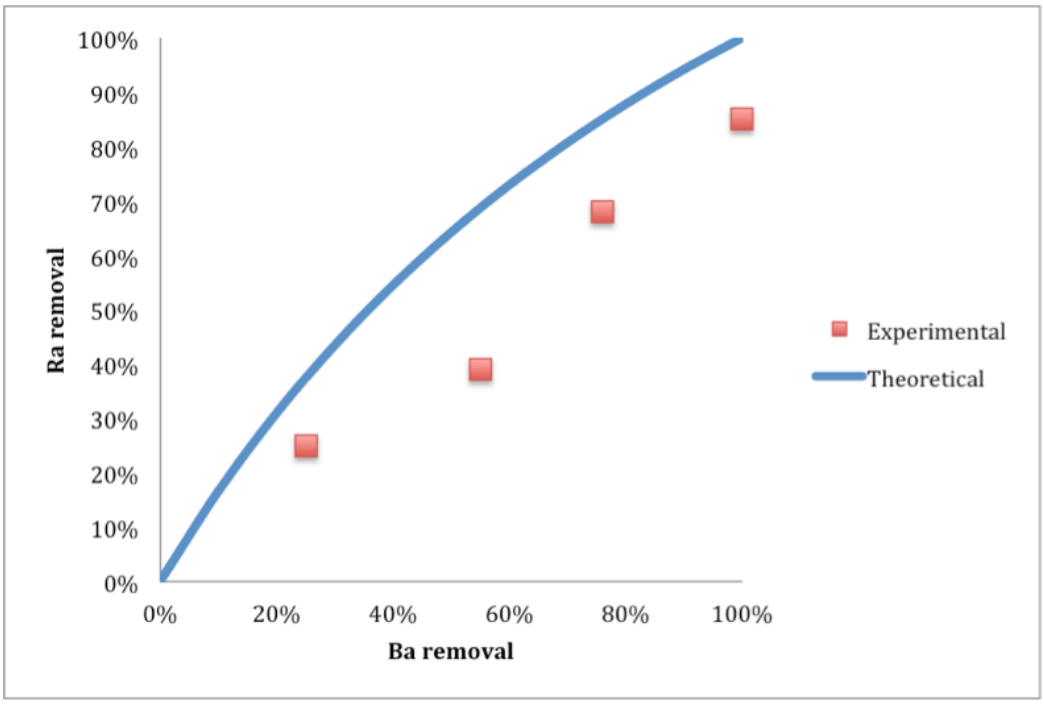

Figure 2.3 Relationship between Ra and Ba removal for co-precipitation of barium and radium sulfate

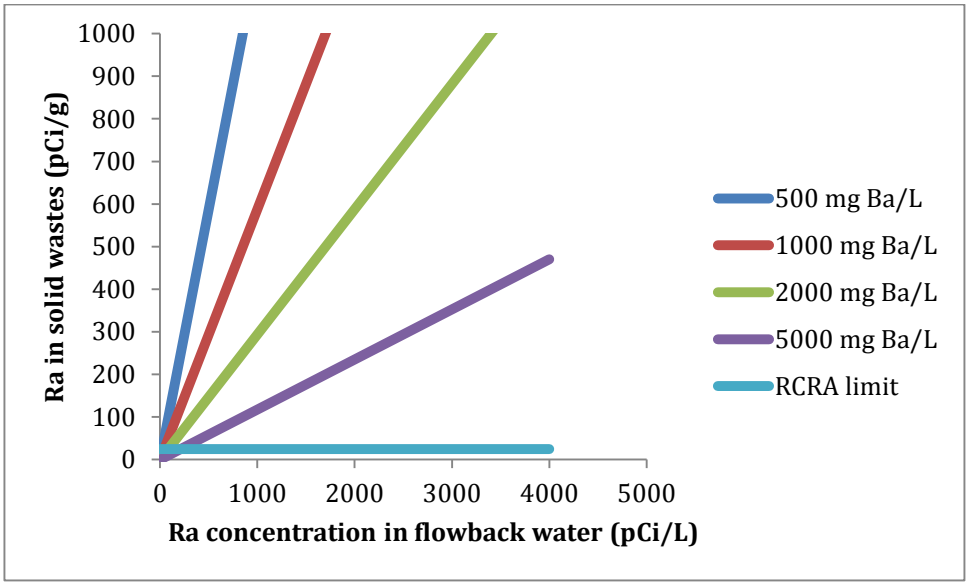

Figure 2.4 Radium activity in solids that would precipitate when high-sulfate AMD is mixed with flowback water

2.5.5 Regulatory concerns

Water withdrawals for Marcellus Shale drilling activities are under the jurisdiction of either interstate basin commissions or state agencies. The Code of Federal Regulations states that water withdrawal must be limited in both quantity and rate to avoid any adverse impact on water level, competing supplies, aquifer storage capacity, water quality, fish and wildlife, and low flow of perennial streams [32]. Based on the water demand, a minimum passby flow may be required to maintain adequate health of the stream ecosystem. Withdrawal of AMD falls under the same legislation as surface and groundwater, although it is technically a waste and the main source of surface water pollution in Pennsylvania.

For the operators who intend to use AMD for natural gas extraction activities, one of the key concerns is the potential for long-term liability for AMD "treatment" (withdrawal and use can be construed as treatment) as claimed in The Clean Streams Law. Recently, the Pennsylvania Department of Environmental Protection (PA DEP) published a "white paper" to encourage the use of AMD for hydraulic fracturing. Two possible solutions for the liability concern associated with the use of AMD for hydraulic fracturing have been proposed by PA DEP. One option is to treat the project that uses AMD for fracturing within the Environmental Good Samaritan Act (EGSA), which is a law intended to encourage pollution abatement caused by abandoned mines. Based on EGSA, participants in a water pollution abatement project are not responsible for any pollution coming from the water treatment facilities used to treat AMD. The other option is to use a Consent Order of Agreement where PA DEP could agree to exempt the operators who use AMD for hydraulic fracturing from long-term liability of the treatment.

Alternatives for AMD storage stipulated by PA DEP include non-jurisdictional impoundment, centralized impoundment and on-site pits and tanks. If AMD is to be stored in

non-jurisdictional impoundment it must meet water quality stored is listed in Table 2.2, while this standard is not enforced for centralized impoundment and on-site pits. In other words, storage of AMD in large non-jurisdictional surface impoundments is not permitted unless substantial treatment of AMD is implemented. In addition, some existing AMD treatment facilities, such as polishing ponds or wetlands, can also serve as AMD storage prior to hydraulic fracturing.

Table 2.2 Storage standards for MIW stored in non-jurisdictional impoundments [33]

Preliminary Results Table **Storage Standards For MIW Stored In Nonjurisdictional Impoundments**		
Parameter	**Units**	**MIW storage standards for nonjurisdictional impoundments**
Alkalinity	mg/L	Minimum of 20 mg/L
Aluminum	mg/L	0.2
Ammonia	mg/L	1.0
Arsenic	µg/L	10.0
Barium	mg/L	2.0
Bromide	mg/L	0.2
Cadmium	µg/L	5.0
Chloride	mg/L	250
Chromium	µg/L	100
Copper	mg/L	1.0
Iron	mg/L	0.3
Lead	µg/L	15
Manganese	mg/L	0.5
Nickel	µg/L	470
pH		6.5-8.5
phenol	µg/L	5.0
Selenium	µg/L	50
Specific Conductance (Conductivity)	µmho/cm	1,000
Sulfate	mg/L	250
TDS	mg/L	500
TSS	mg/L	45
Zinc	mg/L	5.0

2.6 TREATMENT PROCESSES AFTER MIXING AMD AND FLOWBACK WATER

When AMD and flowback water are mixed, barium and strontium sulfate will co-precipitate and result in large amount of suspended solids in solution. Several batch tests were conducted with actual flowback water from two different Marcellus Shale wells and two different AMD sources in the vicinity of each of these wells to determine key parameters for the design of the treatment process. Water quality of AMD and flowback sources selected for this study is listed in Table 2.3. As shown in Figure 2.5, barium sulfate precipitation can be completed within 30 min if the initial supersaturation ratio (square root of quotient of ion activity product and solubility product) is high. However, when supersaturation ratio is low, as was the case for Flowback Water A mixed with AMD 1, it took more than 5 hours to achieve equilibrium. Barite precipitation could also be inhibited in the presence of Ca ion and scaling inhibitors that remain in flowback water [34]. Solids that are created by mixing AMD and flowback water would have to be removed prior to use of this mixture in hydraulic fracturing. Coagulation/flocculation followed by sedimentation or membrane microfiltration are the two potential approaches to achieve this separation.

Table 2.3 Water Characteristics of Flowback Water and AMD

	Flowback water A	Flowback water B	AMD 1	AMD 2	AMD 3	AMD 4
Na+ (mg/L)	27,946	11,860	687	281	139	104
Ca2+ (mg/L)	15,021	2,170	245	353	144	175
Mg2+ (mg/L)	1,720	249	33	53	40	49
Sr2+ (mg/L)	1800	362	3	<DL	0.8	1.5
Ba2+ (mg/L)	236	730	ND	ND	ND	ND
Fe total (mg/L)		32.1	ND	27	0.5	32
Cl- (mg/L)	104,300	29,000	373	101	264	71
SO42- (mg/L)			242	696	328	709
TSS (mg/L)			1	69	9	118
pH	6.40	7.42	7.03	5.68	7.56	6.14
Alkalinity (mg CaCO3/L)			394	62	47.5	40.5
AMD reclaimed	-	-	yes	no	yes	no

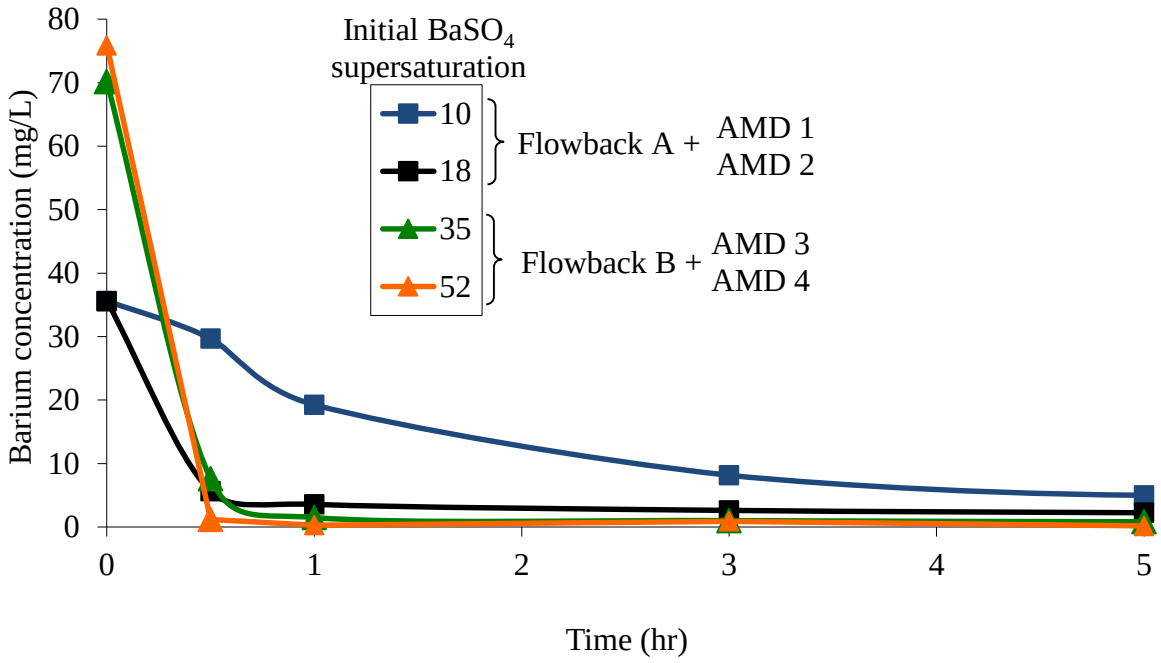

Figure 2.5 Barite precipitation as a function of supersaturation ratio

The advantage of microfiltration (MF) is that it requires smaller footprint compared with conventional gravity-based solids separation process (membrane microfiltration unit can be mounted on a truck in a mobile treatment systems). However, bench-scale experiments demonstrated that the colloidal particles that could be present in some flowback waters can cause severe membrane fouling and permeate flux decline, which limits the application of MF in Marcellus Shale flowback water treatment [35].

Coagulation/flocculation followed by sedimentation is the most economical approach to separate particles created by mixing AMD and flowback water. The key design and operating parameters (e.g., solution pH, mixing time, chemical addition, sedimentation time, etc.) for coagulation-flocculation-sedimentation treatment process were evaluated in bench-scale studies using actual flowback and AMD samples [36]. These studies revealed that the finished water quality in terms of final sulfate concentration can be controlled below 100 mg/L by adjusting the mixing ratio of AMD and flowback water and that the effluent turbidity was consistently below 3 NTU. These water quality characteristics meet the requirements for unrestricted use in hydraulic fracturing operations in Marcellus Shale.

2.7 SUMMARY AND CONCLUSION

Flowback water generated during unconventional gas extraction in Marcellus Shale and abandoned mine drainage (AMD) in Pennsylvania are both major environmental concerns in Pennsylvania. The use of AMD as makeup water for flowback water reuse in hydraulic fracturing operations could benefit both gas developers and watershed associations. The benefits of using AMD water include less pressure on fresh water sources, reduced water transportation

costs, reduced energy consumption and greenhouse gas emissions by the unconventional gas industry, reduced costs for flowback water treatment, and reduced risk for adverse environmental impacts of both mine drainage and flowback water on water resources in Pennsylvania. Detailed studies on technical limitations of AMD use for hydraulic fracturing, potential negative impacts of AMD withdrawals and development of appropriate regulations are required to eliminate the concerns associated with combined AMD-flowback water used for shale gas extraction activities.

3.0 MANAGEMENT OF MARCELLUS SHALE PRODUCED WATER IN PENSYLVANIA: A REVIEW OF CURRENT STRATEGIES AND PERSPECTIVES

This work has been published as:

He, C.; Zhang, T.; Zheng, X.; Li, Y.; Vidic, R. D., Management of Marcellus Shale Produced Water in Pennsylvania: A Review of Current Strategies and Perspectives. *Energy Technology* (2014), *2*(12), 968-976.

Reuse of flowback/produced water generated by natural gas extraction from Marcellus Shale for hydraulic fracturing is the dominant management option in Pennsylvania. Advantages and disadvantages of this management approach are discussed together with long-term concerns and technology development needs.

Abandoned mine drainage is a promising alternative make-up water but high sulfate concentration will lead to barite precipitation once it is mixed with produced water. Conventional processes are very effective in separating these solids but Ra co-precipitation may cause concerns with the disposal in municipal landfills.

When the produced water volume exceeds the reuse capacity for hydraulic fracturing, lime-soda ash softening can be used to remove divalent cations, including Ra, to enable production of pure salts in subsequent thermal processes.

3.1 INTRODUCTION

Unlike conventional gas that is contained in relatively porous sandstone and carbonate reservoirs, unconventional gas is entrapped in low-permeability reservoirs or the source rock itself. Because of the advancement in horizontal drilling [1] and hydraulic fracturing [2], the extraction of gas contained in shale formations became technically and economically feasible. The economic success in the Barnett Shale in Texas has spurred the development of shale gas extraction all over the world [3]. The Marcellus Shale formation is one of the largest known shale gas reservoirs in the US with an estimated natural gas reserve of 262-500 trillion cubic feet (Tcf) [4].

Compared with coal, natural gas is considered a relatively clean energy source with higher heat of combustion and fewer pollutant emissions, which potentially enables it to serve as a transition fuel towards renewable energy. U.S. Energy Information Administration (EIA) projected that the U.S. shale gas production will reach 16.6 Tcf in 2040 and will account for 50 % of the total U.S. natural gas production [5].

While shale gas is an attractive energy source that may reduce the reliance on energy imports for a number of regions in the world, it comes with its own environmental challenges in terms of water needs and wastewater management [6, 7]. Extraction of natural gas from the shale rock requires large amount of water for hydraulic fracturing and generates significant quantity of highly polluted wastewater over a lifetime of each well. Lack of Class II UIC (disposal) wells in Pennsylvania creates challenges for the management of this wastewater. Current solution relies on reusing it for hydraulic fracturing operations. As the well fields mature and the number of new wells declines, the reuse will not be able to consume the entire volume of wastewater produced from the existing wells. Due to extremely high salinity of Marcellus Shale produced

water, conventional desalination approaches like reverse osmosis are likely to have limited application and it is expected that thermal desalination process (e.g., distillation and crystallization) would be needed to ensure economical and environmentally acceptable management of this wastewater. Marcellus Shale produced water is among the most radiogenic of all sedimentary basins in the U.S. [7] and the selection of treatment and disposal solutions will have to address the fate of naturally occurring radioactive material (NORM) in this wastewater in environmentally acceptable manner.

Abandoned mine drainage (AMD) is one of the most significant environmental problems in Pennsylvania as it impacts the quality of over 4,000 miles of rivers and streams. The use of this impaired water for hydraulic fracturing in Pennsylvania would have enormous environmental and economic benefits, including reduced pressure on fresh water sources, reduced cost and environmental impacts of water transportation, reduced overall energy consumption for unconventional gas extraction, and reduced adverse environmental impacts of AMD on water resources in Pennsylvania [8].

This study analyzes the state of the art regarding environmental challenges associated with the wastewater generated by natural gas extraction from Marcellus Shale. Furthermore, the potential use of AMD as make-up water for hydraulic fracturing is evaluated with regards to the fate of radium and separation and disposal of solids that will precipitate when AMD is mixed with produced water. Long-term concerns with the development of Marcellus Shale are discussed together with technology development needs to minimize potential environmental impacts of this industry in Pennsylvania.

3.2 STATE OF THE ART

3.2.1 Flowback water management

Hydraulic fracturing is employed in unconventional gas extraction to create a network of fractures that enable natural gas trapped in the source rock to escape into the production casing. Large quantities of water (3 - 5 million gallons) are required to fracture each Marcellus Shale well. During the first 2-3 weeks after well completion (i.e., flowback period), approximately 10 - 30% of injected fluid is recovered from each well [6, 9]. After the flowback period, the well is placed in production and the wastewater denoted as produced water will be generated throughout the lifetime of each gas well [10, 11]. Both of these wastewaters are jointly referred to as produced water.

Produced water generated by shale gas extraction raised significant health and environmental concerns due to its chemical characteristics. The produced water generated in Marcellus Shale is characterized by high concentrations of total dissolved solids (TDS), metals (e.g., Ba and Sr), organic matter and NORM (e.g., Ra-226 and Ra-228) as illustrated in Table 3.1 [11]. For example, the average barium concentration in the flowback water exceeds the drinking water regulation by more than 1,000 times. Presence of NORM in the produced water is of particular concern because of the potential health effect for on-site workers and long-term soil and water contamination.

Because of the high salinity, toxicity and radioactivity of the produced water, the most common management approach is disposal by deep well injection. The approximately 144,000 Class II wells in operation in the United States are injecting over 2 billion gallons of brine every day. Due to the abundance of Class II disposal wells in Texas and low cost of deep well

injection, water reuse in TX accounts for only 5% of the total amount of water that is used for shale gas extraction [12]. Although water usage for shale gas extraction is less 1% of the total statewide water withdrawals in Texas, the impact of water use for hydraulic fracturing on the local water resource may be significant for the arid regions at peak time of well completion activities [3, 12]. In contrast, there are only seven Class II wells that are available for produced water disposal in Pennsylvania [6], which limits the available management options.

Table 3.1 Typical Marcellus Shale produced water characteristics [11]

	minimum	maximum	average	number of samples
TDS (mg/L)	680	345,000	106,390	129
TSS (mg/L)	4	7,600	352	156
oil and grease (mg/L)	4.6	802	74	62
COD (mg/L)	195	36,600	15,358	89
TOC (mg/L)	1.2	1530	160	55
pH	5.1	8.42	6.56	156
Alkalinity (mg/L as CaCO3)	7.5	577	165	144
SO4 (mg/L)	0	763	71	113
Cl (mg/L)	64.2	196,000	57,447	154
Br (mg/L)	0.2	1,990	511	95
Na (mg/L)	69.2	117,000	24,123	157
Ca (mg/L)	37.8	41,000	7,220	159
Mg (mg/L)	17.3	2,550	632	157
Ba (mg/L)	0.24	13,800	2,224	159
Sr (mg/L)	0.59	8,460	1,695	151
Fe dissolved (mg/L)	0.1	222	40.8	134
Fe total (mg/L)	2.6	321	76	141
gross alpha[a] (pCi/L)	37.7	9,551	1,509	32
gross beta[a] (pCi/L)	75.2	597,600	43,415	32
Ra228 (pCi/L)	0	1,360	120	46
Ra226 (pCi/L)	2.75	9,280	623	46
U235 (pCi/L)	0	20	1	14
U238 (pCi/L)	0	497	42	14

[a]Data for Northeast Pennsylvania only.

In the early stages of Marcellus Shale development, discharge of produced water into publicly owned treatment works (POTWs) was allowed under certain conditions (i.e., less than 1% of the average daily flow). However, typical treatment processes employed by POTWs (e.g., sedimentation, biological treatment, filtration) are not capable of removing dissolved solids and the TDS contained in the produced water was only diluted with municipal wastewater and discharged into the receiving waterways. As a result, level of barium in the POTW effluent and salt loading in the rivers in Pennsylvania increased during this period [13]. It was reported that disposal of flowback water into POTWs resulted in elevated bromide levels in the Allegheny River, which is a health concern because of a potential to create brominated disinfection by-products [14]. In addition, increased Ra concentration was found in river sediments downstream of a waste treatment facility that received produced water [15]. Aiming to resolve these environmental concerns, the disposal of water produced from unconventional gas wells into POTWs has been curtailed by the Pennsylvania Department of Environmental Protection since 2010 [16].

Because of the lack of disposal options, close to 90% of the produced water generated in Pennsylvania is reused for hydraulic fracturing [7]. Figure 3.1 summarizes the dominant produced water management approach in Pennsylvania. Impoundments or storage tanks are often constructed near well sites to store produced water for subsequent treatment and reuse and a small fraction is shipped for disposal in Class II wells in neighboring states (i.e., Ohio and West Virginia).

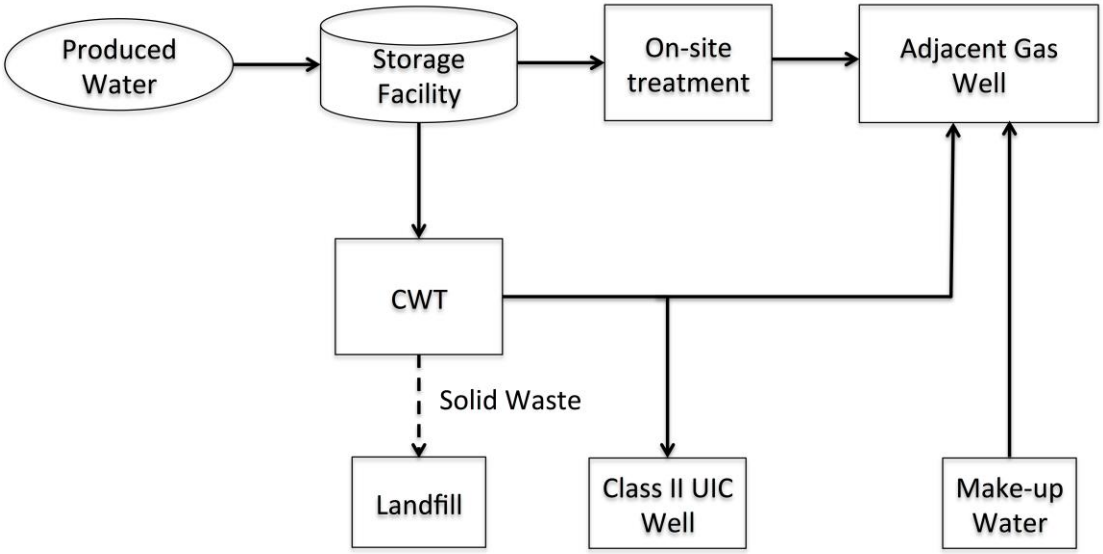

Figure 3.1 Dominant Marcellus Shale produced water management approach in Pennsylvania

On-site treatment may include filtration to remove coarse suspended solids from the produced water and enable unrestricted use in subsequent hydraulic fracturing operations. Regional centralized wastewater treatment plants (CWTs) play an important role in managing wastewater from unconventional shale gas extraction activities. In comparison to POTWs, the CWTs are equipped to remove barium and strontium using sulfate precipitation. This process removes over 90% of barium, strontium and radium [8], but the major dissolved ions (i.e., Na, Ca and Cl) are not affected and the TDS of the finished water cannot meet the requirements for the discharge into surface streams. Therefore, the only options for treated wastewater include reuse for hydraulic fracturing and disposal by deep well injection.

It is important to note that wastewater reuse for hydraulic fracturing represents a temporary solution in Pennsylvania because the capacity to reuse this wastewater is limited by the development of new wells. When the well fields mature and the drilling of new wells slows considerably, it will not be possible to reuse all produced water generated by the existing gas

wells. It is difficult to predict when a given well field will become a net water producer because of the unique well completion schedule for each field and the estimates range from 12-20 years [17-19]. In the absence of a large number of Class II disposal wells that are distributed throughout Pennsylvania, it would be necessary to employ effective and economical technologies for separation of dissolved salts, including NORM, from produced water so that the treated effluent would meet regulatory limits for unrestricted disposal to surface waters. This is a formidable challenge considering that there are currently no operating desalination facilities in this region. In addition, it will be necessary to develop industrial capacity that would use around 7 million tons of chloride salts (e.g., NaCl and $CaCl_2$) that could be recovered annually from estimated 80,000 Marcellus Shale gas wells that are likely to be eventually developed in Pennsylvania when each well is generating approximately 8 bbl/day (1.3 m^3/day) of produced water. This significant industrial development will be needed to ensure continued use of this important natural resource in an environmentally responsible manner.

3.2.2 NORM in Marcellus Shale produced water

Marcellus Shale is an organic-rich formation that contains uranium-238 and thorium-232 and their decay product, Ra-228 and Ra-226 [7]. The radioactive decay chains for U-238 and Th-232 are shown in Figure 3.2. Once formed, radium may be released into the adjacent pore water as Ra^{2+} ion that is soluble in water for a wide range of pH and redox conditions [20-22]. Ra-226 and Ra-228 have half-lives of 1,600 and 5.75 years, respectively. Considering that approximately 10 half-lives are required for radium isotopes to decay to negligible quantities [23, 24], it is clear that the presence of Ra-226 in produced water from Marcellus Shale is the main reason for environmental and public health concern.

(a)

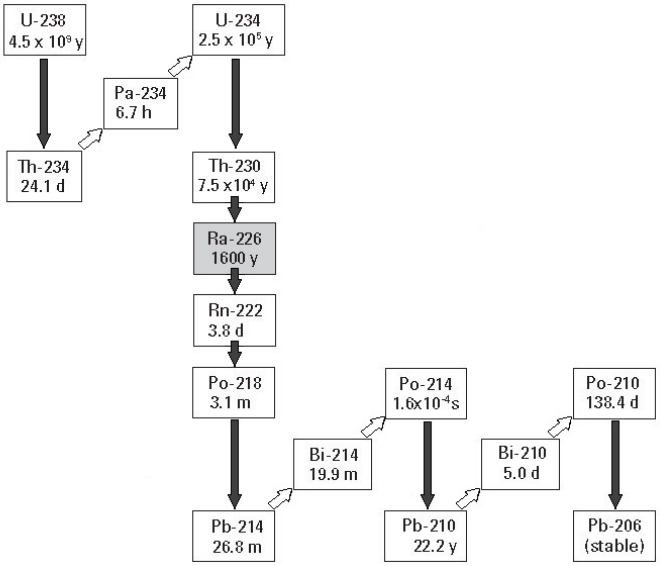

(b)

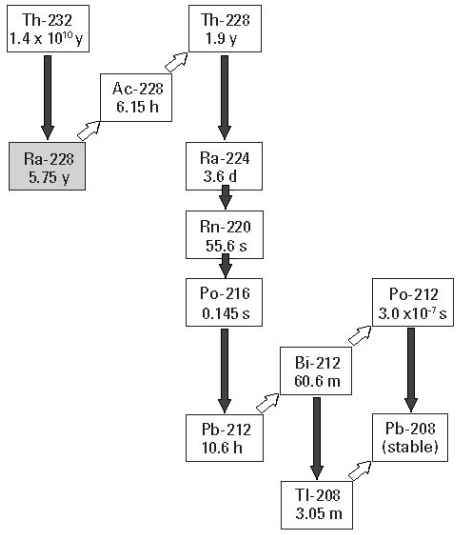

Figure 3.2 Decay chains of (a) U-238 and (b) Th-232

Uranium and thorium are present in their insoluble forms under typical environmental conditions in shale formations (reducing environment) and will have limited mobility. Hence, U and Th are minor components of NORMs in the Marcellus Shale produced water compared with Ra (Table 3.1). Ra tends to adsorb onto clays or oxide grains but the adsorption affinity is inversely related to the ionic strength of the solution [25]. Considering that the formation brines have extremely high ionic strength, it is most likely that the majority of Ra will remain in the solution [21, 26]. Therefore, Ra is generally considered a proxy of NORM that is brought to the surface by the extraction of natural gas from shale formations.

Radium concentration in the produced water from oil and gas extraction activities in Pennsylvania and New York reported by the USGS [24] can be as high as 18,000 pCi/L with a median value of 2,460 pCi/L. In comparison, non-Marcellus produced waters contain as much as 6,700 pCi/L of radium with a median value of 734 pCi/L (Figure 3.3). The Marcellus Shale produced water contains significantly higher total radium concentration compared with the produced water from other formations ($p=0.0002$, Wilcoxon-Mann-Whiney test).

Natural decay of Ra-226 and Ra-228 emits alpha and beta particles, respectively, which is accompanied by gamma radiation. Alpha and beta radiation have relatively weak penetrating ability and are only a concern if radium is accumulated in the body through inhalation or ingestion. On the other hand, gamma radiation can lead to exposure even at a distance [27, 28]. Because radium is naturally present in the environment at low levels, there is a minor exposure to radium in everyday life. However, health problems, such as teeth fracture and cataract, can be induced when an individual is exposed to higher levels of radium [29].

Long-term exposure to high level of radium can cause cancer and even fatalities [27, 30]. It is therefore important to properly asses the radiation risk from the NORM brought to the surface with the produced water from Marcellus Shale.

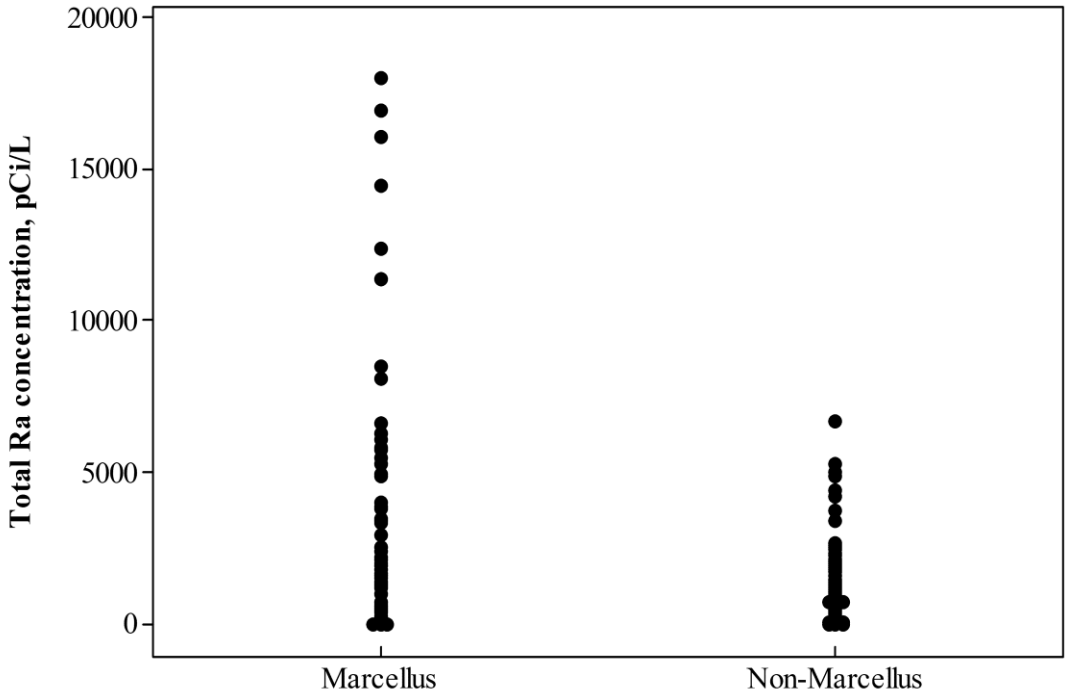

Figure 3.3 Comparison of the total radium concentration in the produced water from Marcellus Shale and non-Marcellus Shale formations [24]

3.3 PERSPECTIVE

3.3.1 Co-treatment of produced water and AMD

As only 10% - 30% of the injection fluid is typically returned to surface during the flowback period, significant volume of make-up water is required to offset the fluid loss and enable fracturing of the next gas well. Utilization of fresh water as a make-up water is a common practice in Pennsylvania [31]. AMD is a promising make-up water source for flowback water reuse considering that it is available in the vicinity of shale gas wells [8]. According to some estimates [32], just six largest AMD sources could meet all water requirements for Marcellus Shale development in Pennsylvania.

One of the key concerns with the use of AMD is the potential for long-term liability stemming from the concern for the stream quality when AMD is no longer needed for hydraulic fracturing. In order to encourage the use of AMD for hydraulic fracturing, PA DEP published a "white paper" that provides potential solutions for the long-term liability concerns when using AMD [33].

Current well completion practice in the Marcellus Shale region limits the sulfate content in the fracturing fluid to 100 mg/L to minimize the potential for well productivity loss due to barium sulfate (barite) scale formation downhole. AMD typically contains several hundred to several thousand mg/L of dissolved sulfate [34], which can react with Ba, Sr and Ca in the formation water. As the solubility product of barite ($BaSO_4$) is the lowest followed by celestite ($SrSO_4$) and gypsum ($CaSO_4$), barite precipitation is the key reaction that governs the fate of dissolved sulfate downhole [8]. Barite precipitation can also be utilized to control the concentration of sulfate in AMD by mixing it with the Ba-rich produced water. The mixing ratio

of AMD and produced water needs to be controlled to achieve a proper Ba/SO_4 ratio in the influent and ensure complete sulfate precipitation. The schematic of a treatment system that would be suitable for combined treatment of produced water and AMD is illustrated in Figure 3.4. This conventional treatment system includes a rapid mix reactor followed by coagulation/flocculation and sedimentation processes. Solids recirculation back to the rapid mix reactor would be required to enhance the kinetics of chemical precipitation in the reactor and ensure better quality of the finished water.

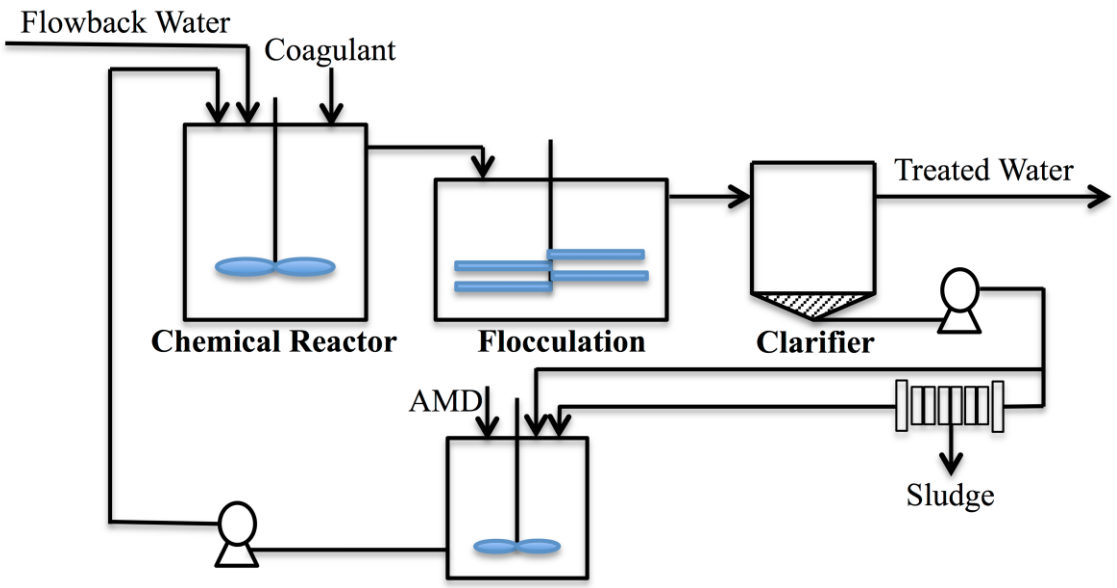

Figure 3.4 Schematic diagram of the system for the co-treatment of flowback water and AMD

The solids that are formed in the rapid mix reactor need to be removed to prevent plugging of the proppant pack and shale fractures. He et al. [35] evaluated the feasibility of membrane microfiltration for the separation of solids from the mixture of AMD and flowback

water and found that severe membrane fouling by submicron particles in the flowback water occurred after several minutes of filtration. As depicted in Figure 3.4, flocculation/sedimentation is proposed as a cost-effective solids removal process. Both conventional and ballasted flocculation can be utilized for this purpose. Ballasted flocculation is a compact process that utilizes micro-sand as the seed for floc formation and requires the addition of flocculant aid (polymer) to facilitate floc attachment to micro-sand and reduce the clarification time.

In order to demonstrate the feasibility of flocculation process for solids removal, bench-scale coagulation/flocculation experiments were conducted using produced water samples from four Marcellus Shale gas wells and six samples from AMD sites located in the vicinity of these four gas wells. Characteristics of the produced water and AMD samples collected in Southwestern Pennsylvania for this study are listed in Table 3.2. Appropriate pairs of produced water and AMD are mixed using the ratios listed in Table 3.3 that were determined based on the initial barium and sulfate concentrations and the desired sulfate limit in the effluent of 100 mg/L.

Table 3.2 Composition of produced water and AMD samples from Southwestern Pennsylvania

Constituent	Flowback water				AMD					
	A	B	C	D	1	2	3	4	5	6
Na^+ (mg/L)	27,946	18,766	28,643	28,368	281	687	104	145	1,899	1,424
Ca^{2+} (mg/L)	15,021	3,496	28,249	34,247	353	245	76	77	50	6
Mg^{2+} (mg/L)	1,720	614	3,513	5,060	53	33	49	38	104	67
Ba^{2+} (mg/L)	236	1,204	5,887	2,350	0	0	0	0	0	0
Sr^{2+} (mg/L)	1,799	625	9,000	7,000	0	3.0	1.5	0.7	0	0
Fe (Total) (mg/L)	ND	2.8	53.5	33.6	24.1	0	32.1	23.0	1.5	3.6
Cl^- (mg/L)	104,300	35,380	ND	ND	101	373	71	252	ND	ND
SO_4^{2-} (mg/L)	15	19	1	1	696	243	709	309	560	540
Alkalinity (mg)	44	ND	ND	ND	62	394	41	50	ND	ND
pH	6.4	7.4	3.9	2.4	6.0	7.0	6.1	6.1	2.8	2.7

Table 3.3 Mixing ratios and initial concentrations of sulfate and barium for the combinations of produced waters and AMDs located in their vicinity

No.	Flowback water	AMD	Initial SO_4^{2-} (mg/L)	Initial Ba^{2+} (mg/L)
1	20% FB A	80% AMD 1	560	47.2
2	30% FB A	70% AMD 2	174.2	70.8
3	40% FB B	60% AMD 3	432.7	496.0
4	25% FB B	75% AMD 4	236.3	291.0
5	12% FB C	88% AMD 5	492.8	706.4
6	25% FB D	75% AMD 6	405.0	587.5

Preliminary studies revealed that the optimum pH for conventional coagulation with ferric chloride is 6.5 [36]. Experiments designed to optimize the coagulant dose revealed that 25 mg/L of ferric chloride was sufficient to achieve effluent turbidity below 10 NTU with 30 min of flocculation and 30 min of sedimentation for all mixtures of produced water and AMD evaluated in this study (Figure 3.5).

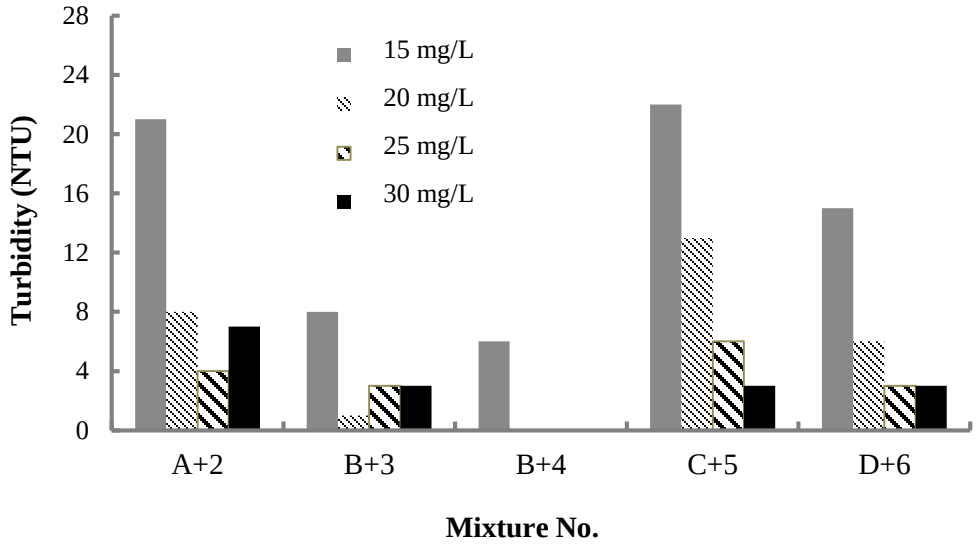

Figure 3.5 Impact of ferric chloride dose on the turbidity of supernatant from conventional flocculation treatment

Optimization of the ballasted flocculation was performed using bench-scale experiments at pH 6.5 with 25 mg/L of ferric chloride as the optimal dose obtained from preliminary studies. A total of 2.5 grams of micro-sand was added to a total mixture volume of 500 mL to achieve typical micro-sand concentration in the ballasted flocculation process of 5 g/L. The initial mixing period of 2 min was followed by another 3 min of rapid mixing at 300 rpm. At that time, flocculant aid was added to the solution and rapid mixing continued for another 15 seconds. Mixing speed was then reduced to 200 rpm for 45 seconds, followed by four minutes of settling.

As can be seen in Figure 3.6, effluent turbidity from the ballasted flocculation process improved when 0.2 mg/L of anionic polymer was added to the solution. Further improvement in effluent turbidity was observed when the polymer dose was increased to 0.5 ppm and it remained below 5 NTU for all combinations of produced water and AMD evaluated in this study.

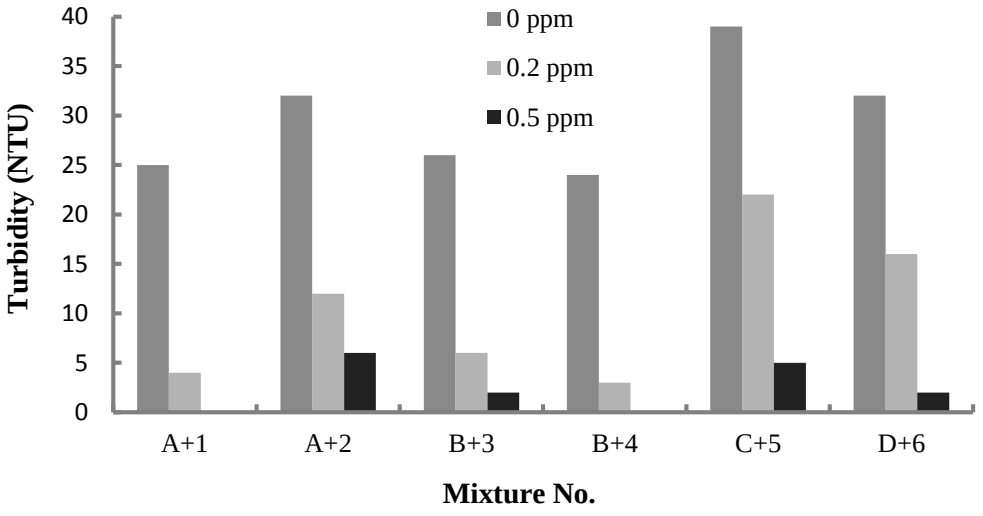

Figure 3.6 Impact of polymer dose on turbidity of the supernatant from ballasted flocculation treatment

After the solids removal process, the effluent can be stored for hydraulic fracturing while the solid waste needs to be properly disposed. As the radium concentration in Marcellus Shale produced water is very high, it is important to evaluate the fate of radium during the proposed

treatment process for its impact on the disposal alternatives for the solid waste generated when the produced water is mixed with AMD.

3.3.2 Fate of Radium during co-treatment of produced water and AMD

Although the solubility of radium sulfate is the lowest among all sulfates that may form when produced water is mixed with AMD, it is unlikely that pure radium sulfate will precipitate because radium concentrations are several orders of magnitude lower than other divalent cations. Radium is a member of alkaline earth metals with similar chemical properties as barium and strontium and will co-precipitate with barite ($BaSO_4$) and celestite ($SrSO_4$). Radium co-precipitation can be described by the distribution law:

$$\frac{RaSO_4}{MSO_4} = K_d \frac{Ra^{2+}}{M^{2+}}$$

where, K_d is the distribution coefficient, MSO_4 and $RaSO_4$ are relative mole fractions of carrier (e.g., Ba, Sr, Ca) and radium sulfates in the solid phase, respectively, and M^{2+} and Ra^{2+} are equilibrium concentrations in the liquid phase.

It is likely that barite, celestite and gypsum will be formed when AMD and flowback water are mixed. However, it is expected that radium removal will be controlled by barite precipitation because it is thermodynamically and kinetically the most favorable reaction [22]. As reported by Zhang et al. [31], the distribution coefficient (K_d) for Ra co-precipitation with barium sulfate increases with an increase in the ionic strength of the solution. Analysis of Ra removal through co-precipitation with barite was conducted in this study assuming the distribution coefficient of 1.5 (lowest theoretical value) [20, 22, 37] and 7.49 (highest value

reported by Zhang et al. [22]) and the initial Ba and Ra concentrations of 500 mg/L and 1,500 pCi/L, respectively, which are representative values for Southwestern Pennsylvania [11]. As can be seen in Figure 3.7, Ra removal increases with barium removal resulting in Ra concentration in the precipitate that ranges from 1,800-13,000 pCi/g. In comparison, NORM limit for unrestricted disposal in RCRA-D nonhazardous landfill ranges from 5-50 pCi/g depending on the state regulations [38]. Therefore, the disposal of the Ra-enriched solid waste generated by the co-treatment of produced water and AMD needs to be carefully managed to avoid any adverse environmental impacts.

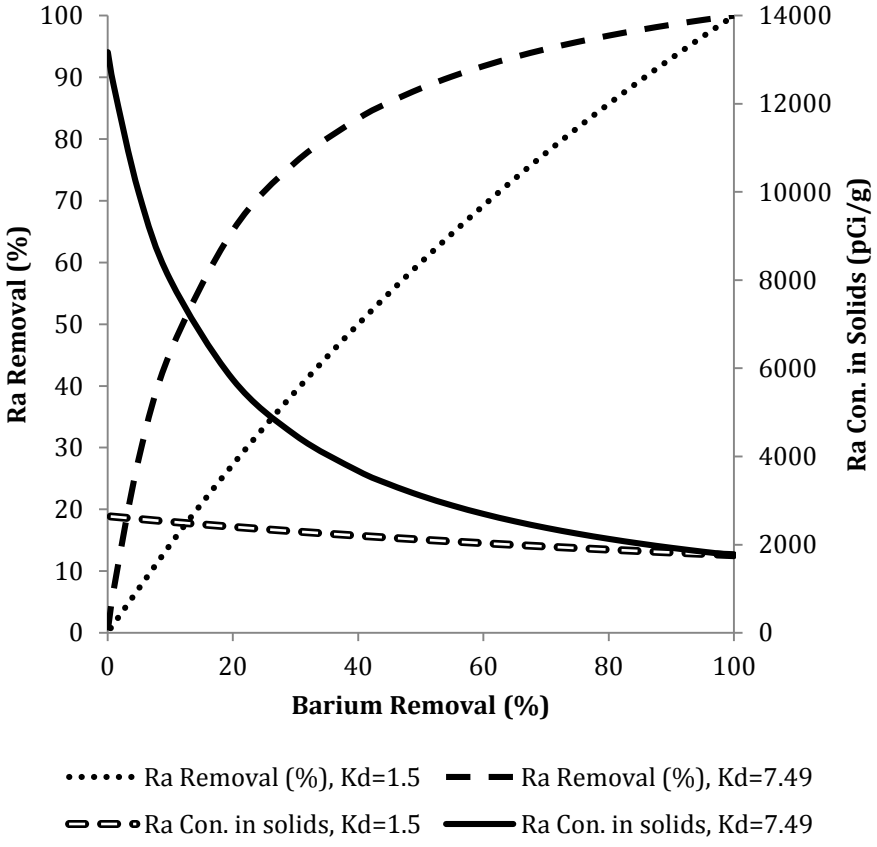

Figure 3.7 Ra removal and Ra concentration in the precipitate for the initial Ba and Ra concentrations in produced water of 500 mg/L and 1,500 pCi/L, respectively

In 2004, PA DEP issued a guidance document for monitoring radioactivity at solid waste processing and disposal facilities using a suitable Gamma radiation detection devices (e.g., Geiger counter or ionization chamber) [39]. The solid waste that contains NORM can be disposed in these landfills without DEP approval if the following conditions are satisfied: (a) volume of solid waste is lower than $1m^3$; (b) gamma radiation monitored by Geiger counter at a distance of 5 cm from any surface is lower than 50 μR/h; and (c) total radium concentration in solid waste is lower than 5.0 pCi/g.

When the solid waste generated by co-treatment of produced water and AMD is disposed in a municipal landfill, Ra concentration in that landfill can be calculated assuming complete Ra removal from the solution and even distribution of Ra-enriched solids in the landfill. If one million gallons of flowback water (i.e., the average flowback volume generated by one Marcellus Shale gas well) containing 1,500 pCi/L Ra is mixed with AMD and the solid waste generated by this process is disposed into a landfill that has an annual loading of 100,000 t, the average Ra concentration in that landfill will be just 0.057 pCi/g. Therefore, the average landfill in Pennsylvania can receive the solid waste created by treating the flowback water generated by approximately 100 Marcellus Shale gas wells without exceeding the allowable NORM limit. However, it is crucial to monitor and control the NORM in the incoming waste to ensure environmental compliance. Once a landfill reaches the maximum capacity for NORM disposal, it will no longer be able to accept Ra-enriched solids generated by produced water treatment.

3.3.3 Alternative management approach for produced water in Pennsylvania

Although the co-treatment of produced water and AMD is a promising option to reduce the pressure on fresh water resources and manage the wastewater generated from shale gas

extraction activities in Pennsylvania, it will be of no use once the supply of produced water exceeds the reuse capacity in a well field [17-19]. At this point, the growing volume of high-TDS produced water must be concentrated for disposal by deep well injection, while the solids (e.g., NaCl and $CaCl_2$) can be recovered and used for other applications (e.g., de-icing salt, chlor-alkali plants). However, these solids are not likely to pass the Toxicity Characteristic Leaching Procedure (TCLP) test for unrestricted industrial use because of high barium and radium concentrations in produced water. Therefore, radium and barium will have to be removed prior to concentrating the produced water to recover reusable solids.

This study revealed that the addition of sulfate can effectively remove both Ba and Ra through co-precipitation but will generate insoluble solids (i.e., barite) with high Ra concentration. These solids may be disposed in municipal solid waste landfills as long as the maximum capacity for NORM disposal is not exceeded. After that, they will have to be sent to landfills approved for low-level radioactive waste, which is a significantly more expensive alternative (e.g., $6,500/ton vs. $50/ton).

The alternative to sulfate precipitation is lime-soda ash softening that can be used to remove divalent cations (e.g., Ca, Mg, Sr and Ba) from the produced water as solid carbonates. During the softening process, radium will also be removed from the produced water by co-precipitation with these carbonate salts [39]. Removal of these major divalent cations from produced water would be beneficial in terms of reducing the potential for scale formation in subsequent treatment steps to recover usable solids. The finished water after softening can be further treated with thermal desalination processes (e.g., evaporation, membrane distillation, crystallization) to concentrate the solution for disposal and recover the solid product (e.g., NaCl, $CaCl_2$), which can be used for other applications (e.g., road salt, chlor-alkali plants). The

carbonate precipitates formed in the lime-soda ash process can be dissolved by acidification and disposed in Class II wells together with concentrated liquid stream from the thermal desalination process. The schematic of the complete treatment process is summarized in Figure 3.8.

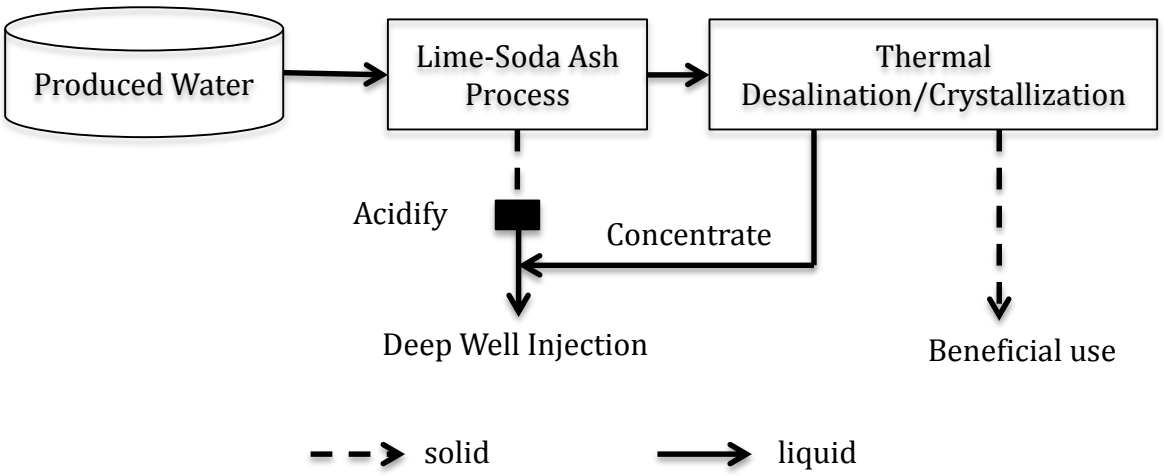

Figure 3.8 Schematic flow chart for the flowback/produced water desalination with pretreatment by lime-soda ash process

Radium has limited affinity for $CaCO_3$ as shown by the theoretical K_d value of just 0.013 and experimental K_d value under ideal condition (i.e., homogeneous nucleation of $CaCO_3$) of 0.15±0.006 [40]. Batch tests using simulated produced water containing 15,000 mg/L of calcium and 5,000 pCi/L of radium were conducted in this study to evaluate the potential of lime-soda ash softening for the treatment of Marcellus Shale produced water, Sodium carbonate dose was adjusted to achieve different levels of calcium removal through precipitation as calcite. Calcium and radium concentrations in the liquid phase at equilibrium were measured using atomic absorption spectrometry and liquid scintillation, respectively. Experimental results showed distinctively higher Ra removal when compared with predictions using both theoretical and experimental K_d values (Figure 3.9). The discrepancy might be attributed to additional

mechanisms for Ra incorporation into the solid phase (e.g., adsorption and/or occlusion) during heterogeneous $CaCO_3$ nucleation [22]. Thus, the distribution equation cannot be used to predict Ra removal during lime-soda ash treatment and further studies are required to overcome this knowledge gap.

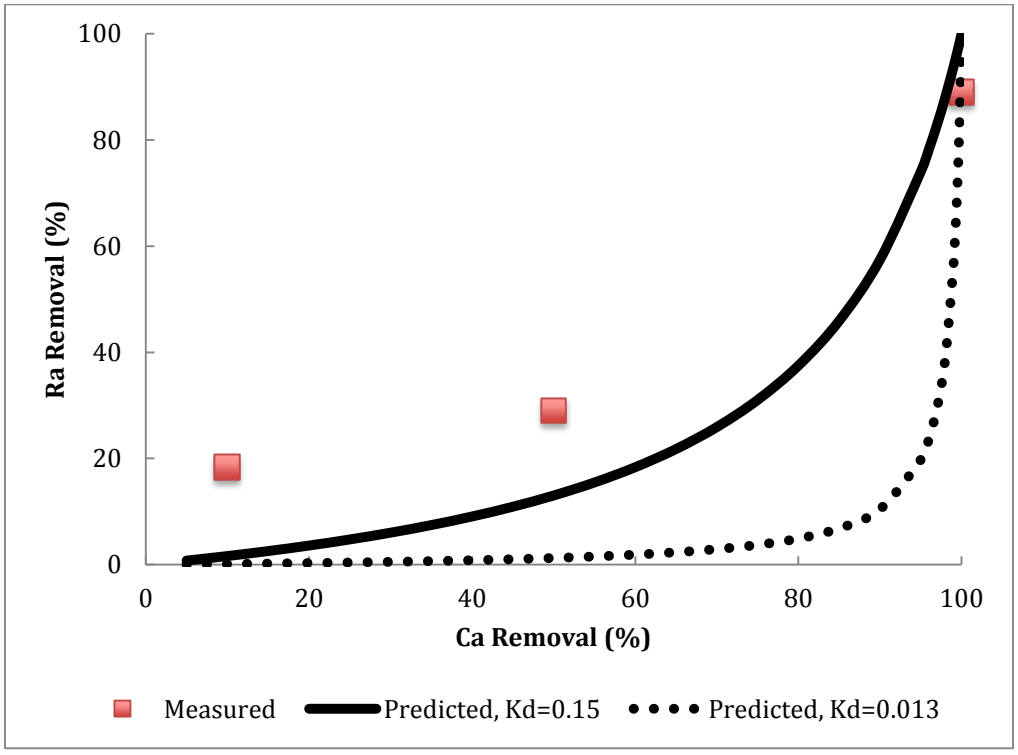

Figure 3.9 Ra removal by co-precipitation with $CaCO_3$ as a function of calcium removal using theoretical and experimental [40] distribution coefficients

3.4 SUMMARY AND CONCLUSIONS

Marcellus Shale flowback/produced water generates significant public health and environmental concerns in Pennsylvania due to its high salinity that includes toxic metals and naturally

occurring radioactive materials. Because of the lack of suitable disposal wells, the most appropriate produced water management option is currently its reuse for hydraulic fracturing.

AMD is a promising make-up water source to compensate for the unrecovered portion of the injection fluid and enable the reuse of flowback water for hydraulic fracturing of subsequent gas wells. Conventional and ballasted flocculation processes were found to be effective in separating the solids that would be formed when produced water is mixed with AMD. Adjusting the mixing ratio of these impaired waters will enable accurate control over the sulfate concentration in the finished water and its unrestricted use for well completions. Ra co-precipitation with barium sulfate is a concern for the disposal of solid waste generated in this process. Review of a guidelines issued by the PADEP suggests that strict monitoring and control of landfill disposal practice is needed to ensure environmentally acceptable management of the NORM-laden solid waste created by the unconventional gas industry.

When produced water supply exceeds the reuse capacity for hydraulic fracturing, this wastewater must be concentrated and disposed in Class II disposal wells. Lime-soda ash softening can be used to remove the divalent cations, including Ra, to facilitate the recovery of reusable solids (i.e., NaCl, $CaCl_2$) and prevent scaling problems in thermal desalination facilities that would be needed to ensure development of unconventional gas resource in Pennsylvania in environmentally and economically acceptable manner.

4.0 EQUILIBRIUM AND KINETICS OF CHEMICAL REACTIONS PROMOTED BY THE USE OF AMD FOR FLOWBACK WATER TREATMENT AND REUSE

Flowback water/produced water generated from shale gas extraction activities is of great environmental concern in terms of its high total dissolved solid (TDS), organic content, and naturally occurring radioactive materials (NORMs). Abandoned mine drainage (AMD) is a degraded water source with significant environmental impact on the surface water and associated groundwater. Application of AMD for flowback water reuse for hydraulic fracturing provides a potential solution to reduce the adverse environmental impact from both wastewaters and relieve the pressure on fresh water by unconventional gas industry. This study evaluated the kinetics and equilibrium of chemical precipitation that occurs when flowback water and AMD are mixed above ground.

Sulfate concentration predicted by thermodynamic calculations was very close to that measured after 60 min of reaction, which was due to the rapid barite precipitation and the minimal impact of celestite precipitation on the finished water quality. An empirical model was developed to predict kinetics of barite precipitation in a mixture of flowback water and AMD. This model offers excellent agreement with experimental results for the mixture that has low percentage of flowback water.

4.1 INTRODUCTION

Unconventional (shale) natural gas has emerged as an important energy source in United States, which can potentially reduce the reliance on gas imports. Horizontal drilling and hydraulic fracturing are the two key technologies that enabled economical recovery of natural gas from shale formations that are characterized by extremely low permeability [1, 2]. As natural gas is more environmentally benign compared to coal, it can serve as a transient fuel between coal and renewable energy to mitigate the greenhouse effects [3].

Marcellus shale formation that is located in the northeastern U.S. is one of the largest shale gas reservoirs in the world, with an estimated 262-500 Tcf (trillion cubic feet) of natural gas reserves [4, 5]. While the unconventional shale gas is a promising and significant energy source, its extraction raises significant environmental challenges in terms of fresh water requirement and wastewater management. Large quantity of water is required for hydraulic fracturing (3-5 million gallons/well), while roughly 10%-30% of the fracturing fluid will be recovered during the flowback period [6, 7]. Flowback typically includes high concentration of total dissolved solid (TDS), high level of naturally occurring radioactive materials (NORMs) and organic matter [8]. Reuse of flowback water for hydraulic fracturing is currently the most common practice for management of this water in Pennsylvania (the reuse rate is about 90% based on PA DEP data) [9, 10].

AMD generated from coal mining industry is the largest source of surface water contamination in Pennsylvania, impacting the quality of over 3,000 miles of surface streams [11]. Uncontrolled discharge of AMD to surface water typically leads to elevated concentration of metals, metalloids and sulfate and possibly a reduction in pH of the receiving stream [12]. AMD sources are often located in the vicinity of permitted gas extraction well sites [3].

Therefore, AMD can potentially serve as an alternative make-up water to supplement flowback water for hydraulic fracturing of subsequent wells and alleviate the fresh water demand, reduce the transportation cost, and reduce potential adverse environmental impacts of these two wastewaters.

Dissolved sulfate presence in AMD is of great concern for the use of AMD in hydraulic fracturing fluid [3]. High level of dissolved sulfate in the injection fluid will cause precipitation of alkaline earth metals (e.g., Ca, Sr, Ba) in the shale formation, which may cause the reduction in well permeability and productivity. Because of very low solubility, barite ($BaSO_4$) precipitation is the most significant scaling concern and requires careful control strategies. Therefore, sulfate concentration in the fracturing fluid is typically limited to 100 mg/L while AMD may contain several hundred to several thousand mg/L sulfate [13]. Mixing AMD with flowback water above ground will lead to precipitation of $BaSO_4$, $SrSO_4$ and $CaSO_4$, which reduces the dissolved sulfate concentration in the finished water. Coagulation/flocculation [14] or microfiltration [15] are required to ensure effective separation of solids that are formed after AMD and flowback water are mixed.

The main objective of this study is to evaluate the kinetics and equilibrium of complex precipitation reactions under process conditions that would occur when AMD is used as make-up water for treatment and reuse flowback water for hydraulic fracturing.

4.2 MATERIALS AND METHOD

4.2.1 Flowback water and AMD sampling

Flowback water (FW) samples were collected from two well sites (Wells A and B) in southwestern PA and one well site (Well C) in northeastern PA. Well A was fractured with reused flowback water, while Well B was fractured with tap water. Flowback water samples from these two wells were collected at various times from Day 1 to Day 16 and stored individually in clean HDPE buckets and covered with lids. Composite flowback water samples for these wells were prepared in proportion to flow rate on each day (i.e., flow composite sample). Flowback Water C was sampled from a storage tank.

Five AMD sites located near the gas wells were selected in this study. AMD 1 and AMD 2 are located near Well Site A; AMD 3 and AMD 4 are available in the vicinity of Well Site B; and AMD 5 is located near Well Site C. AMD 1, 3 and 4 are untreated, while AMD 2 and 5 underwent a passive treatment process. Characteristics of AMD and flowback water samples used in this study are summarized in Table 4.1.

Flowback water and AMD samples were mixed at ratios ranging from 10% to 70% in a 200-mL beaker covered with plastic film to minimize evaporative losses. Samples were collected at pre-determined time points, filtered through 0.45-μm nylon membrane and immediately diluted to prevent subsequent chemical reactions. Atomic absorption spectroscopy (AAS Model 1000, PerkinElmer, Waltham, MA) was used to analyze Ba and Sr ions while ion chromatography (Dionex ICS-1100, Thermo Scientific, Waltham, MA) was used to analyze the dissolved sulfate.

The samples for AAS analysis were diluted with 2% HNO_3 solution with 0.15% KCl, while the samples for IC analysis were diluted with DI water. Analysis of each ion was conducted 3 times and the average values were reported as long as the relative standard deviation did not exceed 5%.

Table 4.1 Characteristics of flowback water and AMD

Parameter	Flowback Water			AMD				
	FW A	FW B	FW C	AMD 1	AMD 2	AMD 3	AMD 4	AMD 5
Na^+(mg/L)	27,950	14,910	81,440	281	687	104	145	1,900
Ca^{2+}(mg/L)	15,020	2,970	32,900	353	245	76	77	50
Mg^{2+}(mg/L)	1,720	530	3,510	53	33	49	38	104
Ba^{2+}(mg/L)	236	850	6,260	-	-	-	-	-
Sr^{2+}(mg/L)	1,800	870	11,910	-	3	1.5	0.7	-
Cl^-(mg/L)	104,300	35,380	188,730	101	373	71	252	-
SO_4^{2-}(mg/L)	15	0		696	243	709	309	560
pH	6.43	7.38	3.86	5.97	7.03	6.14	6.12	2.82

4.2.2 Empirical kinetic model for barite precipitation

Batch experiments were conducted with synthetic model solutions (Table 4.2) to assess the kinetic parameters. The solutions that are supersaturated with respect to barite were prepared by adding Na_2SO_4, $BaCl_2$ and NaCl from stock solutions. The samples were collected and analyzed as described above.

Table 4.2 Composition of model solutions

Run	NaCl (mM)	Ba (mM)	SO_4 (mM)	Saturation Index (SI)
M1	0	2	0.1	3.05
M2	10	2	0.1	2.89
M3	50	2	0.1	2.59
M4	100	2	0.1	2.39
M5	0	0.1	2	3.06
M6	10	0.1	2	2.9
M7	50	0.1	2	2.59
M8	100	0.1	2	2.39

4.3 RESULTS AND DISCUSSION

4.3.1 Mixing experiments and equilibrium prediction

AMD 1 and 3 have relatively high sulfate concentration compared to AMD 2 and 4. As depicted in Figure 4.1, the mixtures made with low-sulfate AMD samples (AMD 2 and 4), require lower percentage of flowback water to achieve the desired sulfate concentration in the effluent. As the sulfate concentration in AMD increases, so does the percentage of flowback water required to achieve the acceptable final sulfate concentration. These simple experiments clearly illustrate that the mixing ratio between flowback water and AMD is the key factor governing the residual sulfate concentration in the finished water (Figure 4.1) because the increase in the percentage of flowback water in the mixture leads to greater dilution of sulfate contributed by AMD and higher barium concentration in the mixture. The flowback with lower Ba concentration (e.g., FW B) requires lower percentage of AMD in the mixture to achieve acceptable sulfate concentration in

the finished water. As the make-up water typically accounts for 70%-90% of the volume required to hydraulically fracture the gas well, it is necessary to conduct preliminary calculations similar to those on Figure 4.1 to determine the appropriate AMD candidates based on the barium concentration in the flowback water.

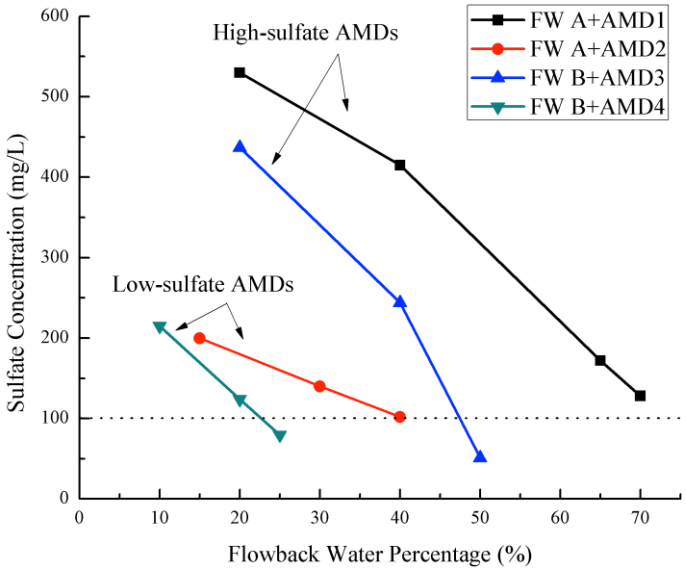

Figure 4.1 Measured sulfate concentration as a function of mixing ratio and composition of flowback and AMD

The AMD samples used in this study have moderate sulfate concentrations ranging from 243 - 709 mg/L. Calcium, strontium and barium in flowback water can all potentially react with dissolved sulfate to form precipitates. The saturation indices (SI) for $CaSO_4$, $SrSO_4$ and $BaSO_4$ were calculated for all FW-AMD mixtures, using PHREEQC software with the Pitzer database. As shown in Table 4.3, gypsum ($CaSO_4$) is undersaturated for all mixtures tested in this study even when using FW A that contains over 15,000 mg/L dissolved calcium. This is due to the fact that the solubility product for gypsum is two and five orders of magnitude higher than that for celestite and barite, respectively.

Table 4.3 Mixtures of flowback water and AMD and the associated saturation indices for barite, celestite and gypsum

Mixture	Composition	Saturation Index (SI)		
		$BaSO_4$	$SrSO_4$	$CaSO_4$
1	15%FW A+85%AMD1	2.58	0.12	-0.45
2	40%FW A+60%AMD1	2.49	0.07	-0.52
3	65%FW A+35%AMD1	2.3	-0.06	-0.65
4	70%FW A+30%AMD1	2.25	-0.09	-0.69
5	15%FW A+85%AMD2	2.16	-0.33	-0.9
6	30%FW A+70%AMD2	2.1	-0.35	-0.94
7	40%FW A+60%AMD2	2.04	-0.38	-0.97
8	20%FW B+80%AMD3	3.61	0.23	-0.73
9	35%FW B+65%AMD3	3.56	0.2	-0.78
10	50%FW B+50%AMD3	3.46	0.11	-0.87
11	10%FW B+90%AMD4	3.23	-0.16	-1.07
12	20%FW B+80%AMD4	3.26	-0.12	-1.07
13	25%FW B+75%AMD4	3.25	-0.12	-1.09
14	70%FW B+30%AMD4	2.89	-0.44	-1.43
15	10%FW C+90%AMD5	3.79	0.6	-0.44

Although celestite is supersaturated for some mixtures (e.g., Mixtures 9 and 10), thermodynamic predictions obtained using PHREEQC suggest that precipitation of $SrSO_4$ will occur only in Mixtures 1 and 7. Such conclusion is due to the fact that $BaSO_4$ precipitation is thermodynamically more favorable than celestite precipitation and because standard thermodynamic calculations do not account for Sr coprecipitation with $BaSO_4$. Therefore, initial barium sulfate precipitation results in the consumption of dissolved sulfate, which in turn leads to undersaturation with respect to celestite for Mixtures 9 and 10.

While Sr coprecipitation will occur, barium sulfate precipitation is the dominant reaction that governs the overall rate of sulfate removal. The measured sulfate concentrations after 60 min of reaction and the predicted values using PHREEQC with Pitzer's activity corrections are compared in Figure 4.2. As illustrated in this figure, the PHREEQC software offers excellent

prediction of sulfate concentration in the finished water and the goodness of prediction suggests that the main reaction responsible for sulfate removal (i.e., barite precipitation) is essentially equilibrated within 60 min.

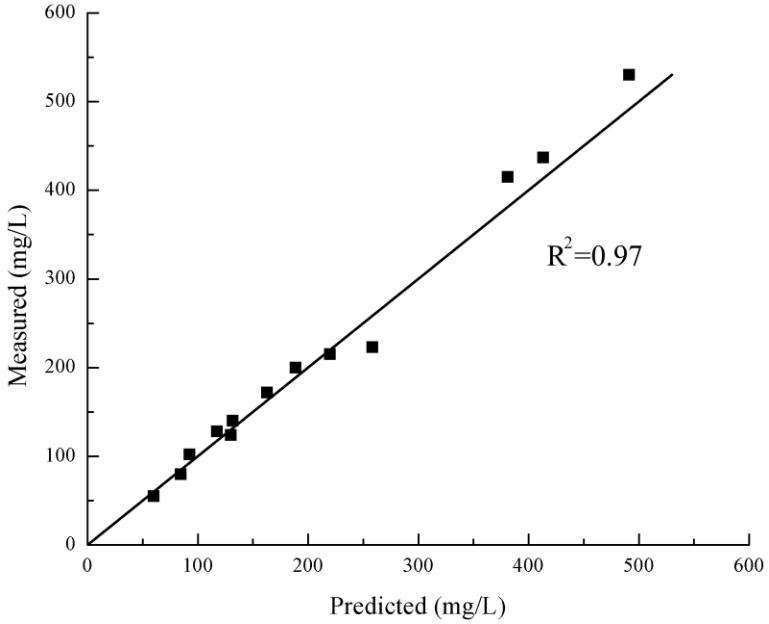

Figure 4.2 Comparison between measured sulfate concentration after 60 min of reaction and values predicted by PHREEQC

4.3.2 Kinetics model for $BaSO_4$ precipitation

Because all solutions are undersaturated or had very low saturation with respect to celestite (Table 4.3), precipitation of "pure" celestite is expected to have minimal contribution to sulfate removal. An example illustrated in Figure 4.3 clearly shows that barite precipitation reached equilibrium after 60 min of reaction, while slight Sr reduction was observed during the first 30

min of reaction, which is most likely due to coprecipitation of barium-strontium sulfate. When Ba essentially reached equilibrium, further decline in Sr concentration was not observed as the mixture became undersaturated with respect to celestite.

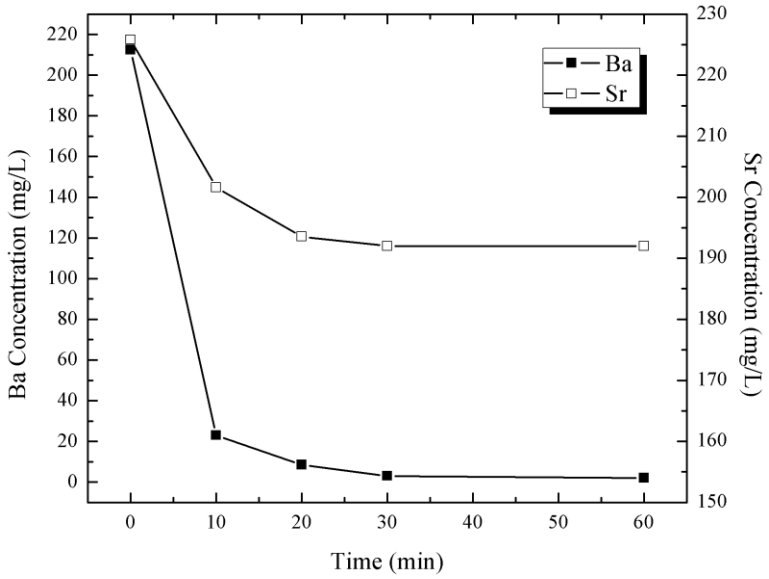

Figure 4.3 Variation of Ba and Sr concentration with time for Mixture 13**.**

Although pure celestite precipitation was not observed in this study because both sulfate and strontium initial concentrations were relatively low, it is possible that pure celestite precipitation would proceed if the saturation index of celestite was high after the initial barite precipitation reached equilibrium. Kondash et al. studied the kinetics of precipitation for AMD and flowback mixture where celestite precipitation was inevitable after all barium was consumed[16]. By monitoring conductivity, Kondash et al. found that roughly 10 hr was needed to reach equilibrium[16], which was most likely due to the slow celestite precipitation after barite precipitation reached equilibrium [17].

In order to evaluate the effect of celestite precipitation on the overall reaction kinetics, the initial Sr concentration of Mixture 13 was adjusted to 1,200 mg/L by the addition of $SrCl_2$. As can be seen in Figure 4.4, rapid sulfate decline was observed during the first 10 min of reaction followed by very slow sulfate reduction for 9 more hours. The initial sulfate decline corresponded to barium-strontium sulfate co-precipitation. After barium concentration essentially equilibrated within 60min, the second phase of sulfate concentration decline that corresponds to pure celestite precipitation was very slow. Even after 9 hr of reaction, sulfate concentration was still far from equilibrium state (dotted line) predicted by PHREEQC. Slow celestite precipitation is consistent with previous study on the removal of barium and strontium from flowback water by the addition of Na_2SO_4, which showed that over 24 hours is needed for Sr concentration to reach equilibrium [17].

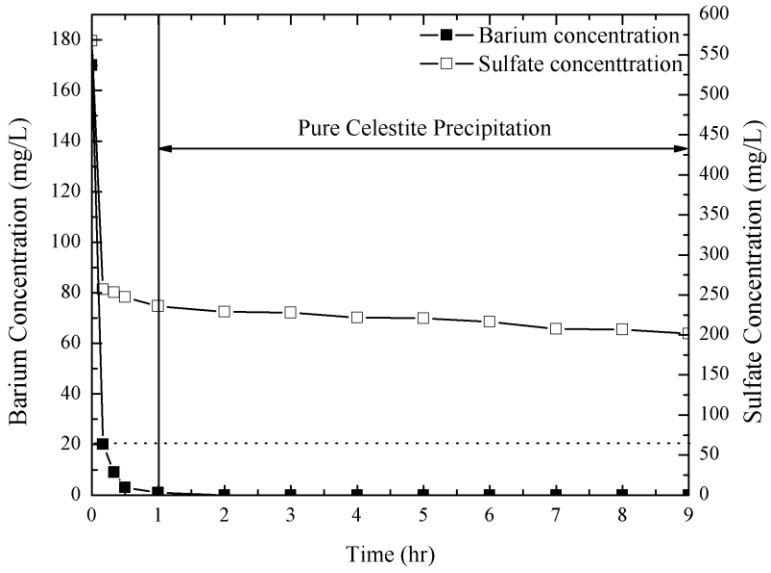

Figure 4.4 Precipitation kinetics of the Mixture 8 with adjustment of Sr concentration. The dotted line is the sulfate concentration at equilibrium as predicted by PHREEQC software.

The slow celestite precipitation is not likely to contribute significantly to sulfate removal in a treatment plan where the reaction time is typically on the order of 1-2 hr. Therefore, the

AMD to flowback water mixing ratio should be adjusted to achieve equal barium and sulfate molar concentrations in the mixture to ensure that complete dissolved sulfate removal will be achieved through barite precipitation (Sr coprecipitation will also occur) in a relatively short period of time.

4.3.3 Empirical kinetic model for barite precipitation

Previous experiments clearly show that barite precipitation governs the overall reaction kinetics when mixing flowback water and AMD. Nucleation and crystal growth kinetics of barite precipitation have been widely studied [18-21] but it cannot be used to predict the variation in sulfate concentration under conditions that are typical for centralized waste treatment plants that utilize sulfate precipitation to control divalent cations in treated flowback water that is used for hydraulic fracturing. The homogeneous nucleation models predict the rate of nuclei formation (number of nuclei formed per volume per time), while the crystal growth models are used to account for the growth rate of seeded particles (length/time). Several kinetics models were developed using rate equation to describe the crystal growth in the seeded experiments [22, 23]. However, the seeded growth model is applicable only at very low supersaturation conditions where homogeneous nucleation is negligible. In this study, an empirical kinetic model for rapid barite precipitation was developed using the rate law shown in Equation 4-1. The difference between the concentration product of barium and sulfate at time t and at equilibrium ($C_{Ba}C_{SO4}$-K'_{sp}) describes the extent of disequilibrium, which drives the precipitation reaction.

$$R = -\frac{dC_{Ba}}{dt} = -\frac{dC_{SO4}}{dt} = k_r\left(C_{Ba}C_{SO4} - K'_{sp}\right)^n \quad (4\text{-}1)$$

where, R is the reaction rate, C_{Ba} and C_{SO4} are the molar concentrations of barium and sulfate at time t, K'_{sp} is the solubility of barite and n is the reaction order with respect to barium and sulfate, respectively.

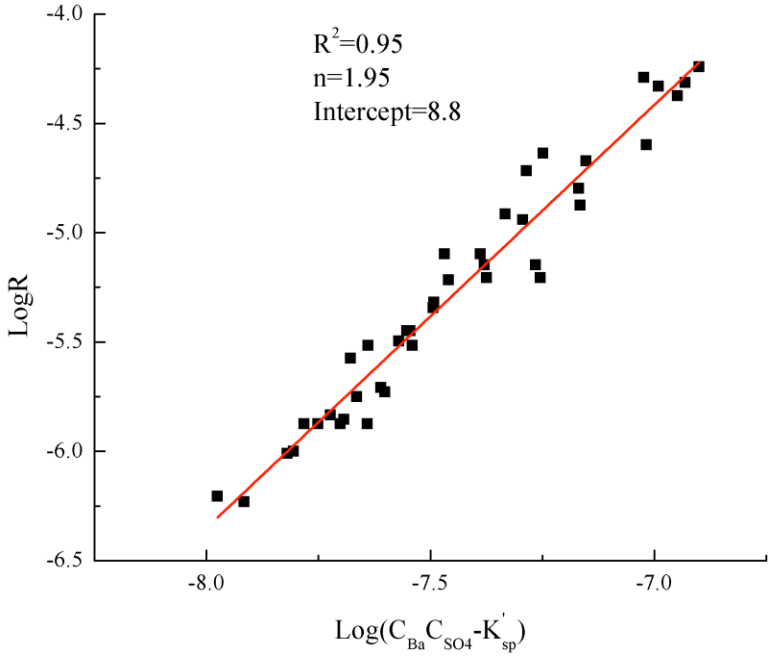

Figure 4.5 Analysis of barite precipitation rate obtained using model solutions (Table 4.2)

The plot of logR vs $\log(C_{Ba}C_{SO4}-K'_{sp})$ shown in Figure 4.5 can be used to determine the apparent reaction order and the reaction rate constant. As illustrated in this figure, the experimental data agreed with the empirical model fairly well (R^2 =0.95) with a slope of approximately 2, which suggests that the reaction is approximately second order with respect to Ba^{2+} and SO_4^{2-} concentration. Equation 4-1 can be integrated to obtain the relationship between barium and sulfate concentration with time:

$$\frac{-C_{Ba}-C_{SO4}}{[4(C_{Ba,0}C_{SO4,0}-K'_{sp})-(C_{Ba,0}+C_{SO4,0})^2](C_{Ba}C_{SO4}-K'_{sp})}+\frac{4ArcTan\left(\frac{-C_{Ba}-C_{SO4}}{\sqrt{4(C_{Ba,0}C_{SO4,0}-K'_{sp})-(C_{Ba,0}+C_{SO4,0})^2}}\right)}{\left[4(C_{Ba,0}C_{SO4,0}-K'_{sp})-(C_{Ba,0}+C_{SO4,0})^2\right]^{1.5}}=k_r t+C \qquad (4\text{-}2)$$

where, C_{Ba} and C_{SO4} are barium and sulfate concentrations at time t, respectively, and C is the constant of integration which can be calculated at t=0.

Mixtures 10, 13, 14 and 15 were used to assess the accuracy and limitations of the empirical kinetics model (Equation 4-2) and the comparison between predicted and measured Ba or SO_4 concentrations are illustrated in Figure 4.6. The model proposed in this study offers excellent prediction of precipitation kinetics for Mixtures 13 and 15 that have 25% Flowback Water B and 10% Flowback Water C, respectively (Figures 4.6b and 4.6d). However, the model over-predicted barite precipitation rate for Mixtures 10 and 14 that have 50% and 70% Flowback Water B, respectively (Figures 4.6a and 4.6c). Such behavior suggests that barite precipitation in these mixtures is inhibited by the constituents in the flowback water, which is most likely due to lattice poisoning and ion-pair formation induced by elevated concentrations of calcium and strontium [17, 24]. Therefore, the kinetic model developed in this study is applicable for mixtures with low percentage of flowback water, which is typically the case in practice where make-up water usually accounts for 70-90% of the mixture to compensate for the unrecovered portion of fracturing fluid.

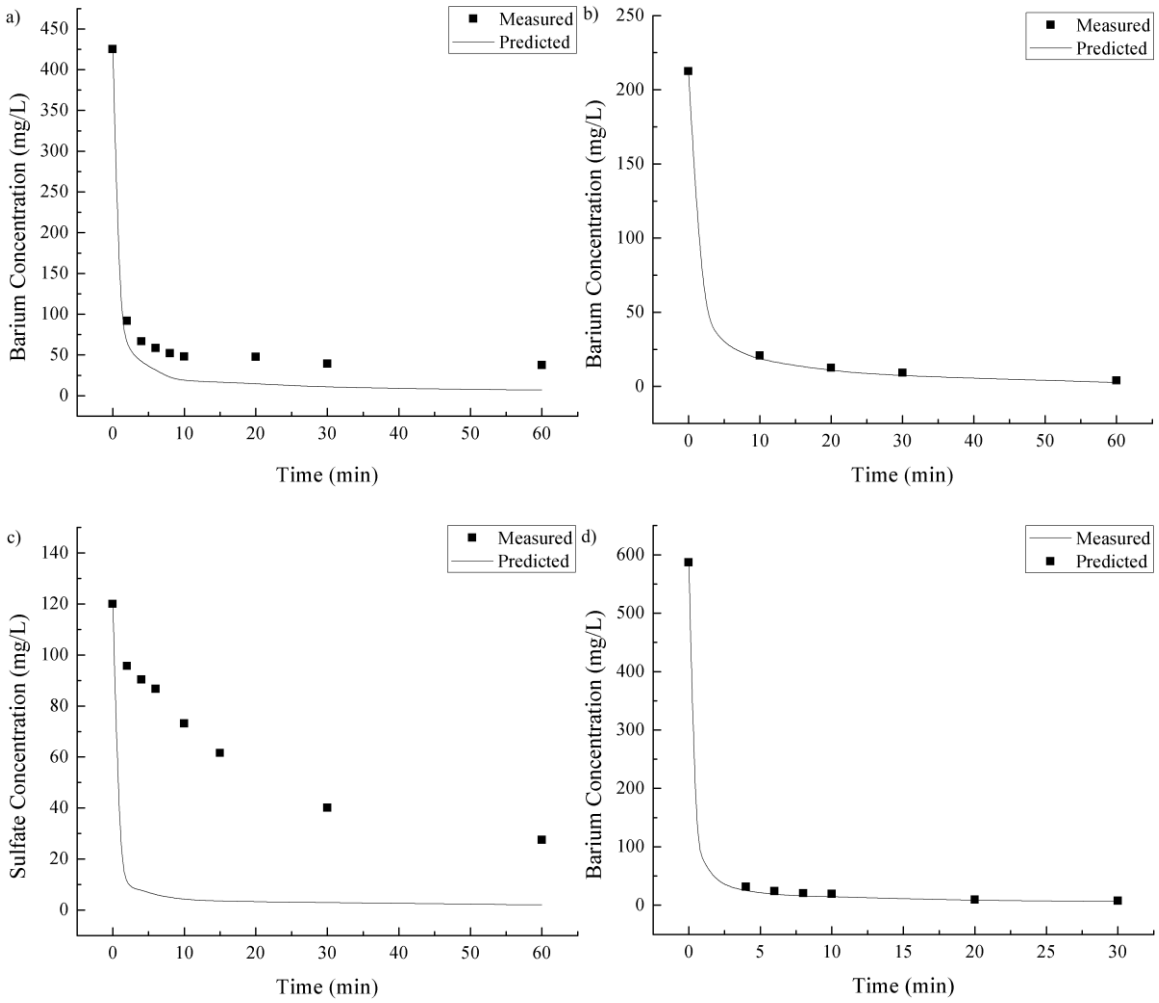

Figure 4.6 Measured and predicted barium or sulfate concentrations as a function of time for a) Mixture 10, b) Mixture 13, c) Mixture 14 and d) Mixture 15. Sulfate concentration was reported for Mixture 14 because its reduction is more significant compared to barium concentration.

4.4 SUMMARY AND CONCLUSIONS

Laboratory experiments conducted in this study demonstrated that the mixing ratio of flowback water and AMD is the key factor governing the sulfate concentration in the finished water. The acceptable sulfate concentration can be achieved by increasing the percentage of flowback water in the mixture.

Barite precipitation controls the fate of sulfate in these mixtures because celestite precipitation is very slow and most of the Sr removal occurs through coprecipitation with barite. Pure celestite precipitation will only occur if the mixture of flowback and AMD is supersaturated with respect to celestite after barite precipitation is completed. Although the celestite precipitation could result in additional sulfate removal, the slow reaction kinetics makes it irrelevant in full-scale waste treatment plants that typically have 1-2 hours of contact time.

An empirical kinetic model to predict sulfate concentration during the treatment process was developed in this study. The apparent reaction order and reaction rate constant were obtained by fitting the empirical model to a set of experimental results and the accuracy and limitations of this model were validated by the comparison of predicted and measured barium (or sulfate) concentrations as a function of time for the remaining experimental results. This model offers excellent prediction for the mixtures that incorporate low percentage of flowback water. When the flowback water accounts for over 50% in the mixture, the kinetic model is not applicable due to the inhibition of barite precipitation by lattice poisoning or ion-pair formation caused by other consitutents in the flowback water.

5.0 MICROFILTRATION IN RECYCLING OF MARCELLUS SHALE FLOWBACK WATER: SOLIDS REMOVAL AND POTENTIAL FOULING MECHANISM

This work has been published as:

He, C.; Wang, X.; Liu, W.; Barbot, E.; Vidic, R. D., Microfiltration in recycling of marcellus shale flowback water: Solids removal and potential fouling of polymeric microfiltration membranes. *Journal of Membrane Science* (2014), *462*, 88-95.

Flowback water generated during unconventional gas extraction is of great concern due to its high total dissolved solids (TDS), radioactive elements and organic matter. Abandoned mine drainage (AMD) is a water source that is often located in the vicinity of gas wells and can be mixed with flowback water to reduce fresh water usage for hydraulic fracturing. The feasibility of microfiltration to separate solids created by mixing actual flowback water and AMD was evaluated using a bench-scale setup. Hydrophilic polyvinyldiene fluoride (PVDF) membrane with a pore size of 0.22 μm was as a model polymeric microfiltration membrane.

Severe membrane fouling occurred during the first 5 minutes of filtration with one flowback/AMD mixture while no significant fouling was observed for a different mixture. It was found that the flowback water that caused membrane fouling contained stable iron-based colloids with an average particles size of 0.2 μm, especially in the samples collected early in the flowback period. These colloids were not formed by mixing flowback water containing high barium

concentration with AMD rich in sulfate but were originally present in the flowback water. Stability of these sub-micron colloidal particles at high ionic strength of the flowback water is attributed to organic coating on the particle surface.

5.1 INTRODUCTION

Natural gas contained in various shale formations around the world represents an important energy source that is projected to grow in the future. Recent report by the US Energy Information Administration indicated that over 860 trillion cubic feet (Tcf) of technically recoverable natural gas is available in the United States [1]. The Marcellus Shale formation that lies from upstate New York, as far south as Virginia, and as far west as Ohio, covering 70% of the surface of Pennsylvania is one of the largest shale gas reservoirs in the US with an estimated 262-500 tcf of natural gas reserves [2, 3].

Horizontal drilling and hydraulic fracturing are the key technologies that enabled economic recovery of this natural resource [4, 5]. Hydraulic fracturing involves injection of fracturing fluid and proppant under high pressure to create a network of fractures that allow gas trapped in the source rock to be released into the production casing of a gas well [6]. Water usage for hydraulic fracturing in Marcellus Shale ranges from 3 - 7 million gallons for a single well [7]. About 10% - 30% of the injected fracturing fluid returns to the surface during the first 10-14 days, which is defined as flowback water [8].

Flowback water contains chemicals that come from the fracturing fluid, such as diluted acids, biocides, viscosity modifiers, friction reducers and scale inhibitors, and those that come

from the formation water or dissolution of shale [9, 10]. The flowback water is typically impounded at the surface for subsequent disposal, treatment, or reuse. Due to the large water volume and high concentration of organic and inorganic constituents, there is growing public concern about management of flowback water. This concern results from the potential for human health and environmental impacts associated with the release of untreated or inadequately treated flowback water to the environment [11]. Flowback water management options in Marcellus Shale are confounded by high concentrations of total dissolved solids (TDS) and the lack of Class II underground injection control wells [8, 12]. Hence, the best management alternative for the flowback water in Marcellus Shale is its reuse for hydraulic fracturing of subsequent gas wells.

Abandoned mine drainage (AMD) is a potential water source that could alleviate low flowback water recovery by serving as a makeup water for the recycling and reuse of wastewaters in the Marcellus Shale region. AMD is particularly attractive water source due to its proximity to natural gas well sites [13]. In addition to serving as source water for hydraulic fracturing, AMD also provides source of sulfates that can be used to precipitate Ba, Sr, and Ca in the flowback water and reduce the potential for scale formation in the gas well [14]. Precipitates formed by the reaction of AMD with flowback water will have to be removed prior to water reuse in order to minimize the potential for porosity reduction of the proppant pack in the well [13]. Cross-flow ceramic membranes were evaluated for the removal of total suspended solid (TSS) in the flowback water from Marcellus Shale and it was found that 0.2 μm ceramic membrane was fouled faster compared with membrane that had larger pores (e.g., 0.8 μm and 1.4 μm) [15].

Particulate matter that is larger than 0.45 μm is relatively unimportant in fouling of microfiltration membranes [16]. The degree of membrane fouling by colloidal particles is dependent on the properties of colloidal particles (e.g., size, shape, chemical structure) and water quality (e.g., amount and type of electrolytes, pH, temperature, chemical additives) [17]. It is difficult for colloidal particles to remain stable in high salinity solution like flowback water since rapid aggregation would occur at high ionic strength conditions [18]. However, if the colloids are coated with organic material, such as natural organic matter (NOM) or manmade polymers, the stability of such colloidal dispersion would increase significantly [18], resulting in greater potential for membrane fouling.

Natural organic matter or manmade polymers that have high molecular weight and linear structure are likely to be effectively retained by the membrane and fill up the interstices between inorganic particles [19]. Chemical oxidation can be used to break down the organic coating on the particle surface as well as free organic matter in the flowback water, which would lead to aggregation of colloid particles when the steric-repulsion forces are reduced and reduce the potential for microfiltration membrane fouling [20].

The objective of this study was to evaluate the feasibility of using polymeric membrane microfiltration to assist in flowback water recycling and reuse program. Detail characterization of submicron particles that caused membrane fouling and the impact of pretreatment methods on permeate flux were analyzed to fully understand the mechanism of membrane fouling and develop solutions that could enable the use of membrane filtration in recycling of wastewater produced during unconventional gas extraction.

5.2 MATERIALS AND METHODS

5.2.1 Feed water

Chemical composition of flowback water varies with location and well completion practice [21]. Samples of Marcellus Shale flowback and produced waters were collected from three separate well sites located in southwestern Pennsylvania. All samples were individually stored in clean buckets and covered with lids. Geographic information and general water quality characteristics of flowback water samples used in this study are listed in Table 5.1. High TDS concentration in Flowback Water B is due to the fact that this well was fractured with reused flowback water, while the wells at Sites A and C were fractured with municipal water. Samples collected at different days from Sites A and B were stored individually and were used to prepare flow composite samples for each site (i.e., samples of the flowback water collected at different days were added to the composite sample in proportion to the flow rate on each day). As the flow rate of Flowback Water C was not available for each day when the samples were collected, its composite water sample was not studied.

Table 5.1 Location and characteristics of flowback water samples

Sample	Location	Description	TDS(mg/L)	TOC(mg/L)	Turbidity(NTU)
Flowback Water A	Westmoreland County, PA	Day 1	17785	4.9	68
		Day 5	54915	5.2	10
		Day 7	65521	6.9	8
Flowback Water B	Washington County, PA	Day 1	135564	19	15
		Day 3	155811	18.6	12
		Day 5	158406	11	10
Flowback Water C	Westmoreland County, PA	Day 1	1910	7.8	60
		Day 5	7440	8.2	17
		Day 7	93220	10.8	8

AMD 1 represents untreated discharge in the vicinity of Well A and AMD 2 represents a discharge in the vicinity of Well B that was treated in a passive water treatment system comprised of lime addition followed by aeration and sedimentation. Water quality characteristics of AMD and composite flowback water samples are shown in Table 5.2. Mixture 1 was prepared using 10% Flowback water A and 90% AMD 1, while Mixture 2 was prepared using 15% Flowback water B and 85% AMD 2. Mixing ratios were determined based on water recovery from these wells during the flowback period. Each mixture was allowed to react for at least 12 hours before filtration experiments to ensure chemical equilibrium during the filtration tests. Diluted flowback water and AMD samples were prepared by mixing them with DI water based on the mixing ratios listed above (e.g., diluted Flowback water A sample contained 10% Flowback Water A and 90% DI water).

Table 5.2 Characteristics of composite flowback water and AMD

	Flowback water A	AMD 1	Flowback water B	AMD 2
Na (mg/L)	11860	104.1	27946	687.31
Ca (mg/L)	2170	76.2	15021	244.65
Mg (mg/L)	249	49.1	1720	33.25
Fe (total) (mg/L)	-	32.1	-	ND
Ba (mg/L)	730.5	ND	236	ND
Sr (mg/L)	362	1.5	1799	3
Cl^- (mg/L)	29000	70.8	104300	373.4
SO_4^{2-} (mg/L)	-	708.7	14.8	242.5
TSS (mg/L)	98	118	776	1
TDS (mg/L)	38000	1328	166484	1574
Turbidity (NTU)	32	7.4	11	0.5
TOC (mg/L)	5.2	-	19.4	-
pH	7.42	6.14	6.40	7.03

Particle size distribution of suspended solids in composite flowback water samples A and B and in mixtures of flowback water and AMD was measured by Microtrac S3500 (Microtac, Inc., PA) and are shown in Figure 5.1. The dominant particle sizes for Flowback Water A and B samples were 30 and 23 μm, respectively while the dominant particle sizes for Mixtures 1 and 2 were 10 and 20 μm, respectively. Analysis of submicron particles was performed by first filtering the actual sample through 0.45 μm nylon membrane so that the permeate could be analyzed using dynamic light scattering (ALV/CGS-3 compact goniometer system, ALV-GmbH, Germany) at 90 degree angle. Several tests were performed and the one with the best correlation function was selected to determine size distribution of submicron particles using a built-in software package.

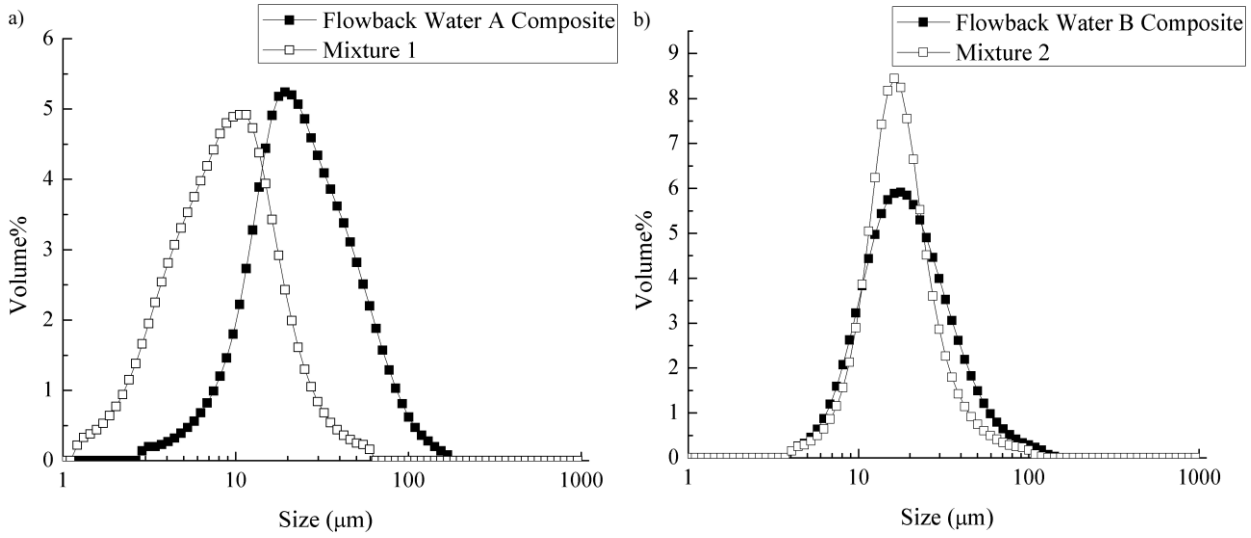

Figure 5.1 Particle size distribution of (a) Flowback Water A and Mixture 1 and (b) Flowback Water B and Mixture 2

5.2.2 Membrane filtration experiment

Membrane filtration experiments were conducted using magnetically stirred dead-end cell with 340 mL volume operated in a constant pressure mode. A 2.5 L feed tank was connected to the dead-end cell and was pressurized with compressed nitrogen to allow filtration of a larger suspension volume. The membrane filtration experiments were conducted using hydrophilic PVDF 0.22 μm microfiltration membranes with porosity of 70% (Durapore® Millipore, Billerica, MA). The membrane was cut into a circle with a diameter of 7.5 cm and was supported by a porous metal plate located at the bottom of the dead-end cell. Permeate was collected and weighed throughout the filtration test. For each membrane filtration experiment, new membrane was used after filtering 1L of deionized water to wet the membrane. All experiments were performed at room temperature (20 - 22°C) with a constant pressure of 0.5bar (7.2psi). The morphology of the membrane surface was inspected using Scanning Electron Microscopy (SEM, Philips XL30, FEI Co., Hillsboro, OR) and the elemental composition of selected samples was determined using Energy Dispersive X-ray Spectroscopy (EDX, EDAX Inc., Mahwah, NJ). Membrane samples were carefully removed from filtration unit and gently washed with DI water prior to EDX analysis.

5.2.3 Fouling mechanism identification

Experimental data can be used to determine which of the four fouling mechanisms control the permeate flux: 1) Cake filtration, 2) Intermediate blocking, 3) Standard blocking, and 4) Complete blocking [22]. The fouling mechanisms were identified using the approach developed by Ho and Zydney [22].

5.2.4 Stability evaluation

Stability of colloidal particles remaining in Day 1 samples of Flowback Water A and C after settling for 12 hours was evaluated as a function of ionic strength and oxidant addition. Ionic strength was adjusted to be identical to Day 1 sample of Flowback Water B (i.e., TDS around 120,000 mg/L) by the addition of NaCl and $CaCl_2$ and sample turbidity was measured every 12 hours for 7 days. In order to test the hypothesis that organic coating on the surface of submicron particles affects the stability of these particles, hydrogen peroxide (Fisher Scientific, PA) was added to Day 1 sample of Flowback Water A to oxidize organic coating and its turbidity was measured every 12 hours for 5 days.

5.3 RESULTS AND DISCUSSION

5.3.1 Membrane filtration of mixture of AMD and flowback water

Mixtures 1 and 2 were filtered using 0.22 μm PVDF membrane to evaluate the membrane fouling caused by the particles that would form after mixing AMD and flowback water. Variations in relative flux (J/J_0) with permeate volume for Mixtures 1 and 2 are compared with the variations in relative flux for diluted flowback water and AMD samples on Figure 5.2. As can be seen from this figure, Mixture 1 caused severe membrane fouling while Mixture 2 did not. Both AMD samples collected for this study exhibited limited membrane fouling, which suggests

that flowback water itself and/or barite particles formed after mixing of AMD and flowback water may be responsible for severe flux decline caused by Mixture 1.

The extent of membrane fouling caused by barite particles was evaluated by mixing AMD 1 samples with $BaCl_2$ solution (concentration of Ba was identical to that in the Flowback Water A). The flux decline was nearly identical to that observed when filtering AMD A alone, which suggests that barite particles created in the mixture had no impact on membrane fouling that occurred when filtering Mixture 1. Because the average particle size of barite formed after the addition of $BaCl_2$ to AMD is larger than 2-3 μm [23], this result is consistent with previous conclusion that particulate matter larger than 0.45 μm is relatively unimportant in fouling of microfiltration membranes [16]. Therefore, it is hypothesized that submicron particles contained in flowback water are the main reason for membrane fouling, since the overall particle size distribution of Mixture 1 and 2 were not that different as indicated on Figure 5.1. It can be seen from Figure 5.2 that the flux decline during filtration of diluted Flowback Water A was more severe compared with Mixture 1. Such behavior is likely due to removal of submicron particles by adsorption or co-precipitation with barite particles that were created by mixing Flowback Water A and AMD 1.

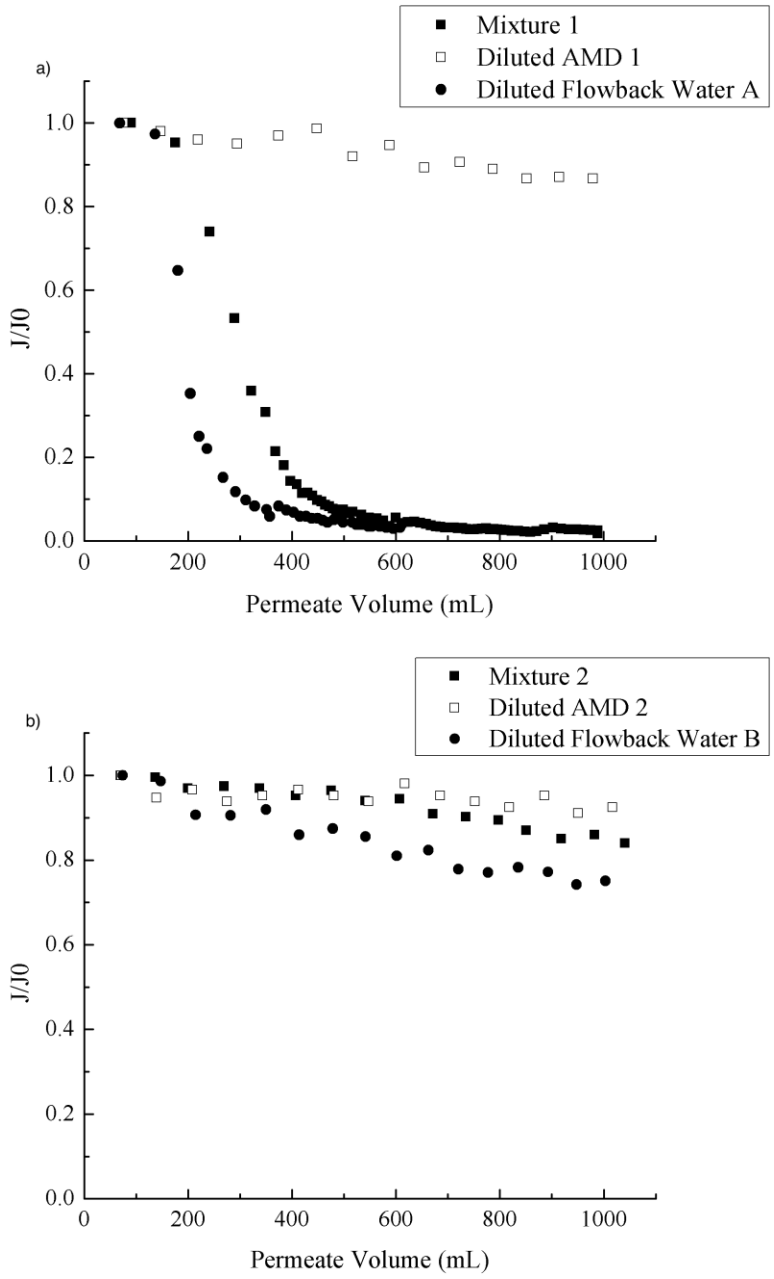

Figure 5.2 Relative flux as a function of permeate volume for filtration of (a) Mixture 1, diluted AMD 1 and Flowback Water A and (b) Mixture 2, diluted AMD 2 and diluted Flowback Water B

5.3.2 Membrane fouling analysis

Flowback water samples collected on different days and at different well sites, as well as composite Flowback Water A and B, were allowed to settle for 12 hours and the supernatant from each sample was diluted based on the flowback water recovery and used in membrane filtration experiment to investigate the extent of membrane fouling by colloidal particles remaining in each sample. Variation in relative permeate flux with permeate volume during the filtration of Flowback Water A, B and C shown in Figure 5.3 revealed that composite Flowback Water A caused much more severe fouling compared with composite Flowback Water B. In addition, water samples that were collected on the first day of the flowback period caused more severe membrane fouling compared with samples collected on later days. Filtration results for Flowback Water A and C exhibited very fast permeate flux decline, while Flowback Water B that was collected from another county had a gradual permeate flux decline. Therefore, the potential of flowback water to foul 0.22 μm PVDF membrane is likely dependent on the location of the unconventional gas well.

SEM image of membrane surface after filtration of diluted composite Flowback Water A is shown on Figure 5.4. As can be seen from this figure, a cluster of densely packed small particles formed a cake layer on the membrane surface. Membrane drying in preparation for SEM analysis resulted in the crack in Figure 5.4, which indicates the thickness of the cake of about 1 μm [24]. Densely packed cake layer with low porosity is the result of high ionic strength of the flowback water that leads to a decrease in Debye length of the charged particles and enables close packing of these particles [25-27].

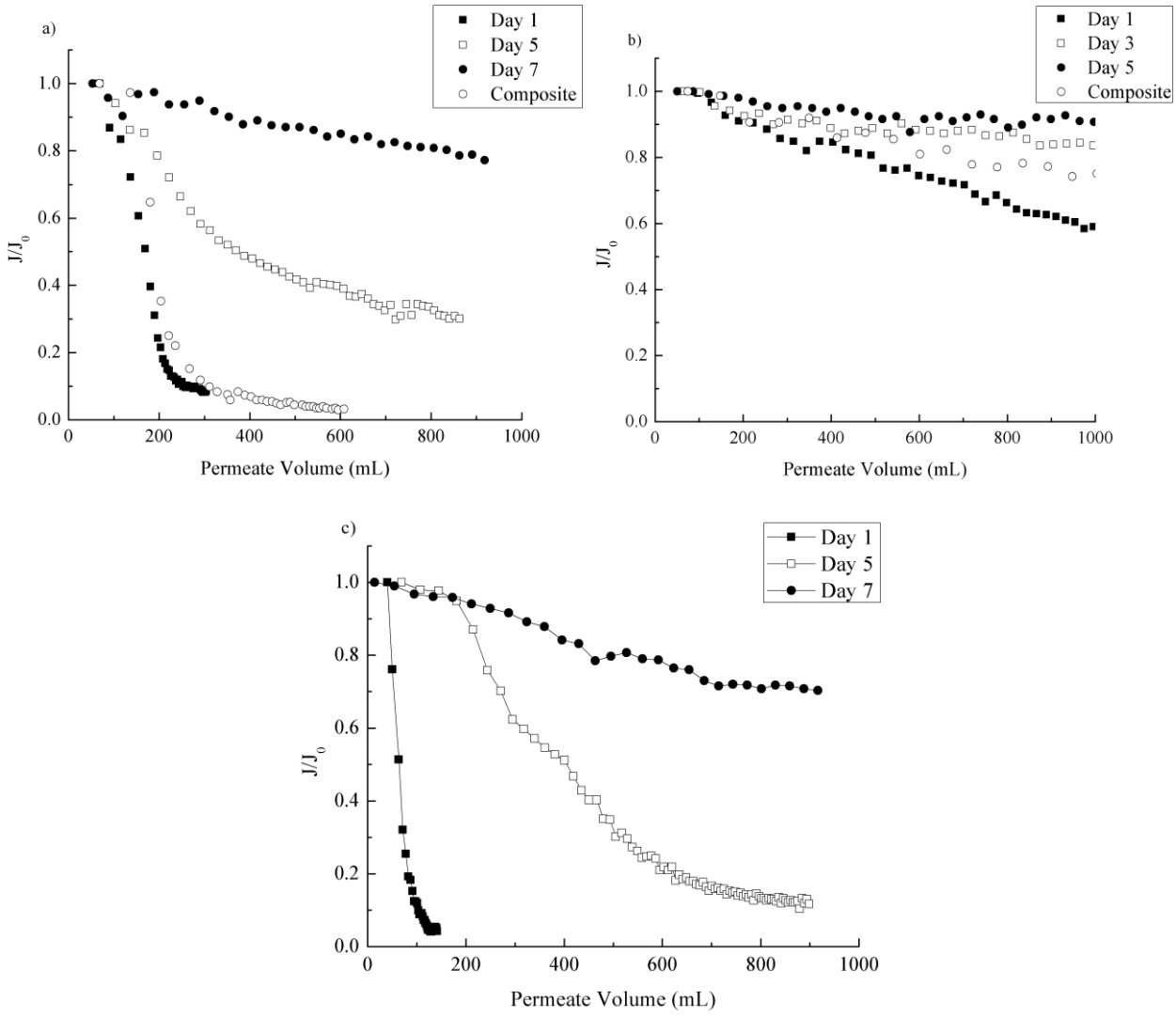

Figure 5.3 Variation of permeate flux with permeate volume for flowback water samples collected on different days as well as flow composite sample after settling for 12 hours: (a) Flowback water A; (b) Flowback water B; and (c) Flowback Water C.

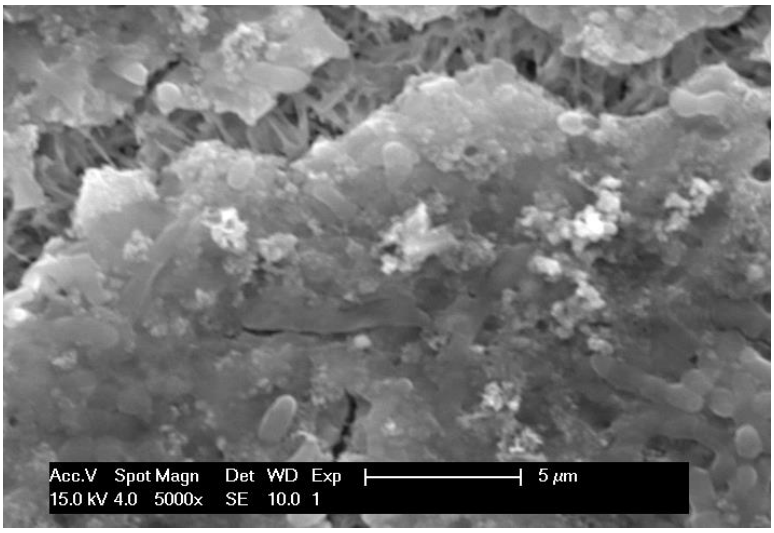

Figure 5.4 SEM image of the cake layer on PVDF membrane after filtration of composite Flowback Water A.

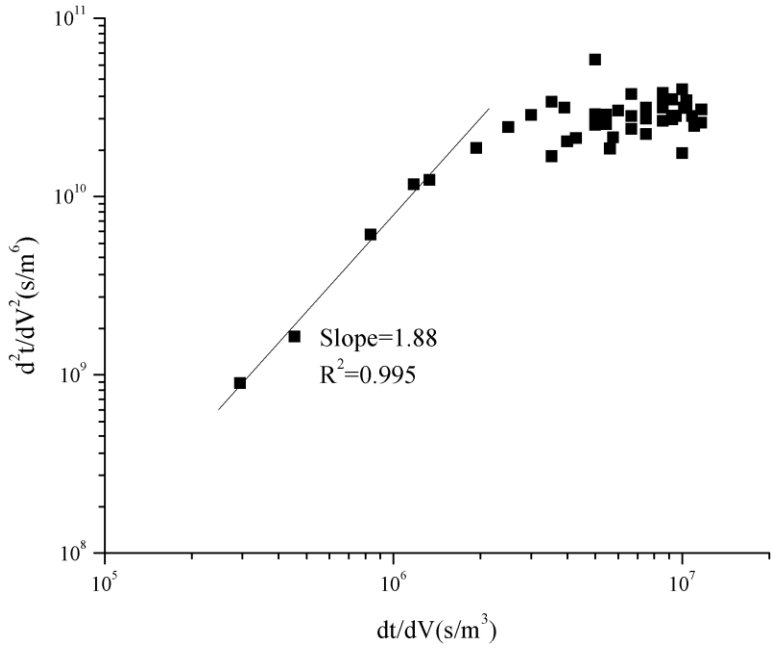

Figure 5.5 Fouling mechanism identification according to the approach developed by Ho and Zydney [22].

The fouling mechanism identification approach reported by Ho and Zydney [22] was applied to determine the type of fouling caused by the pre-settled composite Flowback Water A sample. The results shown in Figure 5.5 indicate a linear relationship during the early stage of the filtration experiment (i.e., low dt/dV) with the slope of 1.88 (R^2=0.995). Such behavior clearly indicates pore blockage as the dominant membrane fouling mechanism. During the later stage of the filtration experiment, the data on Figure 5.5 exhibit a plateau (i.e., the d^2t/dV^2 becomes constant as its slope equals zero), which indicates that the membrane fouling is governed by cake formation. The membrane fouling identified by this analysis further supports the hypothesis that submicron particles present in the original flowback water are mostly responsible for severe microfiltration membrane fouling.

In order to identify the elemental composition of the submicron particles contained in Flowback Water A, Day 1 sample of this water was first filtered through 0.45 μm nylon membrane. The permeate was then filtered through 0.05 μm membrane and the elemental composition of submicron particles collected on 0.05 μm membrane was analyzed using EDX. Typical EDX spectrum of these submicron particles is shown on Figure 5.6. High carbon peak is due to 0.05 μm membrane that is made of polyacrylonitrile. Based on the EDX measurement at three different locations on the membrane, final elemental composition (excluding carbon) is shown on Figure 5.7. These results indicate that the submicron particles are mainly comprised of iron oxide.

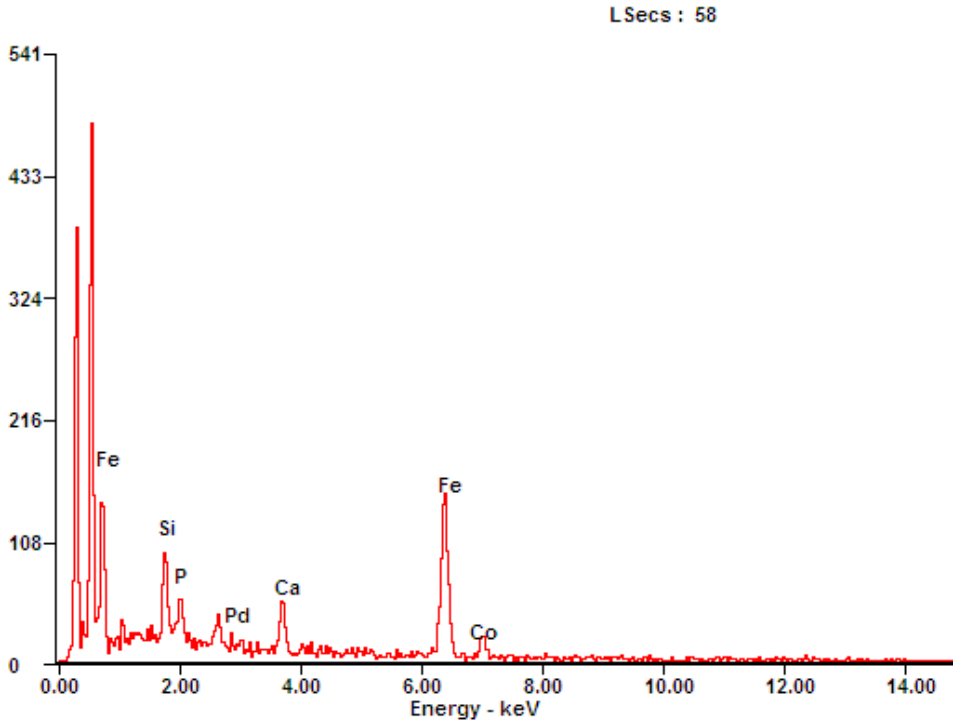

Figure 5.6 EDX spectra of submicron particles collected on the surface 0.05 µm membrane from Flowback Water A collected on Day 1 (raw sample was first filtered using 0.45 µm membrane).

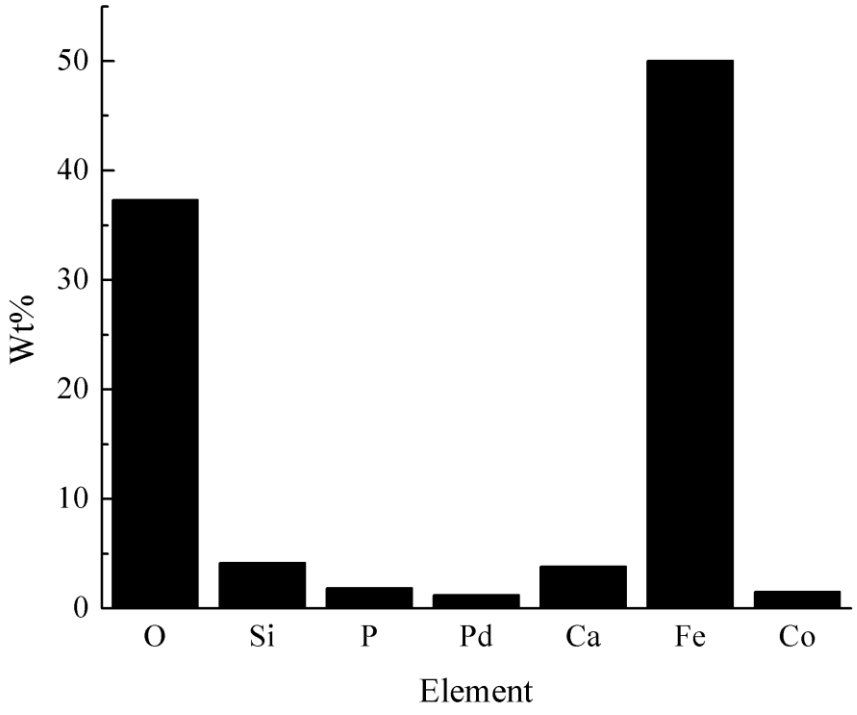

Figure 5.7 Average elemental composition of submicron particles excluding carbon.

Particle size distribution of colloids remaining in the supernatant of the Flowback Water A collected on Day 1 and Day 5 after settling for 12 hours was measured using the ALV dynamic light scattering (DLS) instrument. The results shown in Figure 5.8 indicate that the particles in Day 1 sample of Flowback Water A had a mean particle size of 0.22μm, which is close to membrane pore size. On the other hand, Day 5 sample of Flowback Water A contained particles that were much larger in size with a mean particle size of about 2 μm. Similar results were observed for Flowback Water C (data not shown). Particle size distribution results shown on Figure 5.8 are consistent with the fact that the Day 1 sample of Flowback Water A caused severe membrane fouling, while Day 5 sample caused much less fouling (Figure 5.3a). These results support the hypothesis that the existence of submicron particles in the samples collected during the initial flowback period is the main reason for membrane fouling. Submicron particles in Flowback Water B were below the DLS detection limit, which is consistent with the observation of limited membrane fouling with composite Flowback Water B sample.

It is known that organic matter may contribute to membrane fouling [28]. Although the TOC in Flowback Water B was three times that in Flowback Water A, it caused significantly less fouling compared with Flowback Water A. In addition, salinity and TSS of Flowback Water B are 4 and 8 times that of Flowback Water A but membrane fouling by Flowback Water A was much more severe than by Flowback Water B. Thus, it can be concluded that sub-micron particles in Flowback Water A play a much more important role in membrane fouling when compared to other water quality parameters.

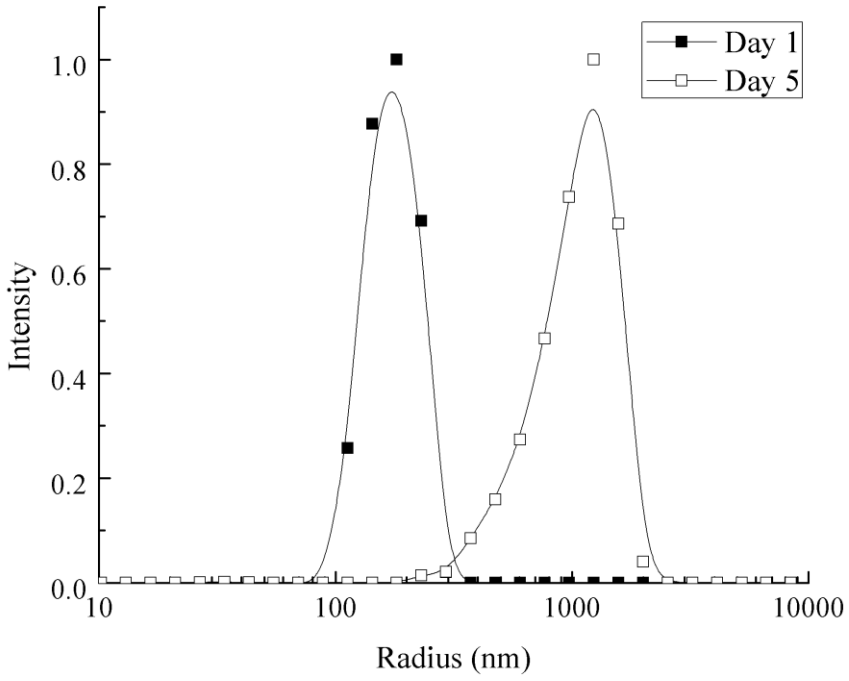

Figure 5.8 Submicron Particle Size Distribution of Flowback Water A. Flowback water samples were allowed to settle for 12 hours to remove large particles

5.3.3 Stability of colloidal suspension

Because stable submicron particles exhibited profound influence on membrane fouling, it is very important to understand the cause of stability of these colloidal suspensions, particularly considering that high ionic strength would normally lead to rapid particle aggregation [18, 29]. Submicron particles that caused severe membrane fouling were only found to be stable in the early samples of Flowback Water A and C, while the later samples did not contain such stable particles. In addition, Flowback Water B samples, which had much higher ionic strength, did not contain measurable concentration of submicron colloidal particles.

Day 1 samples of Flowback Water A and C were selected to investigate the colloid stability under high ionic strength by adjusting Na^+ and Ca^{2+} to the level found in Day 1 sample

of Flowback Water B (i.e., TDS of around 120,000 mg/L). In essence, TDS in Day 1 sample of Flowback Water A and C were elevated more than 7 times compared to their original values. Increase in the ionic strength of solution typically results in lower electrostatic force between particles and should lead to aggregation of small particles. As the aggregates are allowed to settle, a decrease in supernatant turbidity should be observed.

Analysis of turbidity and particle size distribution in Day 1 samples of Flowback Water A and C every 12 hours for seven days after ionic strength adjustment revealed that destabilization of the colloidal suspension did not occur (data not shown). It is hypothesized that the stability of these submicron particles is due to organic matter coating on the particle surface. Based on extended DLVO theory, which takes steric repulsion forces into consideration for particle-particle interactions, once polymer or NOM is coated on particle surface, repulsion forces between particles are largely increased, thereby increasing the stability of coated colloidal or nano-sized particles [18, 30, 31]. Scaling inhibitors and friction reducers, which are injected together with hydrofracturing water [32-34], as well as natural organic matter from the shale matrix could be responsible for such behavior [9].

To test this hypothesis, treatment with hydrogen peroxide was performed to oxidize organic coating on particle surfaces. After adding 1% hydrogen peroxide to Day 1 smaple of Flowback Water A, turbidity of the solution was measured every 12 hours for 5 days. The results in Figure 5.9 compare the turbidity of hydrogen peroxide treated solution together with turbidity in the control sample that did not receive hydrogen peroxide treatment. The turbidity of the treated sample initially increased to 81 NTU, followed by destabilization of the dispersion as indicated by visual observation of large aggregates in the reactor. Aggregation of submicron particles resulted in relatively rapid settling and reduction in sample turbidity to 2 NTU. The

results of filtration experiment with H_2O_2 treated Day 1 sample of Flowback Water A are compared to the results of the filtration experiment with untreated Day 1 sample of Flowback Water A in Figure 5.10. The data shown on Figure 5.10 confirm that the submicron particles are responsible for the severe flux decline for Flowback Water samples and that the stability of these submicron particles at very high ionic strength is due to the organic coatings.

The removal of the organic coating by oxidation leads to rapid agglomeration of these submicron particles and eliminates severe membrane fouling observed for some flowback water samples. Future studies should focus on the origin and characteristics of this organic coating and optimal treatment approached of its removal.

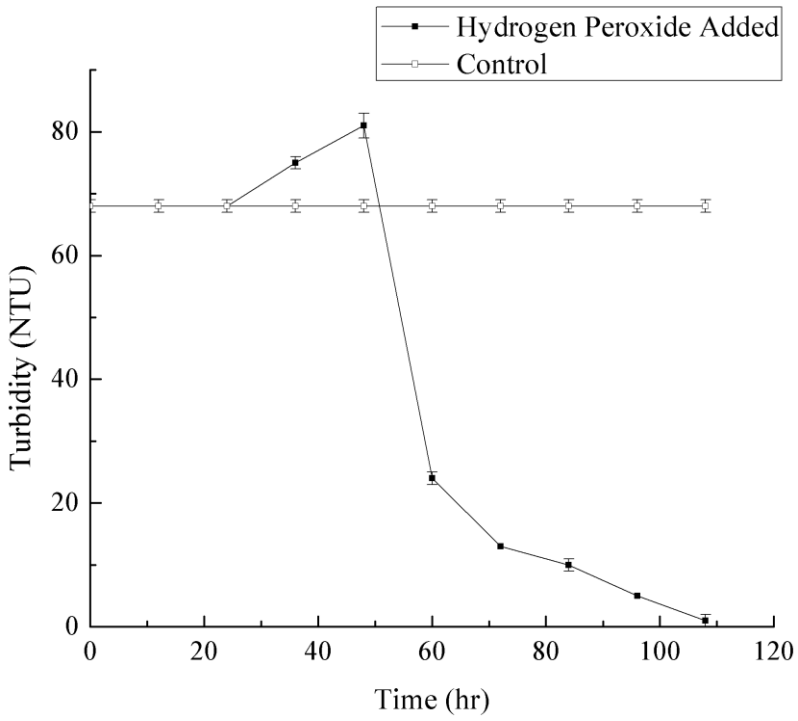

Figure 5.9 Turbidity variation of Day 1 Flowback Water A sample after adding 1% hydrogen peroxide

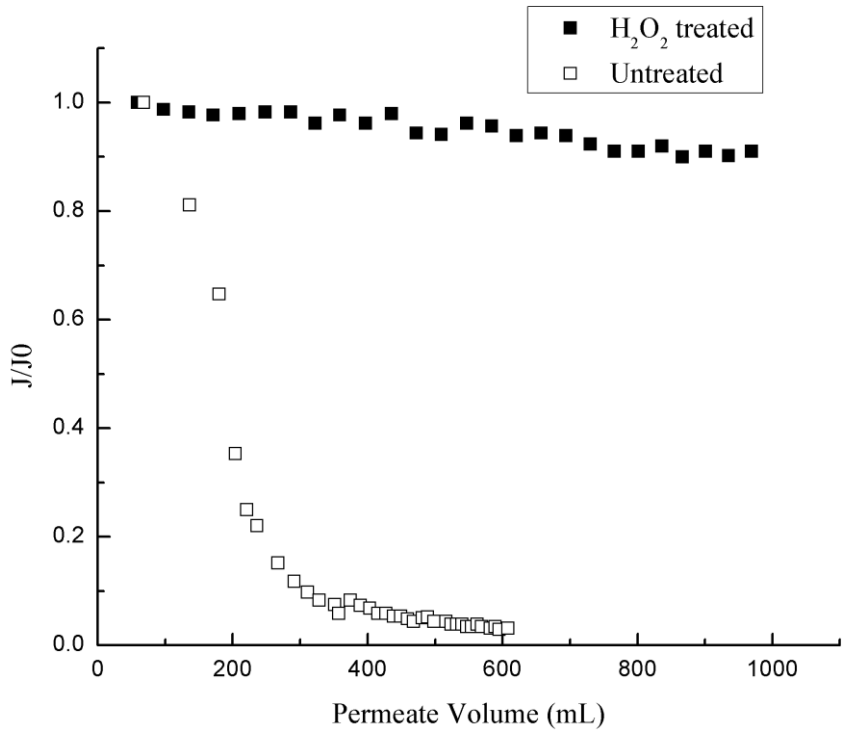

Figure 5.10 Flux decline for H_2O_2 treated and untreated Day 1 sample of Flowback Water A

5.4 SUMMARY AND CONCLUSIONS

A bench-scale dead-end microfiltration unit was used in this study to evaluate microfiltration for treatment of Marcellus shale flowback water to enable its reuse for hydraulic fracturing. In addition, AMD that is located in the vicinity of gas wells was evaluated as a potential make-up water source to reduce the fresh water use for hydraulic fracturing.

Mixing of AMD and flowback water results in the formation of barite solids that need to be removed prior to injection of this solution in the gas well to minimize the potential for well plugging. This study revealed that neither AMD nor barite formed in solution after mixing these two waters caused membrane fouling but that submicron particles present in some flowback waters can cause severe fouling of 0.22 μm PVDF membrane. Severe microfiltration membrane

fouling was observed for two out of three flowback water samples evaluated in this study. Both flowback water samples that caused severe membrane fouling contained submicron particles with a peak particle size close to the average membrane pore size. Analysis of filtration results revealed that complete blocking is the dominant fouling mechanism during the initial stages of filtration with subsequent cake layer formation contributing to the flux decline in the later stages of filtration.

Stable colloids that contributed to severe membrane fouling were only found in water samples collected in the first few days of the flowback period. EDX analysis revealed that these submicron particles are mainly comprised of iron oxide. The stability of submicron particles at very high ionic strength is due to organic coating of these particles. Removal of this organic layer by oxidation leads to particle aggregation and reduction in membrane fouling.

6.0 APPLICATION OF MICROFILTRATION FOR THE TREATMENT OF MARCELLUS SHALE FLOWBACK WATER: INFLUENCE OF FLOC BREAKAGE ON MEMBRANE FOULING

Management of Marcellus Shale flowback water is a rising concern in Pennsylvania. Due to limited capacity for wastewater disposal by deep well injection, flowback water reuse is the dominant management option in PA. Microfiltration is a promising technology to be used in a mobile treatment system for solids removal from Marcellus Shale flowback water prior to reuse. It was found previously that early Marcellus shale flowback water could cause severe membrane fouling due to the presence of stable submicron colloids. Bench-scale cross-flow filtration system was used in this study to evaluate feasibility of microfiltration for treatment of Marcellus Shale flowback water that does not contain these submicron colloids. The performance of alumina (Al_2O_3) and silicon carbide (SiC) ceramic membranes that have distinct surface charge properties was evaluated in this system using a constant transmembrane pressure. The difference in the isoelectric point of theses membranes suggested possible difference in fouling behavior, but extremely high salinity of the flowback water nullified these differences.

For the two flowback waters tested in this study, the one with lower TDS caused more severe fouling of both SiC and Al_2O_3 membranes during the first 15min of filtration. The flux decline analysis revealed that intermediate pore blocking was the dominant fouling mechanism in the early stage. Such behavior was due to the fact that the particulate matter in this flowback

water was in aggregate form and the flocs were prone to breakup at elevated shear stress caused by high pumping rate. Despite having much higher TSS, the other flowback water did not cause excessive membrane fouling due to stability and strength of its original particles.

6.1 INTRODUCTION

The recent development of unconventional natural gas resource in Marcellus Shale play led to significant public concern about the environmental challenges associated with the wastewater management [1-3]. Generally, 10 - 30% of the hydraulic fracturing fluid is recovered after 2 weeks of well completion, which is referred to flowback water. Due to the rock-water interaction and mixing of fracturing fluid and formation brine, flowback water typically contains high levels of total dissolved solids, toxic metals and radioactive elements [4, 5]. The disposal of this wastewater to publicly owned treatment works (POTWs) in the early phase of shale gas development in Pennsylvania elevated salt concentration in receiving waterways, because the treatment in POTWs does not remove total dissolved solids (TDS) from the feed stream [6, 7]. Very high TDS levels in Marcellus Shale flowback water limits the choice of desalination technologies. Reverse osmosis that is generally used for desalination of seawater is not feasible for flowback water treatment, and energy intensive thermal desalination processes would have to be used [3]. While forward osmosis and membrane distillation are two promising membrane technologies for treatment of flowback water, full-scale treatment systems are still not available[8]. Because of limited capacity for wastewater disposal by deep-well injection in Pennsylvania, flowback water reuse for hydraulic fracturing is the dominant management option [2, 3, 9].

Prior to reuse, flowback water is typically treated on-site to remove suspended solids or sent to a centralized wastewater treatment (CWT) plant that is equipped to remove specific constituents that may not be compatible with fracturing fluid chemistry [2, 4]. Microfiltration (MF) membrane unit with a small footprint is well-suited for a mobile system that can be used for on-site treatment of flowback water. It can also potentially be used in the CWT plant to separate particulates in the flowback water or those that are formed during treatment.

However, membrane fouling is the limiting factor for the wide application of microfiltration for flowback water treatment. Jiang et al. studied the use of ceramic microfiltration membrane for the removal of total suspended solids and observed severe fouling of both 0.2 μm and 0.8 μm membranes. He et al. evaluated the mechanisms that are responsible for severe fouling of polyvinyldiene fluoride (PVDF) membrane by flowback water and revealed that the submicron particles that are sometimes present in early flowback water will cause rapid flux decline through complete blocking mechanism [10]. Milier et al. increased the fouling resistance of polysulfone membrane to oil fraction by coating polydopamine-g-poly(ethylene glycol) to increase the surface hydrophilicity [11], but did not address fouling caused by the particulate fraction.

Membrane fouling decreases with an increase in particle size and becomes relatively insignificant when filtrating particles larger than 1 μm [10, 12]. MF membrane can be potentially used for direct filtration of the flowback water that does not contain submicron particles. However, considering high TDS level in the flowback water, the particulate matter may be present in aggregate form due to electric double layer compression. Breakup of these aggregates into fine particles at elevated shear conditions in the membrane module can result in increased

cake layer resistance [13]. This study focuses on feasibility of using ceramic MF membranes to remove solids from Marcellus Shale flowback water.

Ceramic membrane technology is rapidly emerging and has been applied to various fields, including water and wastewater treatment, food processing, bioreactor processes [14-16]. In comparison to conventional polymeric membranes, ceramic membranes have much better thermal stability, resistance to chemical corrosion and mechanical strength [17, 18]. These unique properties allow aggressive chemical cleaning to remove the irreversible fouling and eliminate need for replacement that is common for polymeric membranes. Recently developed silicon carbide (SiC) membranes feature low isoelectric point (pH=2.6) and high hydrophilicity, which may explain greater fouling resistance compared to other ceramic membranes [19].

This study was designed to evaluate the performance of two ceramic MF membranes (i.e., SiC and Al_2O_3) for treatment of Marcellus Shale flowback water, with particular emphasis on the influence of floc breakage on membrane fouling.

6.2 MATERIALS AND METHODS

6.2.1 Characteristics of flowback water

Characteristics of flowback water are dependent on well location and completion practice[20]. Early flowback water can possibly contain submicron particles, which is a key concern for fouling of microfiltration membranes [10]. Marcellus Shale flowback waters collected from two separate well sites were used in this study. Samples were delivered in sealed buckets and stored in the laboratory at room temperature. The quality of these two flowback waters is summarized in Table 6.1. Flowback water samples for this study were collected during later stages to avoid stable colloidal particles.

Table 6.1 Characteristics of Flowback Water Samples

	Flowback Water A	Flowback Water B
TDS (mg/L)	158,406	308,334
TOC (mg/L)	11	ND
TSS (mg/L)	754	1,520
Na (mg/L)	40,339	81,442
Ca (mg/L)	15,269	32,901
Mg (mg/L)	1,632	3,513
Ba (mg/L)	253	6,256
Sr (mg/L)	1,832	11,910
Cl (mg/L)	107,315	188,728
pH	6.1	3.9

6.2.2 Filtration experiments

The filtration experiments were conducted in a bench scale cross-flow membrane filtration unit. The schematic diagram and detail description of this system was reported elsewhere and will not be repeated here [14]. The major units of system include a 15-L feed tank, a centrifugal pump, a vertical membrane module, a heat exchanger, an in-line flow meter and three pressure gauges.

Membralox® α-Al_2O_3 membrane with pore size of 0.2 μm and α-SiC membranes with pore size of 0.25 μm were provided by Pall Corporation (Port Washington, USA) and Saint-Gobain (Courbevoie, France), respectively. General information about the ceramic membranes used in this study is summarized in Table 6.2.

Table 6.2 Description of the ceramic membranes used in this study

Composition	Pore Size (μm)	Surface Area (cm^2)	Isoelectric point
α-SiC	0.25	39	2.6 [21]
α-Al_2O_3	0.2	55	8.5 [22]

All the cross-flow filtration experiments were conducted at a constant transmembrane pressure of 10 psi and flow rate of 2 GPM. The temperature was controlled at 20-21 °C by running cooling water through the heat exchanger to counteract heat generated by the pump. Initial tests with tap water were conducted to establish the baseline permeate flux and to fully wet membrane pores. Filtration tests with flowback water sample started after the tap water was completely drained from the system. Permeate was returned to the feed tank throughout the filtration experiment to maintain the constant composition of the feed solution.

Dead-end filtration system was used to evaluate the influence of shear-induced floc breakage on membrane fouling. Schematic diagram and description of the dead-end system was reported previously [10]. Feed solution was blended with a six-paddle jar tester (PB-700, Phipps & Bird, Richmond, VA) at desired mixing speed for 30 min before the filtration tests with Durapore® hydrophilic PVDF membranes with 0.22 μm pore size (Milipore, Billerica, USA). A new membrane was used for each experiment and it was pre-conditioned by filtering 1L of DI water. The dead-end filtration tests were conducted at room temperature with a constant pressure of 50 kPa.

6.2.3 Membrane cleaning procedure

Ceramic membrane cleaning procedure was initiated by draining the feed solution from the system and flushing several times with tap water for 10 min until the water was visually clean. The cooling line was then disconnected and temperature was allowed to gradually increase to 60 °C, while recirculating surfactant (commercial soap), 1% NaOH and 1,000 ppm NaOCl, 2% nitric acid solutions in the system for 2 hr, 1 hr and 1 hr, respectively. Tap water was used to rinse the system after cleaning with each reagent until the turbidity of the drainage was below 2 NTU and pH was neutral. At the end of acid washing, the permeate valve was opened for 5 min to clean the permeate side of the system.

6.2.4 Fouling mechanism modeling

Hermia developed a common mathematical equation to describe the four fouling mechanisms (i.e., complete, standard, intermediate pore blocking and cake layer formation) for dead-end filtration operated at constant filtration pressure [23]:

$$\frac{d^2t}{dV^2} = k\left(\frac{dt}{dV}\right)^n \tag{6-1}$$

where, t is the filtration time, V is the cumulative permeate volume, k is the kinetic parameter and the exponent n is the indicator of the fouling mode (n=0,1,1.5 and 2 corresponds to cake layer filtration, intermediate, standard and compete pore blocking, respectively).

Although this model cannot describe the effect of shear force, it is often used to fit the flux decline data from cross-flow filtration or stirred dead-end filtration due to the limitation of available model [24-26]. Ho and Zydney proposed an approach for flux data analysis by rewriting the two derivative components as Equation 6-2 and 6-3, and plotting the data as d^2t/dV^2 vs. dt/dV [27].

$$\frac{dt}{dV} = \frac{1}{JA} \tag{6-2}$$

$$\frac{d^2t}{dV^2} = -\frac{1}{J^3A^2}\frac{dJ}{dt} \tag{6-3}$$

where, A is the membrane surface area and J is the permeate flux.

6.2.5 Characterization of floc strength

Shear-based floc strength model proposed by Parker et al. was used to quantify the stability of the particulate matter contained in flowback water at elevated shear conditions (Equation 6-4) [28]:

$$d = CG^{-\gamma} \tag{6-4}$$

where, d is the floc diameter, C is the floc-strength coefficient, G is the average velocity gradient and γ is the stable floc size constant that describes the resistance of flocs to shear-induced breakage, which is considered as an indicator of floc strength. Higher γ values indicate that the floc is more prone to breakup into small particle with the increase in shear rate. In this study, γ was obtained using 95-percentile floc size (d_{95}) [28] as a function of average velocity gradient using Equation (6-5).

$$logd_{95} = logC - \gamma logG \tag{6-5}$$

Floc breakage experiments were carried out using PB-700 jar tester. The flowback water samples were mixed at preselected speeds for 30 min, and 1mL sample was diluted with 100 mL DI water and deposited evenly on 0.45 μm nylon membrane by filtration. After the membrane was air-dried, the particle size was measured using Axio A1 microscope (Zeiss, Germany) fitted with a Canon Powershot A620 camera with halogen light source. Particle size was determined from image analysis with axioVision LE 4.5 software.

6.3 RESULTS AND DISCUSSION

6.3.1 Cross-flow filtration experiments

Variations in normalized permeate flux (J/J_0) with time for SiC and Al_2O_3 membranes treating Flowback Waters A and B are shown in Figure 6.1. Flowback Water A caused severe fouling of both SiC and Al_2O_3 membranes (Figure 6.1a) as evidenced by rapid flux decline during the first 15 min of the experiment. The permeate flux with SiC membrane was essentially stabilized towards the end of the filtration test, while the permeate flux with Al_2O_3 membrane experienced a decline throughout the entire experiment. Figure 6.1b reveals that the membrane fouling caused by Flowback Water B was much less pronounced compared to fouling caused by Flowback Water A.

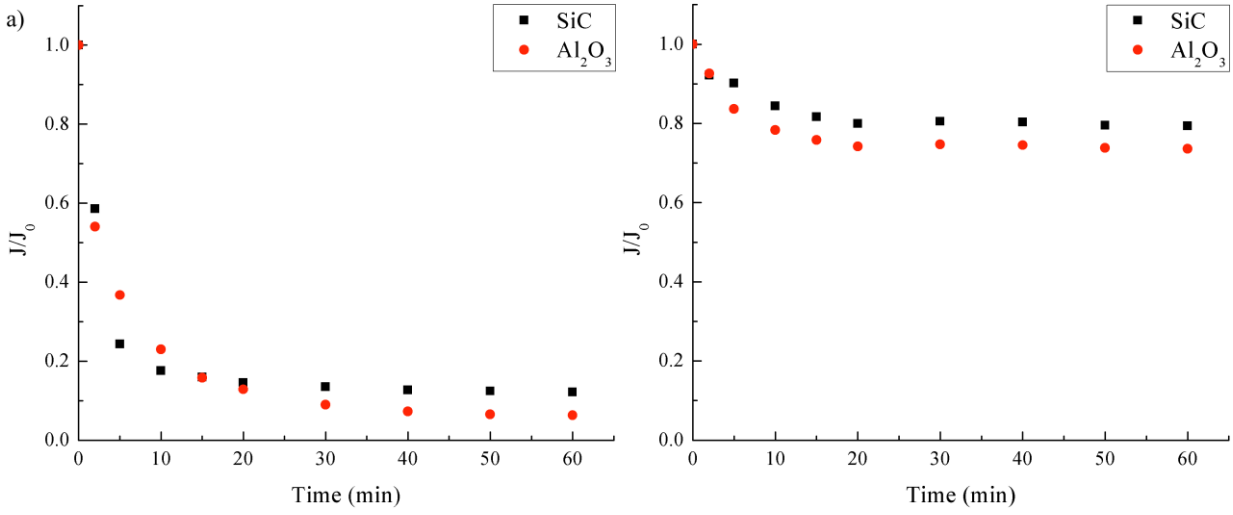

Figure 6.1 Variation of normalized permeate flux during filtration of (a) Flowback Water A and (b) Flowback Water B using SiC and Al_2O_3 membrane

While SiC has unique surface charge characteristics in terms of the isoelectric point, it exhibited limited improvement in fouling resistance caused by Flowback Water A. Particle-membrane interaction controlled by physicochemical properties of the feed solution (i.e., pH and ionic strength) generally have a great impact on membrane fouling behavior [12, 29]. Because the pH of Flowback Water A is between the isoelectric point of SiC (~2.6) and Al_2O_3 (~8.5) membranes, distinct electrostatic interactions (i.e., repulsive vs. attractive) between the membrane surface and the particles were expected to lead to different fouling behaviors. However, this was not the case as indicated by similar flux decline profiles in Figure 6.1a. Therefore, it can be concluded that electrostatic interactions were screened by the high concentration of dissolved salts in flowback water. This result suggests that the surface charge of the membrane is not an important factor in fouling resistance of microfiltration membranes treating flowback water.

He et al. reported that the low concentration of organics in flowback water had minimal impact on microfiltration membrane fouling and that densely packed cake layer of fine organic-coated iron oxide particles at high TDS level was the key reason for severe fouling of polymeric microfiltration membrane [10]. While the submicron particles were absent from the flowback water samples selected for this study, colloids could possibly be released from the particulate matter. Tombacz et al. reported that iron oxide and clay mineral could easily aggregate at ionic strength above 0.1M [30]. Kim et al. demonstrated that pump-induced shear stress caused breakage of microbial flocs, resulting in rapid permeate flux decline for microfiltration and ultrafiltration membranes [31]. Considering the high TDS of Marcellus Shale flowback water, it is very likely that the particulate matter in this water is comprised of aggregates, which can potentially break into fine particles when exposed to high shear stress.

Visual observation of Flowback Water A before and after recirculating in the cross-flow membrane filtration system is shown in Figure 6.2. The suspended particles in raw Flowback Water A settled much faster compared to recirculated Flowback Water A. This behavior suggests that breakage of aggregates originally present in Flowback Water A occurred in the cross-flow filtration system. No such behavior was observed for Flowback Water B.

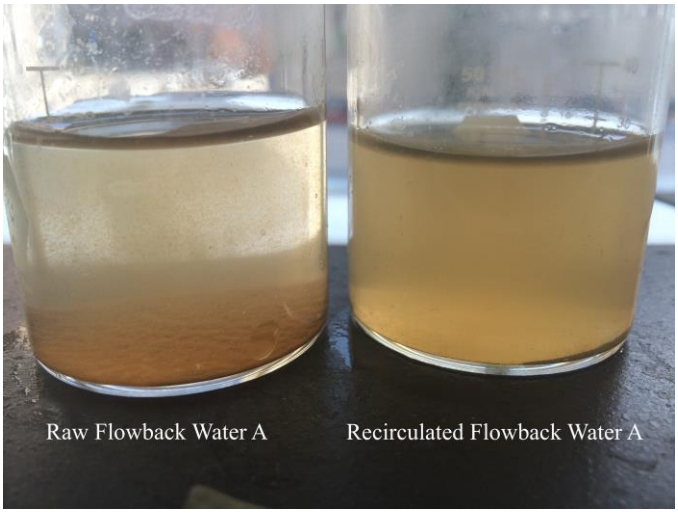

Figure 6.2 Appearance of raw (left) and recirculated (right) Flowback Water A after settling for 10 min.

6.3.2 Fouling mechanism identification

The identification of fouling mechanism during cross-flow filtration of Flowback Water A was evaluated by plotting the permeate flux using Equations 6-2 and 6-3. The linear relationship with the slope of approximately 1 during early stage of cross-flow filtration experiments (i.e., low dt/dV) shown in Figure 6.3 indicates that the intermediate pore blockage is the dominant fouling mechanism for both membranes. The intermediate pore blocking mechanism is characterized by either foulant deposition on the preformed cake layer or directly on membrane pores. Several

studies found that intermediate pore blocking was the dominate fouling mechanism during microfiltration of coagulated water [32, 33] . The duration of intermediate pore blocking is approximately 30 min for Al_2O_3 membrane while only 10 min for SiC membrane. The shorter intermediate pore blocking time observed for SiC membrane is consistent with achieving steady state permeate earlier and slightly less severe fouling when compared with Al_2O_3 membrane (Figure 6.1). Negative slope after the peak value in Figure 6.3 was observed for both membranes and indicates more rapid reduction of the permeate flux decline rate (dJ/dt) than the permeate flux itself. This is not uncommon for the cross-flow filtration or dead-end filtration with stirred cell and is generally considered a transition phase between pore blocking and cake layer filtration[27, 34]. The absence of a plateau of the filtration experiment at the later stage in Figure 6.3 suggests that the cake layer formation was not fully achieved. Yuan et al. found that while stirring-induced shear force had no influence on the fouling mechanism at the initial filtration stage, it affected the transition from pore blocking to cake layer filtration as indicated by the continuous decrease in d^2t/dV^2 after reaching the maximum [35]. Such behavior is likely due to the influence of shear force on the formation and subsequent growth of cake layer.

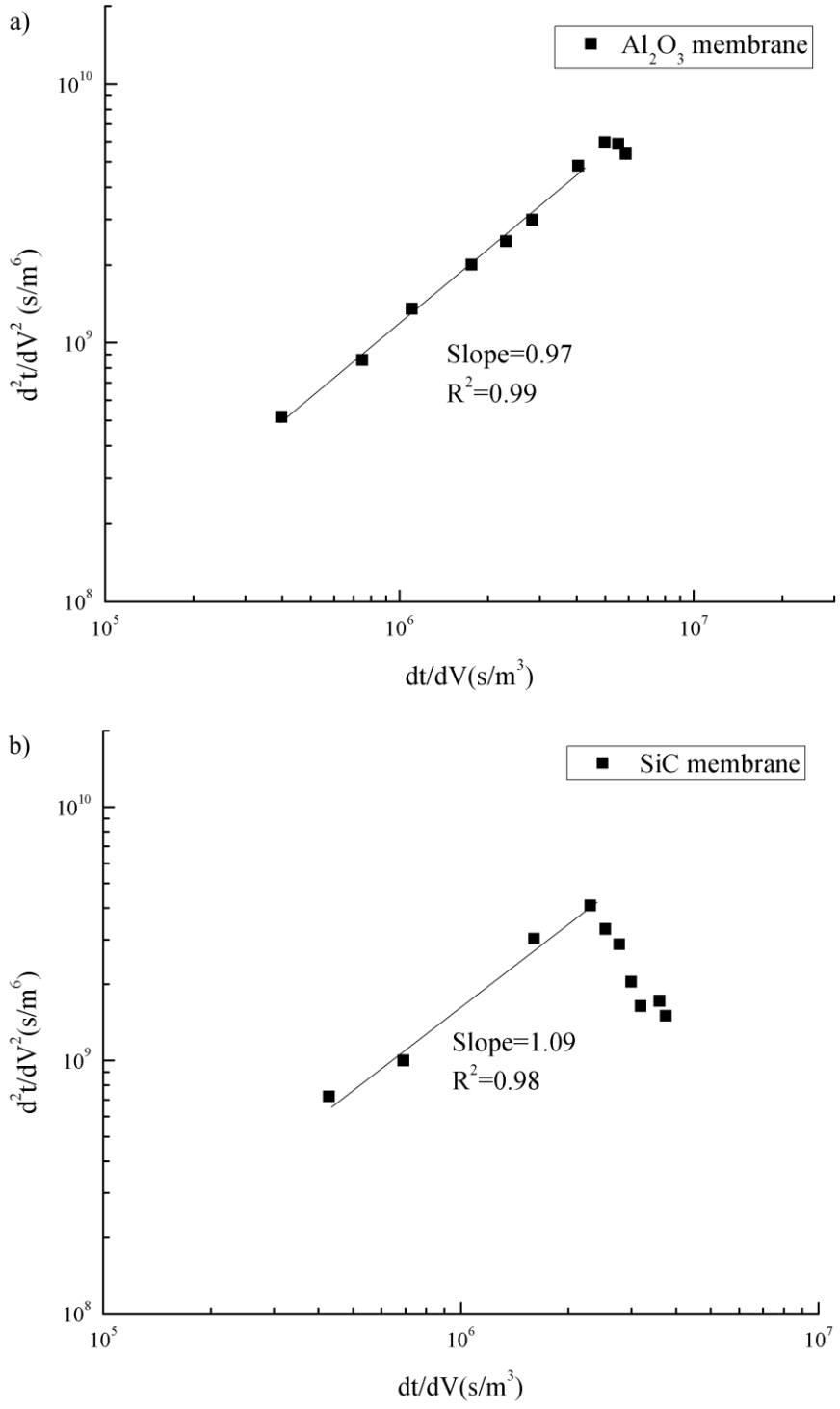

Figure 6.3 Fouling mechanism identification for the filtration of Flowback Water A with (a) Al_2O_3 and (b) SiC membrane

6.3.3 Impact of floc breakage on membrane fouling

Based on the flux decline profiles and visual observations, aggregate breakage may be a potential reason for severe membrane fouling caused by Flowback Water A. Therefore, jar tests were conducted to quantify the aggregate strength and to evaluate the effect of shear stress on aggregate size in the flowback water samples. The particle size distribution for Flowback Water A and B at various shear conditions are shown in Figure 6.4. The histogram and cumulative particle size distribution graphs reveal that the particles in Flowback Water A became smaller with an increase in shear force, while they remained virtually unchanged in Flowback Water B. Particle size distribution in Flowback Water A becomes narrow and shifts toward the smaller size with an increase in shear stress (Figure 6.4a and 6.4c). Such behavior is consistent with visual observation shown in Figure 6.2. The fraction of particles that are smaller than 2 μm increased from 1% to 28% when G value increased from $60s^{-1}$ to $640s^{-1}$. On the other hand, the release of fine particles at elevated shear stress was not observed for Flowback Water B and the fraction of particles that are smaller than 2 μm remained below 1% for all shear rate conditions tested (Figure 6.4b and 6.4d).

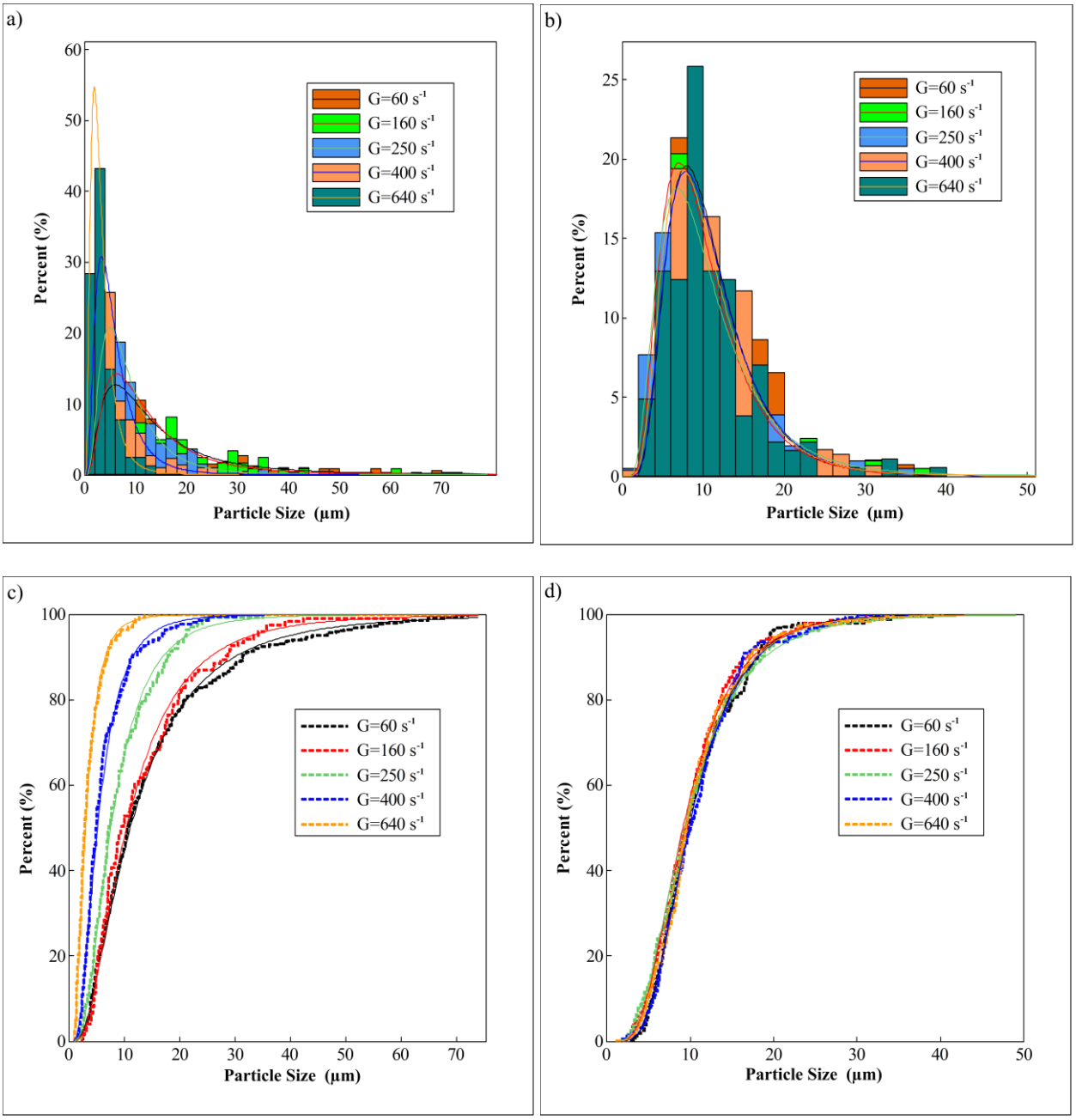

Figure 6.4 Number-weighted histogram and cumulative particle size distribution as a function of shear condition for Flowback Water A (a and c) and Flowback Water B (b and d). The solid lines represent fitted lognormal distribution.

Floc strength model (Equation 6-4 and 6-5) was used to quantify the resistance of aggregates in flowback water samples to shear-induced breakage. Log-log plot of d_{95} as a function of G value for Flowback Waters A and B is shown in Figure 6.5. The steep slope of 0.72 (R^2=0.97) for Flowback Water A indicates that these particles have low strength and are prone to breakup into smaller particles at high shear stress. On the other hand, particles in Flowback Water B are more stable and are not affected by the shear stress as indicated by a very gentle slope (0.06) and a weak relationship between d_{95} and G (R^2=0.41). The resistance of floc to shear-induced breakage (γ) depends on multiple factors, including type of floc and type of coagulant [36, 37]. The value of γ=0.72 for the aggregates in the Flowback Water A is within the range of typical values (0.29-0.81) reported for activated sludge and coagulated flocs [36].

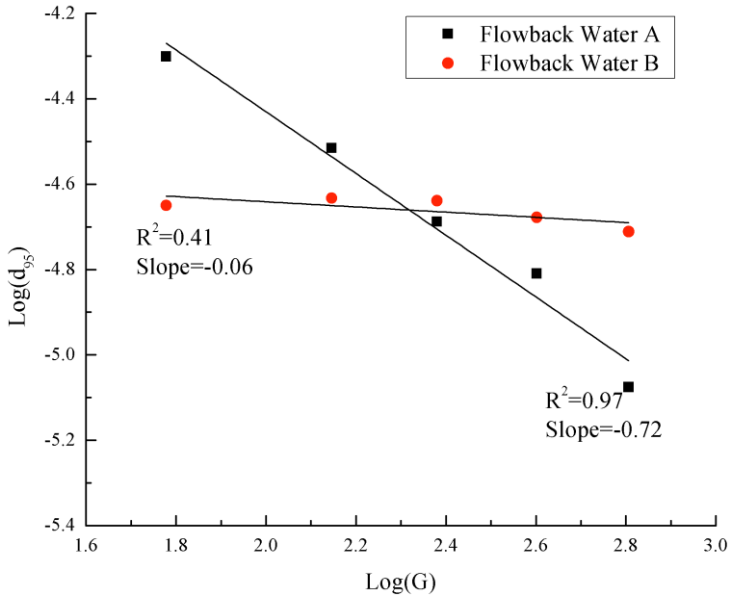

Figure 6.5 Variation of 95-percentile floc size (d_{95}) as a function of average velocity gradient (G)

It was reported that floc strength could significantly influence the performance of microfiltration membrane in the hybrid coagulation-MF and membrane bioreactor processes[20, 37-39]. As the membrane fouling increases with a decrease in particle size [12], breakage of particles is likely the key factor for the severe flux decline observed for Flowback Water A. As the feed solution contains high concentration of dissolved salts, the resulting smaller particles can form a denser cake layer with much lower permeability compared with the original particles because of the screening of particle-particle electrostatic repulsion, which typically cause more severe flux decline [12]. On the other hand, particles in the Flowback Water B exhibited great stability in the range of G values evaluated in this study and did not cause severe membrane fouling.

To validate the hypothesis that membrane performance is greatly affected by floc breakage, dead-end filtration system was used to treat Flowback Water A that was exposed to high shear rate ($G=640\ s^{-1}$) for 30 min. As illustrated in Figure 6.6, the treated Flowback Water A severely fouled the polymeric membrane compared with the raw Flowback Water A. This result further supports hypothesis that the floc breakage is a key factor that led to the severe permeate flux decline during cross-flow filtration of Flowback Water A.

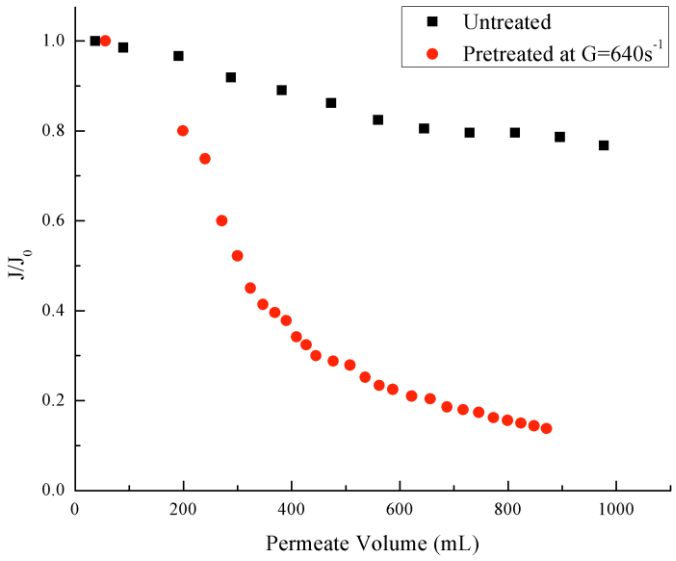

Figure 6.6 Permeate flux decline during filtration of raw (untreated) and treated Flowback Water A using PVDF membrane

6.4 SUMMARY AND CONCLUSIONS

Bench-scale cross-flow filtration with Al_2O_3 and SiC ceramic microfiltration membranes were evaluated for direct filtration of Marcellus Shale flowback water. Although submicron particles were not present in the samples used in this study, one flowback water caused much more severe fouling for both Al_2O_3 and SiC membranes. While the electrostatic interaction is a factor that typically affects fouling behavior, it is relatively insignificant during filtration of flowback water due to the high TDS of this water. Flux decline analysis demonstrated that the dominant membrane fouling mechanism at the early stage of filtration was intermediate pore blockage. Incomplete transition to cake layer filtration that was observed in these experiments is most likely due to the influence of shear stress on the formation and growth of cake layer.

Floc strength model revealed that the particulate matter in Flowback Water A was in aggregated form, which was prone to breakup into smaller particles at elevated shear stress. Such behavior was the main reason for rapid flux decline observed during direct filtration of flowback water. The results of this study suggest that it is necessary to evaluate the floc strength of the particles in the flowback water when considering microfiltration for flowback water treatment. Future studies should evaluate the critical shear stress, at which the floc breakage will not be significant to cause severe membrane fouling to minimize particle deposition and cake layer formation.

7.0 UTILIZATION OF ABANDONED MINE DRAINAGE FOR MARCELLUS SHALE FLOWBACK WATER REUSE: A PILOT STUDY

This chapter, written by Can He and coauthored by Tieyuan Zhang, and Radisav D. Vidic, was submitted for publication.

Flowback water generated during shale gas extraction in Pennsylvania is mostly reused for hydraulic fracturing operation. Abandoned mine drainage (AMD), one of the most serious threats to water quality in Pennsylvania, can potentially serve as a make-up water source to enable flowback water reuse. This study demonstrates co-treatment of flowback water and AMD produced in northeastern Pennsylvania in a pilot-scale system consisting of rapid mix reactor, flocculation tank and sedimentation tank. Sulfate concentration in the finished water can be controlled at a desired level (i.e., below 100 mg/L) by adjusting the ratio of flowback water and AMD in the influent. Fe^{3+} contained in the AMD can serve as a coagulant to enhance the removal of suspended solids, during which Fe^{2+} is co-precipitated and the total iron is reduced to a desirable level.

Solid waste generated in this process (i.e., barite) will incorporate over 99% of radium present in the flowback water. Sludge recycling can be used to increase the size of barite particles formed by mixing flowback water and AMD, so that they can be used as weighting

agent in drilling fluid. This alternative management approach for naturally occurring radioactive materials (NORM) can be used to offset the treatment cost, promote flowback water reuse, reduce environmental impacts of AMD and reduce pressure on fresh water sources.

7.1 INTRODUCTION

Marcellus shale in the Appalachian Basin is one of largest unconventional gas reservoirs in the U.S. and is estimated to contain 7.42 to 14.2 trillion m^3 (262-500 trillion cubic feet) of natural gas reserves [1, 2]. The success in unconventional gas extraction from Marcellus Shale formation has significant economic impacts for Pennsylvania [3]. However, there is an increasing public concern about environmental risks associated with the management of flowback/produced water that has the second highest salinity and highest radioactivity among all sedimentary basins in the U.S. [4-8].

Abandoned mine drainage (AMD) represents one of the most significant and persistent water quality problems in Pennsylvania [9, 10]. Considering the proximity of AMD sites to shale gas wells, AMD can potentially serve as an alternative water source for flowback water reuse [11, 12]. The merits of using AMD for hydraulic fracturing include reduced pressure on fresh water sources, reduced water transportation costs and associated greenhouse gas emissions, and mitigation of adverse environmental impacts caused by AMD. The major technical concerns with the use of AMD are high sulfate and iron concentrations in this impaired water. Dissolved sulfate can react with barium in the formation resulting in severe scaling that may decrease well productivity, while iron may interfere with chemical additives used in hydraulic fracturing [12].

Bench-scale studies were performed to understand precipitation of barite ($BaSO_4$) when mixing flowback water and AMD [13, 14], and to optimize potential subsequent solids separation processes [8, 15]. Creation of fairly small precipitates requires particle coagulation[15] or microfiltration [8] to ensure effective separation of solids that are formed when AMD and flowback water are mixed.

Co-precipitation of Ra with $BaSO_4$ results in the enrichment of NORM in the solid phase, which may be of concern for the management of this solid waste [13, 14]. Ra concentration in the solid waste generated through sulfate precipitation, which is also a common approach in centralized wastewater treatment plants (CWT) that are employed in flowback water reuse, far exceeds the technically enhanced naturally occurring radioactive material (TENORM) limits for disposal in municipal waste landfills (5-50 pCi/g depending on state regulations) [13]. Municipal waste landfill disposal is the main alternative for managing low level NORM waste, but is limited by the allowed source term loading for TENORM on an annual basis (i.e., amount of TENORM that can be disposed in a given landfill) [16]. Therefore, alternative management option for Ra-enriched solids generated by co-treatment of flowback water and AMD is needed in Marcellus Shale play.

As barite is the main component of the solids generated in this process, it can potentially be utilized as a weighting agent in drilling mud. Barite used in drilling mud formulation is typically produced from commercial barite ores. American Petroleum Institute specification for physical and chemical characteristics of barite used in this process includes minimum density (4.2 g/cm^3), maximum water-soluble alkaline earth metals (250 mg/kg), maximum mass fraction of particles that are smaller than 6 μm (30%), and maximum mass fraction of particles that are larger than 75 μm (3%) [17]. Generally, freshly precipitated $BaSO_4$ is relatively small in size (<6

μm) with the mean particle size decreasing with an increase in saturation level [18, 19], which is the main barrier for its use as a weighting agent.

This study was designed based on previous laboratory-scale results to demonstrate the feasibility of using AMD as an alternative make-up water and a source of chemicals for the treatment of flowback water in a pilot-scale treatment system. In addition, the treatment process was optimized to enable recovery of $BaSO_4$ solids that can be used as weighting agent in drilling mud.

7.2 MATERIALS AND METHODS

7.2.1 Characteristics of flowback water and AMD

Flowback water and AMD were collected from sites in northeastern Pennsylvania and stored in 20,000 gallon frac tanks for use in the pilot-scale study. Characteristics of these impaired waters sampled from the storage tanks are summarized in Table 7.1. The flowback water used in this study contains much higher concentrations of divalent cations compared with the flowback water from southeast PA reported previously [8, 11, 12, 14] and is in agreement with the flowback/produced water quality model developed by Barbot et al. [20].

Based on the analysis of 140 AMD samples, Cravotta demonstrated that pH of AMD varies widely from 2.7 to 7.3, with the majority being either acidic or neutral [21]. AMD generally contains dissolved iron that vary from below 0.1 mg/L to a few hundred mg/L [22]. Low-pH AMD can contain both Fe^{2+} and Fe^{3+}, and the ratio depends on geological conditions [23, 24]. The non-treated AMD used in this study is acidic and rich in ferric iron, which is

typical for AMD from this region [25]. Although precipitation of amorphous ferric hydroxide is thermodynamically feasible, it would take several months to reach equilibrium considering the pH and ferric iron concentration of the AMD sample [26].

Sulfate concentration in the AMD collected for this study was very low compared to barium concentration in the flowback water (Table 7.1), and was adjusted by adding Na_2SO_4 to represent more challenging treatment conditions. The initial concentrations of key constituents (i.e., Ba^{2+} and SO_4^{2-}) in the two feed streams to the pilot-scale unit that were tested in this study are shown in Table 7.2.

Table 7.1 Characteristics of flowback water and AMD

Constitutes	Flowback Water	AMD
Na^+(mg/L)	31,382	37.6
Ca^{2+}(mg/L)	31,270	66.3
Mg^{2+}(mg/L)	1,590	82
Ba^{2+}(mg/L)	19,115	-
Sr^{2+}(mg/L)	16,141	-
Cl^-(mg/L)	152,213	266
SO_4^{2-}(mg/L)	-	275
Fe^{3+} (mg/L)	-	29.7
Fe^{2+} (mg/L)	28.2	5.9
Ra-226 (pCi/L)	15570	-
Ra-228 (pCi/L)	1385	-
pH	6.2	2.6

Table 7.2 Initial barium and sulfate in flowback water and AMD after adjustment

Concentration	Barium (Flowback Water)	Sulfate (AMD)	Mixing ratio (Flowback: AMD)
Low (mg/L)	11,474	1,172	1:9
High (mg/L)	19,115	2,150	1:8
The adjustment of barium and sulfate was determined in the field with turbidimetric analytical method and validated by sample analysis in the laboratory.			

7.2.2 Bench-scale tests

Bench-scale beaker tests were conducted to evaluate the reaction rate as a function of saturation index ($SI = \log \frac{\text{Ion Activity Product}}{K_{sp}}$), using various flowback water and AMD samples collected previously as well as synthetic $BaCl_2$ and Na_2SO_4 solution (see Table A1 in the Appendix). The reaction rate was calculated based on in the first two minutes and it was assumed that homogenous nucleation governs the initial phase of the reaction without any seed particles.

Prior to pilot-scale tests, bench-scale jar tests using a six-paddle jar tester (Phipps & Bird, Richmond, VA) were conducted to find optimal operating conditions for turbidity and iron removal. Rapid mixing in these tests was conducted for 1 min at 300 rpm followed by slow mixing for 25 min at 25 rpm and settling for 30 min, during which dissolved iron concentration was measured.

7.2.3 Pilot-scale operation

Unit processes in the pilot-scale treatment system include rapid mixing, flocculation, sedimentation and bag filtration (Figure 7.1). Two 25-gallon tanks equipped with variable-speed electric mixers (80-4000 rpm) were used as rapid mixing tank and AMD mixing tank. The mixing speed of rapid mixers was adjusted to 1600 rpm to ensure effective mixing (Gt value of 87,000). A 300-gallon tank equipped with paddle mixer was used as a flocculation tank. The mixing speed used for flocculation was adjusted to 8 rpm to reach Gt value of 83,800. A 500-gallon cone-bottom settling tank was equipped with tube settler to ensure efficient separation of suspended solids and sludge thickening. The total influent flow rate of flowback water and AMD was targeted at 5 GPM, while the flow rate of the recycled sludge was targeted at 5 GPM. The TSS of the bottom sludge was 7.5% and the diaphragm pump was used to recycle sludge with such high solids concentration back to AMD mixing tank.

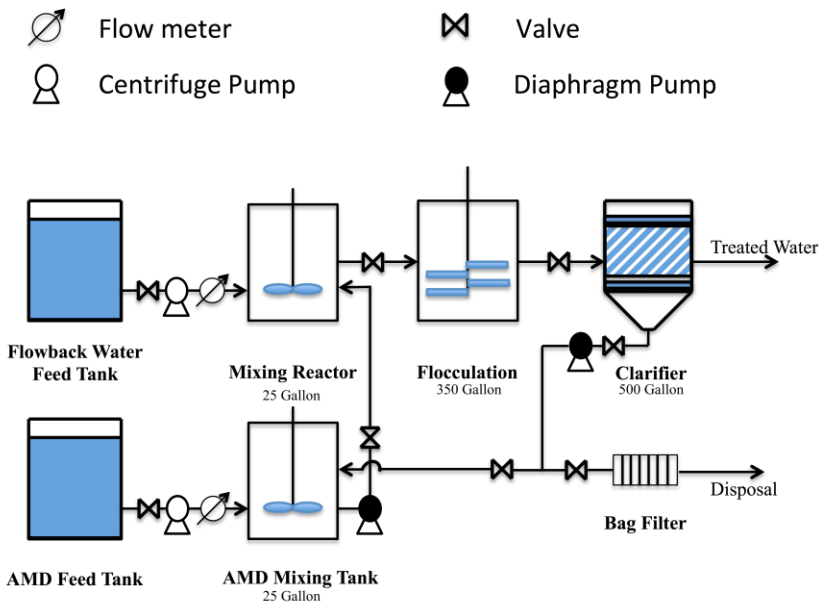

Figure 7.1 Schematic of the pilot-scale treatment system.

7.2.4 Analytical methods

Cation and anion analysis in the laboratory was performed using atomic absorption spectroscopy (AAS Model 1000, PerkinElmer, Waltham, MA) and ion chromatography (Dionex ICS-1100, Thermo Scientific, Waltham, MA), respectively. For AAS analysis, samples were filtered through 0.45-µm membrane, and diluted with 2% nitric acid and 0.15% KCl solution to eliminate ionization interference during AAS analysis for Ba and Sr [14, 20]. For total dissolved iron analysis, samples were filtered through 0.22-µm membrane to eliminate the interference of sub-micron particles with significant iron content [8].

A high-resolution Apex Gamma spectrometry system (Ortec, Oak Ridge, TN) with a high-purity Germanium detector was used to quantify the activity of radionuclides. Prior to Ra analysis, samples were placed in 47 mm petri dishes, sealed with vinyl electrical tape, and kept for at least 2 days to ensure equilibrium between Ra-228 and Ac-228. Ra-226 activity was analyzed by measuring gamma ray emission at 186 KeV, while Ac-228 activity was analyzed based on multiple gamma ray emissions at 270, 338, 911, and 964 KeV. Ra-228 activity was calculated based on the activity of its equilibrium progeny Ac-228.

The on-site analysis for barium and sulfate was conducted using Hach turbidimetric method. Validation of the Hach method was performed by comparison with AAS for dissolved barium and ion chromatography for sulfate measurement under the conditions that are relevant for shale gas wastewater. It was found that dissolved sulfate measurements by these two analytical methods were in good agreement (data not shown). However, the turbidimetric method for barium analysis was reliable only when strontium concentration was close to or less than barium concentration. The total dissolved iron and Fe^{2+} on site analyses were conducted by FerroVer Method (Hach Method 10249) and 1,10-phenanthroline method (Hach Method 8146), respectively. The Fe^{3+} concentration was calculated as the difference between total iron and Fe^{2+} concentration.

Characterization of solids precipitated in the mixing reactor in terms of morphology and chemical composition were performed using scanning electron microscopy (SEM, Philips XL30, FEI Co., Hillsboro, OR) and energy dispersive X-ray spectroscopy (EDX, EDAS Inc., Mahwah, NJ), respectively. The solid samples from the mixing reactor were diluted 500-1,000 times with DI water and deposited on a 0.45 μm nylon membrane on site. After the membrane samples were completely dried in the field, they were transferred to the laboratory and sputter coated with

palladium for 60s in a vacuum at a current intensity of 40 mA to avoid the charging effect [27]. The particle size distribution was obtained by measuring the size of 200 particles observed in the SEM image.

Water-soluble alkaline earth metals content (as calcium) was measured in solid samples collected from the sludge return line. The sludge samples were filtered through 0.7-μm glass fiber membrane, washed with 150 mL of DI water and dried in an oven. 1g of dry solids was collected from the membrane, mixed in 50 mL of DI water, and placed on a rotary shaker to equilibrate for 1 hour. The suspension was then filtered through 0.45-μm membrane and the total alkaline earth metals in the liquid permeate was measured using EDTA titration method (Standard Method 2340).

7.3 RESULTS AND DISCUSSION

7.3.1 Sulfate removal

Presence of dissolved sulfate in the fracturing fluid is of concern because of the potential to cause mineral scaling, particularly in Marcellus Shale that is rich in Ba, Sr and Ca [12, 15]. Therefore, sulfate concentration in the hydraulic fracturing fluid is generally limited to 100 mg/L[12]. It was previously reported that mixing of AMD and flowback water requires more than 10 hours to reach precipitation equilibrium as indicated by conductivity analysis [11]. He et al. reported that barite precipitation is very rapid and will reach equilibrium within 30 min when excess sulfate is added to flowback water, while celestite precipitation will proceed for more than 24 hours [14]. As it is desirable to minimize the size of the treatment plant, slow celestite

and gypsum precipitation reactions were not considered in this study for the control of sulfate in the finished water.

Sulfate analysis throughout the treatment system revealed that barite precipitation proceeded rapidly in the mixing reactor and reached equilibrium after the flocculation tank (Figure 7.2). Such behavior is expected because the saturation index, calculated using PHREEQC software with Pitzer activity corrections was above 4.0 for all experimental conditions evaluated in this study, which corresponds to rapid barite precipitation [14]. As shown in Figure 7.2, sulfate concentration in the finished water was reduced to below 100 mg/L for all three experimental conditions, which was the target concentration to enable unrestricted use of this water for hydraulic fracturing.

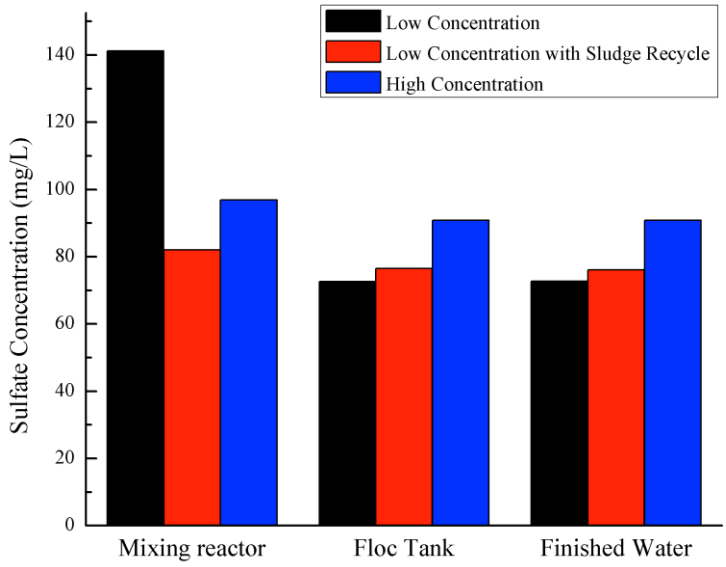

Figure 7.2 Sulfate concentration in the pilot-scale treatment units for various experimental conditions

Decrease in saturation index will lead to slower homogeneous nucleation rate, while the increase in seed concentration will promote the seeded growth rate [28]. The sulfate consumption rate observed in bench-scale and pilot-scale tests as a function of saturation index is shown in

Figure 7.3. As can be seen in this figure, the reaction rate increases sharply for SI>3.0, which is in agreement with rapid barite precipitation reported previously [14]. Bench-scale tests were designed to evaluate homogenous nucleation reaction (Supporting Information) and the rate expression is well fitted with an exponential curve (R^2=0.95). The average sulfate consumption rate in the rapid mix reactor of the pilot-scale test without sludge recycling was 2.0 and 4.2 mM/(L min) in the mixing reactor for low (SI=4.4) and high (SI=4.7) concentration, respectively, and was in excellent agreement with the bench-scale tests (Figure 7.3). Experiments conducted at low concentration with sludge recycle reduced SI from 4.4 to 4.0 due to dilution, but the total suspended solids (TSS) in the mixing reactor increased from 0.2% to 3.9%. The average sulfate consumption rate in the mixing reactor increased from 2.0 to 2.2 mM/(min L) due to sludge recycling and this data point was significantly above the results for homogenous nucleation. This result indicates that the seeded growth was effectively promoted by sludge recirculation and that growth of existing barite particle represented a significant portion of sulfate consumption (48%) under these conditions.

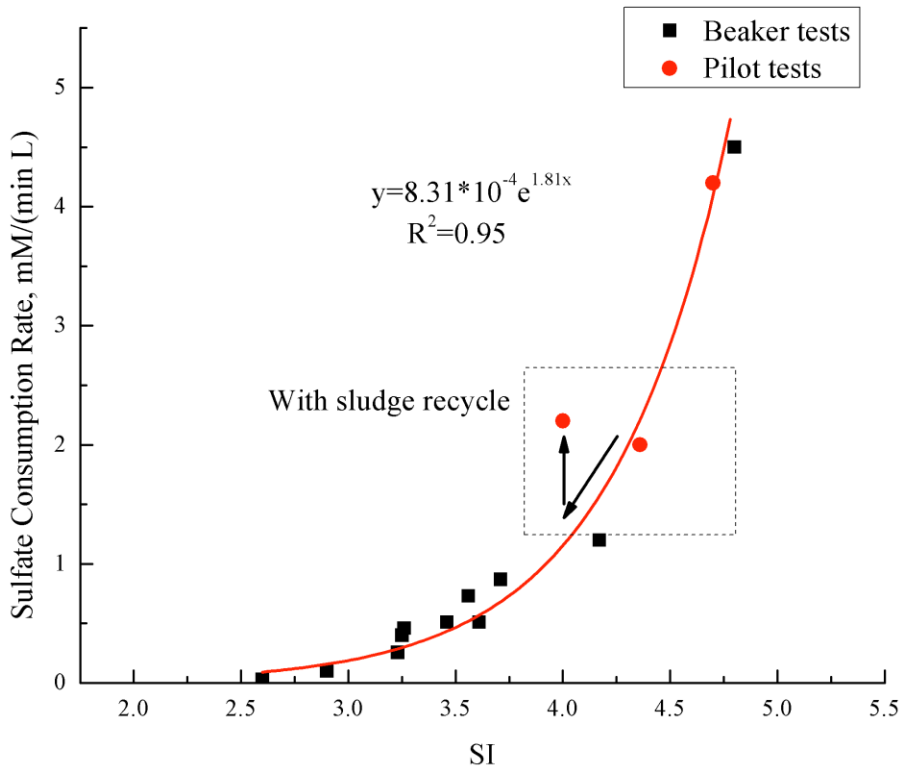

Figure 7.3 Sulfate consumption rate as a function of saturation index.

7.3.2 AMD as a source of coagulant

While dissolved sulfate can be reduced to acceptable level, coagulation may be required to facilitate removal of fine barite particles formed in this process by settling [15]. Dissolved iron typically present in AMD can potentially serve as the internal coagulant to reduce the cost and total life cycle impact of the proposed use of AMD as make up water for hydraulic fracturing. Salama et al. [29] reported that AMD was useful for coagulation of microalgae biomass at pH between 7 and 9, while Sun et al. [30] studied As removal by coagulation with in-situ formed Fe^{3+} from AMD. Previous lab-scale studies found that coagulation with ferric chloride was an

effective process for the removal of the suspended solids formed by mixing flowback water and AMD and that the finished water turbidity can be reduced to below 5 NTU with ferric chloride dosage of 20-60 mg/L as Fe at pH 6.0-7.0 [31].

The pilot-scale experiment with pH adjustment by adding NaOH was conducted at low concentration conditions. Initial concentrations of Fe^{3+} and Fe^{2+} in the mixture were 26.7 mg/L and 8.1 mg/L, respectively. Bench-scale jar tests revealed that the optimum pH for turbidity and iron removal was between 7.0 and 7.5, when the turbidity of the supernatant was reduced to 2 NTU and total iron was reduced to 0.1 mg/L. The coagulant dosage used in this study is in agreement with the range of ferric chloride dosages reported previously [31].

Turbidity and total iron in the effluent from the pilot system operated at pH 7.5 were 3 NTU and 0.1 mg/L, respectively, indicating that iron contained in the wastewater effectively served as coagulant to enhance solids removal. Although aeration was not applied in the pilot-scale system, the total iron was reduced to a desired level at pH 7.5. The Fe^{2+} concentration in the effluent of the rapid mix reactor, flocculation tank and settling tank was 0.66 mg/L, 0.18 mg/L and 0.08 mg/L, respectively, while the Fe^{3+} concentration was reduced to below the detection limit (0.1 mg/L for Hach Method 10249) in the rapid mix reactor.

The rate equation developed by Singer and Stumm [32] was incorporated in the PHREEQC model to predict the Fe^{2+} removal. The kinetic model predicted that Fe^{2+} would be reduced from 8.1 to 5.8 mg/L after 1 min of contact time at the dissolved oxygen concentration of 4 mg/L. Jar tests revealed that the Fe^{3+} concentration decreased from 26.7 mg/L to 0.12 mg/L after 1 minute of rapid mixing, while the Fe^{2+} concentration was reduced from 8.1 mg/L to 0.78 mg/L. The difference between measured and predicted Fe^{2+} concentrations suggests that the reduction of Fe^{2+} in the rapid mix reactor was likely due to incorporation of ferrous ion into

ferric hydroxide by coprecipitation [23, 33] rather than oxidation. As the ferric hydroxide precipitation essentially reached equilibrium in the rapid mix reactor, the subsequent iron removal in the flocculation and settling tanks (from 0.66 mg/L to 0.08 mg/L) is likely due to adsorption of Fe^{2+} and/or oxidation of Fe^{2+} to Fe^{3+} followed by rapid precipitation as ferric hydroxide.

The effective use of iron contained in AMD as coagulant for solids separation reveals the additional merits for using this wastewater as make-up water for flowback water reuse.

7.3.3 Sustainable management of Ra-enriched solid waste

As listed in Table 7.3, the quality of finished water from the proposed treatment process enables unrestricted use for hydraulic fracturing. However, the management of the solid waste generated from this process is still a concern due to its elevated radioactivity.

Table 7.3 Finished water quality for low concentration conditions

Finished Water Quality	
Ra-226 in Effluent	<60 pCi/L
Ra-228 in Effluent	<10 pCi/L
Ra removal	>99%
Total Iron (mg/L)	0.1
Sulfate (mg/L)	73
Turbidity (NTU)	3
pH	7.3

As sulfate concentration in the influent was in excess compared to barium, complete removal of barium resulted in complete Ra removal as evidenced by Ra concentration in the finished water below the detection limit (60 pCi/L for Ra-226 and 10 pCi/L for Ra-228), which is in agreement with previous results [11, 13]. The solids generated in the pilot system contained 648 pCi/g Ra-226 and 53 pCi/g Ra-228, respectively, which far exceeded the limits for NORM disposal in municipal solid waste landfills (5-50 pCi/g depending on state regulations). Reuse of Ra-enriched $BaSO_4$ particles for drilling mud formulation can potentially reduce the TENORM loading in municipal landfill in Pennsylvania. In essence, this approach for management of barite produced in this process will result in the deposition of Ra-enriched $BaSO_4$ in the shale formation due to the loss of the drilling mud during horizontal drilling. However, it will be necessary to increase the size of barite particles formed in this process to meet API standards and allow the use of barite for unconventional well drilling. Growth of precipitated solids is a common goal in many industrial processes [34, 35]. The fundamental idea behind these applications is to promote seeded growth, while limiting the generation of new particles through homogeneous nucleation. At high supersaturation, homogenous nucleation governs the reaction, which is typical for barite precipitation from flowback water due to its high barium concentration[20]. Therefore, sludge recycling was utilized at low concentration conditions in this study to reduce supersaturation by dilution and increase the concentration of seed particles in the mixing reactor, which suppresses homogenous nucleation and promotes seeded growth. Schematic concept of this idea is illustrated in Figure 7.4 using the relationship between supersaturation level and reaction rate from this and other studies [34, 36].

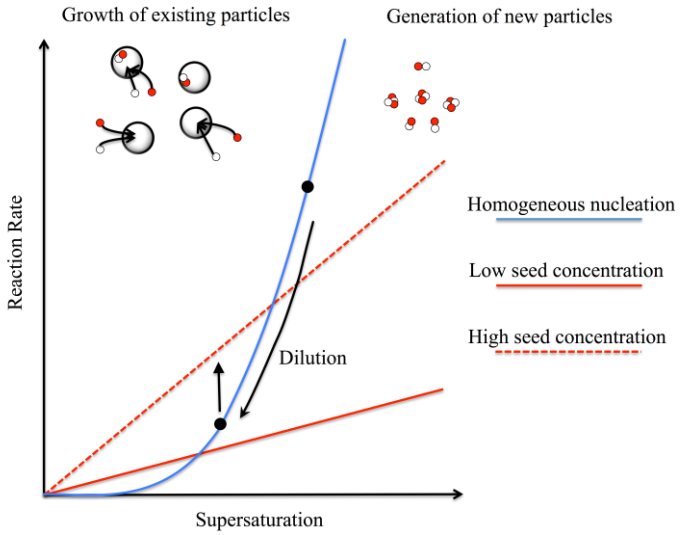

Figure 7.4 Enhanced barite growth at lower supersaturation level and in the presence of higher concentration of primary particles. Growth of existing particles is dominant when the red line (seeded growth) is above the blue curve (homogeneous nucleation)

The feasibility study to demonstrate the possibility to enhance barite growth was conducted in a pilot-scale system without pH adjustment. Particle size analysis of samples collected from the rapid mix reactor revealed the average barite particle size of 5.42±1.61 and 3.77±1.23 μm for low and high concentration conditions, respectively. These results illustrate that the increase in saturation level yields smaller particles (Figure 7.5a), because homogeneous nucleation dominates at high supersaturation [18]. The number percent of particles that are smaller than 6 μm was 63% and 89% for the low and high concentration levels, respectively, which is not compatible with the size requirement for drilling mud specified by API.

As illustrated in Figure 7.5b, introduction of sludge recycling reduced cumulative frequency of the particles that are smaller than 6 μm from 63 to 27%, which meets the API requirement. This result is consistent with the reaction rate analysis discussed earlier (Figure 7.3).

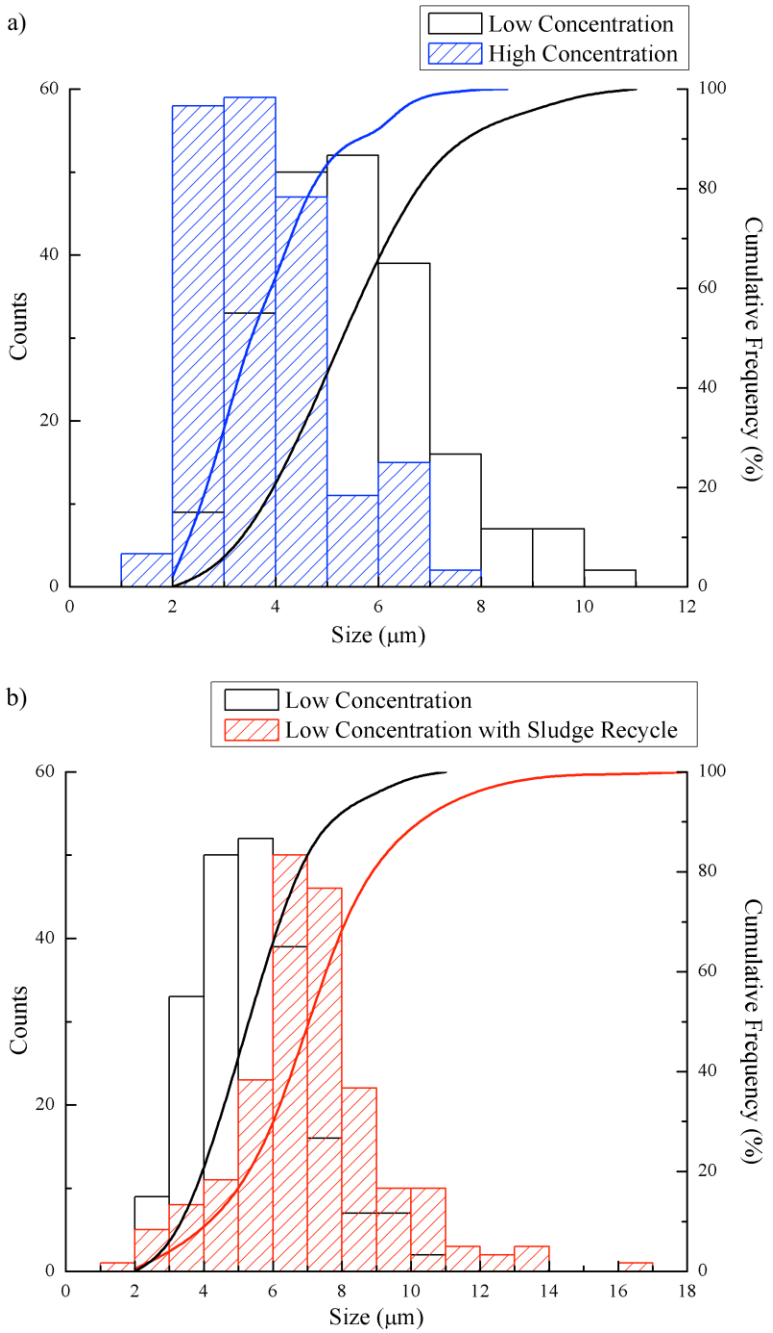

Figure 7.5 Particle size distribution for barium sulfate particles: (a) low sulfate and high sulfate conditions (b) low sulfate condition with/without sludge recycle

EDX analysis revealed that the precipitates formed in the pilot-scale system are strontian barite (i.e., $BaSrSO_4$) with relatively uniform Ba content (about 84% of cations) for all three experimental conditions evaluated in this study. As can be seen in Figure 7.6, Sr content in strontain barite particles is not dependent on the morphology of solids formed in the system. Sanchez-Pastor et al. reported that the incorporation of Sr into barite particles would result in the elongation of the precipitate [37]. However, such phenomenon was only observed under low concentration conditions (i.e., low supersaturation) used in that study. At high concentration condition, the reaction is governed by homogeneous nucleation rather than crystal growth. EDX analysis also revealed that Ca incorporation into the precipitates was negligible, which can be explained by the difference in the ionic radius between barium and calcium [38]. The atom percent of barium in strontian barite obtained in this study is slightly higher than that reported elsewhere [11], which is likely due to differences in the composition of feed solution, reaction time and measurement method.

Particle density measured by submersion method [39] averaged 4.3 g/cm^3 based on triplicate measurements and water-soluble alkaline earth metal (as calcium) was 44 mg/kg. Therefore, $BaSO_4$ particles recovered from this process meet API specification and can be reused in drilling mud formulation, which can potentially reduce the cost of unconventional gas extraction and relieve the pressure on the management of TENORM associated with flowback water reuse. Ra levels in the solids produced in the centralized wastewater treatment (CWT) facilities that employ sulfate precipitation for divalent ion removal (mainly Ba and Sr) are also significantly above the TENORM disposal limit [13]. Therefore, the approach for barite reuse developed in this study can also be used to improve waste management practices in these facilities.

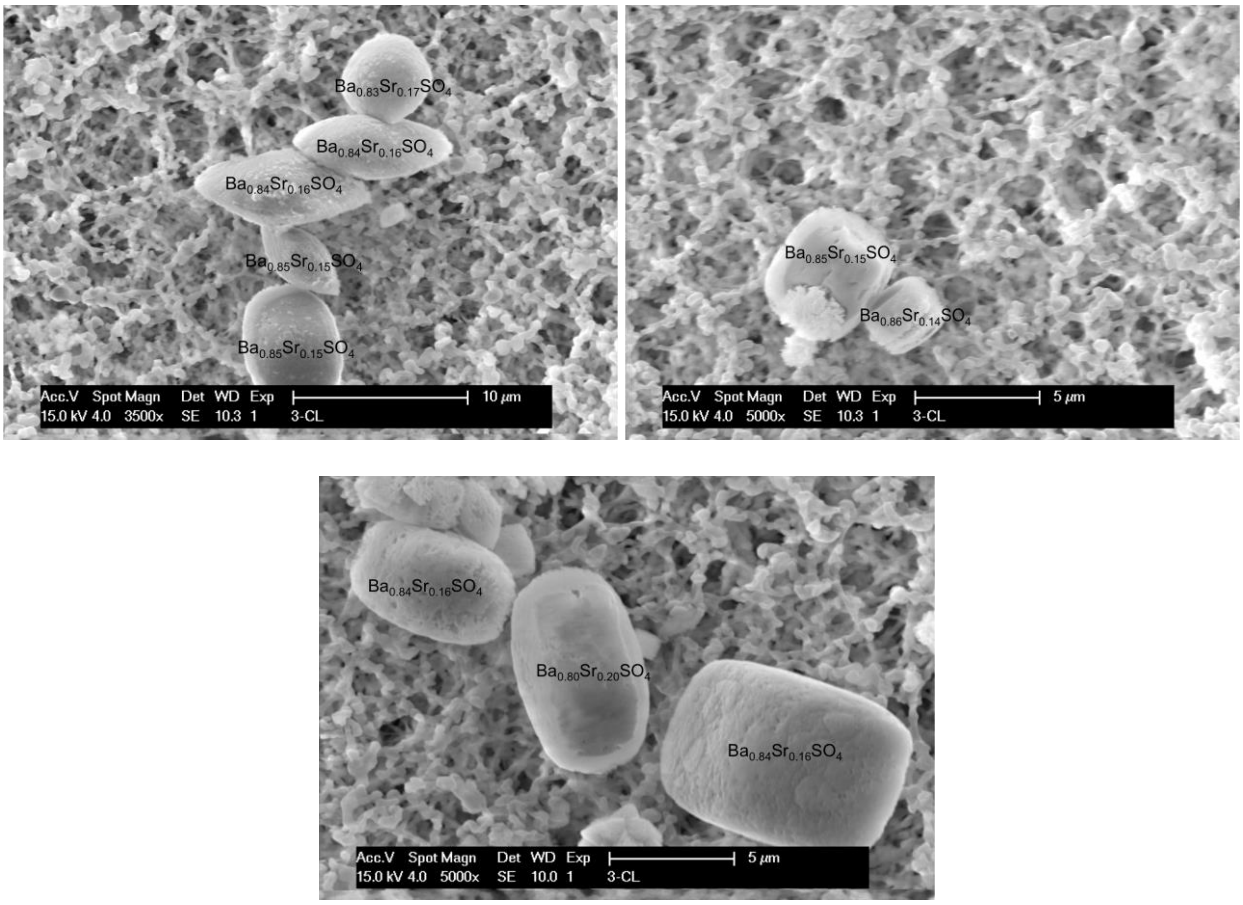

Figure 7.6 Morphology and chemical composition of mineral precipitates formed at various experimental conditions: (a) low concentration; (b) high concentration and (c) low concentration with sludge recycle.

7.4 SUMMARY AND CONCLUSIONS

The results of the pilot-scale tests revealed that the sulfate was rapidly removed from liquid phase at high barite supersaturation levels so that the sulfate concentration in the effluent is

reduced to below 100 mg/L with appropriate mixing ratio between flowback water and AMD. Radium removal through coprecipitation with barium sulfate was in agreement with theoretical predictions and the previous results.

The feasibility of recovering barium sulfate for use as a weighting agent in drilling activities was evaluated. The results of this study demonstrated that the particle size of barium sulfate decreased with an increase in initial barite supersaturation and was below the requirement for barite use as a weighting agent. Sludge recycling was used to increase the surface area of seeded particles and reduce barite supersaturation to promote the growth of barium sulfate primary particles. The physical and chemical properties of the barium sulfate particles formed in this process meet API requirement for use as a weighting agent in drilling mud, which offers an alternative management option for the Ra-enriched solid waste generated from co-treatment of flowback water AMD. In addition, the barium sulfate reuse method developed in this study can be applied for the solid waste generated in centralized wastewater treatment facilities, where sodium sulfate addition is employed for flowback/produced water treatment.

This pilot-scale study revealed that a treatment system with rapid mix reactor, flocculation tank and settling tank is effective for the co-treatment of flowback water and AMD with the treated effluent quality meeting the criteria for reuse in hydraulic fracturing of unconventional wells in Marcellus Shale.

8.0 IMPACT OF ANTISCALANTS ON THE FATE OF BARITE IN THE UNCONVENTIONAL WELLS

Formation of barite ($BaSO_4$) scale is a potential problem during the extraction of unconventional shale gas, as it can potential plug the proppant media. While antiscalants cannot prevent the formation of mineral scales for highly supersaturated solution, they can reduce the size and alter the morphology of $BaSO_4$ particles.

Extensive attachment of $BaSO_4$ particles by proppant media was observed at typical background NaCl concentration and in the absence of antiscalants, due to the relatively large particle size and screened electrostatic interaction. The presence of polymer antiscalants can enhance the mobility of $BaSO_4$ particles by providing electrosteric repulsion force. Ethylene glycol that is commonly added to hydraulic fracturing fluid to prevent scale deposition can reduce the size of $BaSO_4$ precipitates but has no impact on the deposition of $BaSO_4$ particles during transport through proppant sand media.

Polymaleic acid (PMA) and sulfonated phosphino carboxylic acid (SPPCA) that are generally considered when the goal is to inhibit the formation of mineral scales are unlikely to prevent barite formation at high supersaturation conditions that are typical for unconventional gas industry. However, they can inhibit the deposition of bulk precipitates onto proppant surface by limiting the particle size and inducing stronger repulsive interactions.

8.1 INTRODUCTION

In the past two decades, extraction of unconventional natural gas resources that are trapped in the low-permeability shale formation has become economically feasible around the world [1]. Hydraulic fracturing is one of the key technologies for shale gas extraction activities, and involves the injection of large volume of water (3-5 million gallon per well) and proppant sand (9% by volume) to enable transport of trapped natural gas into the production casing of a shale gas well [1, 2]. During well completion, a portion of hydraulic fracturing fluid is recovered to surface as the pressure in the well is released, while proppant sand remains in subsurface to keep the induced hydraulic fracture open. As indicated by produced water quality [2-4], formation brines in shale gas reservoirs contain high concentrations of alkaline earth metals (e.g., Ca, Sr and Ba), which have low solubility as sulfates. Therefore, dissolved sulfate concentration in the fracturing fluid is typically limited to 100 mg/L and antiscalants are added to the hydraulic fracturing fluid to minimize potential for well plugging by sulfate scales [2, 3].

Among the three common sulfate scales (i.e., $CaSO_4$, $SrSO_4$ and $BaSO_4$), barium sulfate (barite) is a unique and troublesome scaling agent in many industrial processes, due to its low solubility and resistance to acid treatment. Previous studies have demonstrated that barium sulfate can be chemically removed with a costly process using chelating agents, such as as diethylenetrinitrilopentaacetic acid (DTPA) and ethylenedinitrilotetraacetic acid (EDTA) [5]. Scaling control strategies, including alteration of feed water quality, optimization of operational parameters and use of antiscalants, are required to mitigate the deposition of barite scales [6].

Antiscalants can function by one or more mechanisms, which depends on the functional groups, molecular weight and dosage [6, 7]. Threshold inhibition is the most common application of antiscalants, which involves addition of substoichiometric amount of antiscalants

(usually below 80 mg/L) to inhibit the formation of mineral scales in the bulk phase for a supersaturated solution [7, 8]. Ion complexation relies on the addition of equimolar concentration of antiscalants to act as a chelating agent and mitigate the tendency of scales formation [5]. Deprotonated antiscalants can adsorb onto newly formed particles to disrupt the crystal growth and prevent particle agglomeration [9]. The common antiscalants used for barite scaling include phosphonate compounds and carboxylic polymers [8, 10]. Various studies have demonstrated that antiscalants can effectively interfere with nucleation and/or crystal growth of barium sulfate at relatively low supersaturation level (SI<3.0) [8, 10]. By limiting the sulfate concentration in the fracturing fluid, the antiscalants can possibly act as threshold inhibitors to prevent the formation of $BaSO_4$ scales in the shale formation.

When sulfate-rich fracturing fluid is injected into shale formation, it is likely that barite will form in the subsurface due to high supersaturation levels that are typical in Marcellus Shale [11]. Preliminary calculations shown in Table 7.1 indicate that the volume of barite that would form downhole can range from 0.1% of the proppant volume in case the fracturing fluid contains 200 mg/L sulfate to as much as 1.2% of the proppant volume when the fracturing fluid contains 2,000 mg/L sulfate. While it seems that the volume of barite particles formed downhole is not significant, the mobility of these particles through proppant sand media is an important factor to assess the potential damage to well productivity. However, the transport of barite particle through porous sand media under elevated ionic strength condition and the potential mobility enhancement by the addition of antiscalant were not studied previously.

Table 8.1 Barite formation downhole

Sulfate in the frack fluid (mg/L)	Barite formed in the well (m^3)	Percentage of the proppant volume (%)
200	1.2	0.1
800	4.9	0.5
2,000	9.8	1.2
Assumptions: • volume of fracturing fluid is 3×10^6 gallons; • proppant fraction is 9% by volume; • barite density is 4500 kg/m^3		

In this study, the impact of antiscalants on barite fomration and subsequent transport through proppant sand media was evaluated in order to obtain some insights into the fate of barite particles formed in the subsurface when sulfate-rich fracturing fluid is used. The anti-deposition function of antiscalants and the associated fundamental mechanism were evaluated together with the transport behavior of antiscalant-modified barite particles through proppant sand media.

8.2 MATERIALS AND METHODS

8.2.1 Chemical reagents

Polymaleic acid (PMA) and sulfonated poly-phosphino-carboxylic acid (SPPCA), both with 50% active content by weight, were provided by Kroff Chemical Company (Pittsburgh, PA) and BWA Water Additives (Tucker, GA), respectively. According to the chemical provider, the molecular weight of PMA and SPPCA is 1,000 g/mol and 3,700 g/mol, respectively. Barium chloride dihydrate (Fisher Scientific), anhydrous sodium sulfate (J.T. Baker), sodium chloride

(Fisher Scientific), sodium hydroxide (Fisher Scientific), ethylene glycol (EG, Fisher Scientific) and hydrochloric acid (37.3%, Fisher Scientific) used in this study were ACS grade reagents.

8.2.2 Preparation and characterization of $BaSO_4$ particles

The suspension of $BaSO_4$ particles used in column experiments was prepared by mixing equimolar $BaCl_2$ and Na_2SO_4 (4.29 mM) in a 200-mL beaker. Antiscalants (1 wt%) and NaCl (1.0 M) solutions were added to reach desirable inhibitor dosage (10 mg/L) and background salt concentration (8.6 to 508.6 mM), before barite precipitation was initiated by the addition of Na_2SO_4. HCl or NaOH solutions (0.1 M) were used to adjust the solution pH between 4 and 8.5. The feed solution was mixed at 400 rpm throughout the experiment using a magnetic stirring bar.

Particle size distribution of precipitates that formed in solution was measured using a laser diffraction analyzer (Microtrac S3500, Microtrac Inc., Montgomeryville, PA). Prior to particle size measurement, 1% sodium hexametaphosphate was added to the suspension to ensure dispersion of barite particles. Scanning electron microscope (SEM, Philips XL30, FEI Co., Hillsboro, OR) was used to analyze the morphology of barite particles under different experimental conditions. The barite particles for SEM analysis were sampled from the feed solution, deposited on a 0.45 μm nylon membrane and washed with DI water. After membrane samples were air-dried for at least 2 days, a section of it was placed on a plate sampler and coated with palladium for 60s in a vacuum at a current intensity of 40 mA. Zeta potential of $BaSO_4$ particles was measured by Malvern Zetasizer (Malvern Instruments Ltd., UK).

8.2.3 Column experiments

A glass chromatography column with inner diameter of 10 mm and length of 10 cm (Omnifit, Toms River, NJ) was used to study $BaSO_4$ transport through saturated porous proppant sand media. A 125-μm nylon mesh screen was placed on each end of the column to retain proppant sand, while enabling the passage of barite particles.

Actual proppant sands used in hydraulic fracturing in Marcellus Shale was used for column experiments. The proppant was sieved through 20 US Mesh sieve to obtain relatively uniform sample with average particle size verified by Microtrac S3500 of 0.249 mm. Sieved proppant was rinsed with DI water for three times to remove fines before use. Proppant was wet-packed into the column to eliminate air bubbles in the porous media. Porosity of packed sand column of 0.36 was determined using the quartz density of 2.59 g/cm^3[12].

Prior to $BaSO_4$ transport experiments, packed column was injected with at least 10 pore volumes (PV) of DI water to remove fines created during column packing. After flushing with DI water, 10 PV of NaCl solution with identical concentration and pH as the feed solution was injected through the column to precondition the proppant sand. Freshly-made $BaSO_4$ feed solution was injected into the column by a peristaltic pump at a constant flow rate of 13 ml/min at room temperature (21 °C). Effluent was sampled every 30 seconds and analyzed by UV/VIS spectrophotometer at a wavelength of 500 nm to determine $BaSO_4$ concentration. The spectrometer was calibrated with barite solution prior to each experimental condition.

8.3 RESULTS AND DISCUSSION

8.3.1 Characterization of $BaSO_4$ particles

Bench-scale experiments were conducted to evaluate the impact of PMA, SPPCA, and EG on industrial process to prevent $BaSO_4$ scaling problem [13-15], while EG is often used by the unconventional shale gas extraction to prevent scales formation and deposition [1, 16]. Many studies focused on the impact of antiscalants on kinetics of nucleation and crystal growth at low supersaturation conditions where threshold inhibition is the dominant mechanism [8, 11, 14]. Under such condition, the presence of antiscalants can interfere with the nucleation phase and result in prolonged induction period.

Batch tests revealed that the three antiscalants evaluated had minimal effect on the retardation of $BaSO_4$ precipitation with the antiscalant dosage as high as 10 mg/L. Induction period was always less than one second based on the visual observation of abrupt turbidity increase while the equilibrium was essentially achieved within 30 minutes of reaction by barium concentration measurements (data not shown). The immediate formation of $BaSO_4$ particles at high initial supersaturation is likely because the formation of nuclei is so rapid that the antiscalant failed to limit their growth beyond the critical size. The inability of antiscalants to inhibit $BaSO_4$ precipitation at high supersaturation condition is consistent with previous studies [9, 11]. These results suggest that the formation of $BaSO_4$ is inevitable when high-sulfate injection fluid is used for hydraulic fracturing. Therefore, it is important to evaluate the transport of $BaSO_4$ particles through proppant sand media at various experimental conditions to fully understand the fate of barite in the subsurface.

While the selected antiscalants were not able to inhibit barite precipitation, SEM images illustrated that the morphology and size of barite particles were significantly altered in the presence of antiscalants (Figure 8.1). The $BaSO_4$ particles for SEM analysis were formed in the presence of 0.5 M NaCl to represent the high salinity of the formation brine in shale gas reservoirs. Barite particles formed in the absence of antiscalants had a rhombohedral shape and relatively larger size (Figure 8.1a). The elongated shape is likely due to difference in growth velocity in selected crystallographic directions [17]. Benton et al. observed the same morphology of barite particles formed at similar experimental condition [18]. The barite particles formed in the presence of antiscalants were visibly smaller and had an ellipsoidal shape (Figure 8.1b-d). Several studies reported similar barite morphology in the presence of organic [8, 18, 19].

The impact of antiscalants on the size of $BaSO_4$ particles formed at different ionic strength was analyzed using Microtrac S3500. As shown in Figure 8.2, the average particle size of $BaSO_4$ increased from 2.0 um to 5.1 um when background NaCl concentration increased from 8.6 mM to 508.6 mM. Risthaus et al. studied the barite growth at background NaCl concentration up to 0.8M using atomic force microscopy and found that the growth rate increased due to reduced interfacial energy at higher ionic strength [17]. On the other hand, the average size of barite particles formed at pH 7 in the presence of three antiscalants was much smaller (Figure 8.2) and it increased only slightly with ionic strength. Among the three selected antiscalants, SPPCA is the most effective in controlling the size of $BaSO_4$ particles. The reduced size and altered shape of barite particles is likely attributed to the adsorption of antiscalants onto nucleating crystals, which leads to distorted crystal growth [8, 9]. The schematic concept for the effect of polymeric antiscalants on $BaSO_4$ precipitation at high supersaturation level is shown in Figure 8.3. For the case where no antiscalants were added (Figure 8.3a), homogeneous

nucleation, seed growth and aggregation of newly formed small $BaSO_4$ particles contributed to the large size of $BaSO_4$. When polymeric antiscalants are present (Figure 8.3b), the seed growth on formed $BaSO_4$ surface is inhibited as polymers take the active growing sites on the surface. Stronger electrostatic and steric repulsion induced by polymer can prevent the particles from agglomeration [9].

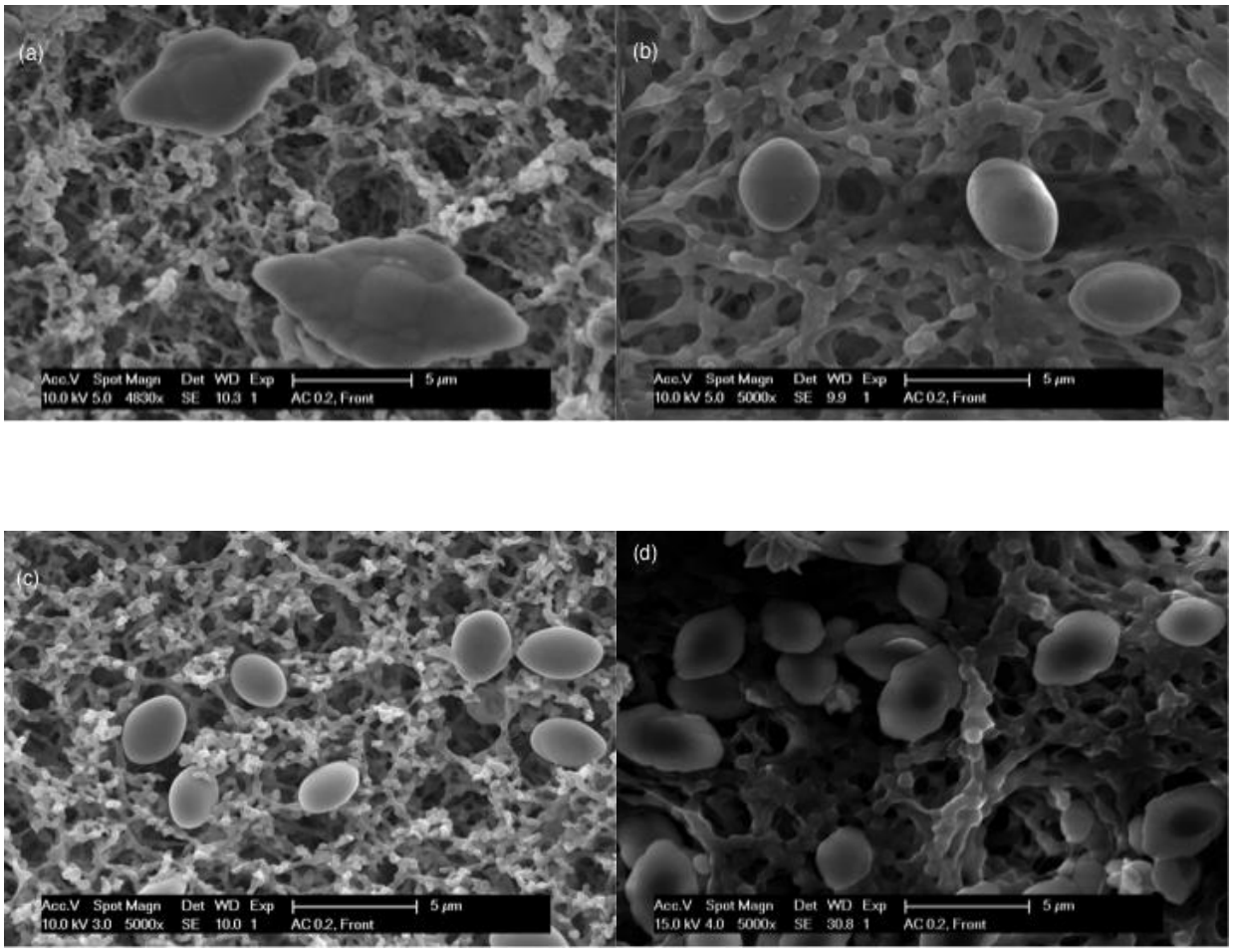

Figure 8.1 SEM images of $BaSO_4$ particles formed in 0.5M NaCl solution with (a) no antiscalants; (b) 10 mg/L SPPCA; (c) 10 mg/L PMA and (d) 10 mg/L ethylene glycol

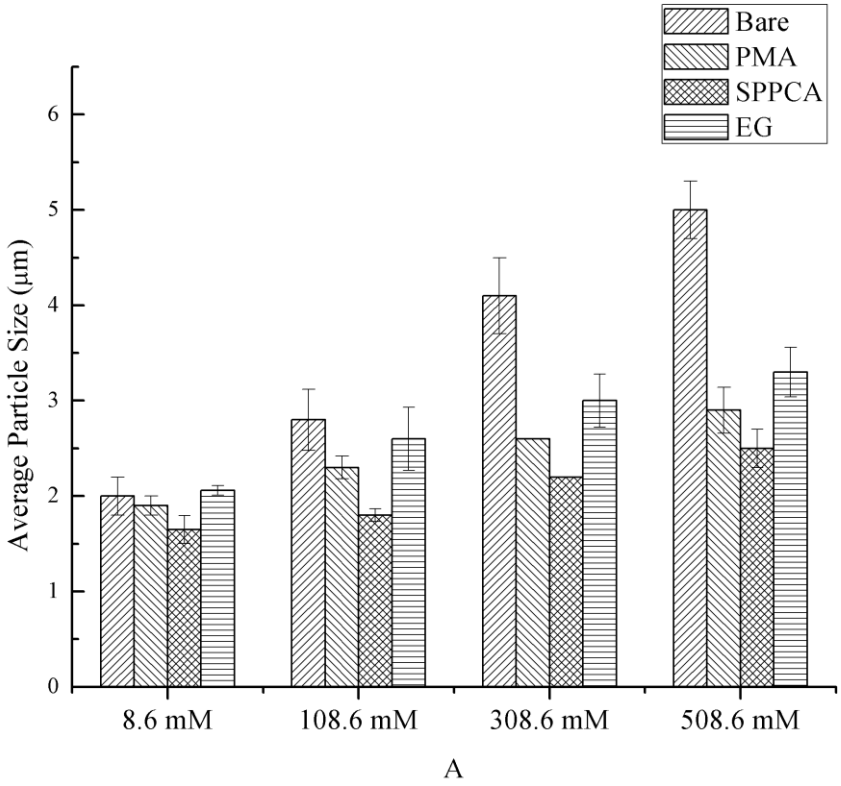

Figure 8.2 Impact of antiscalants on average particle size of $BaSO_4$ formed at different NaCl concentrations

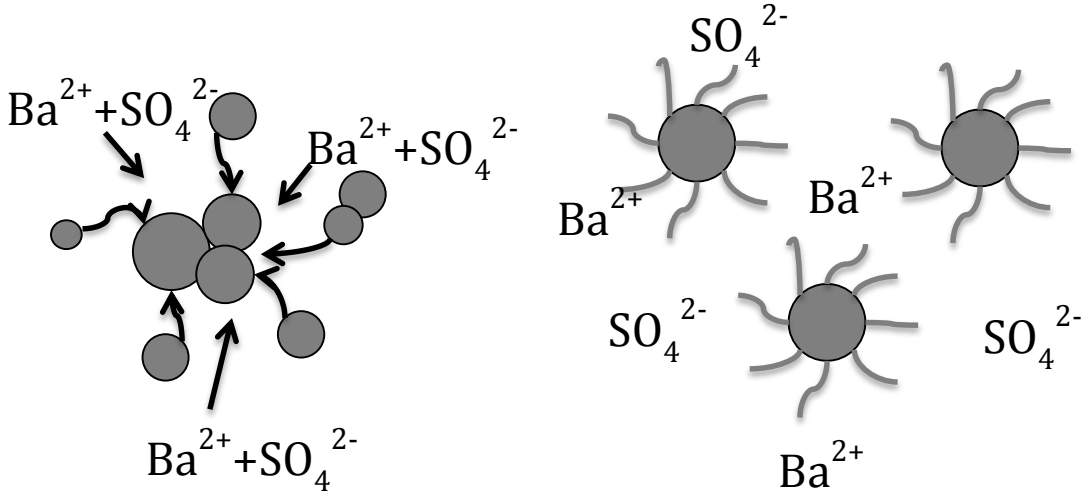

Figure 8.3 Schematic diagram of $BaSO_4$ formation at high ionic strength with (a) no antiscalants; (b) polymeric antiscalants.

8.3.2 Mobility of bare $BaSO_4$ through proppant sand media

Considering the high salinity of shale formation brine, it is important to investigate the impact of background salt concentration on the mobility of barite particles through the proppant pack. Column experiments with barite feed solution formed in the absence of antiscalants revealed that the mobility of $BaSO_4$ particles decreased with background salt concentration. As can be seen in Figure 8.4, when background NaCl concentration was below 0.1M, gradual increase in $BaSO_4$ concentration in the effluent was observed, suggesting the "blocking" of retention sites by previously deposited $BaSO_4$ particles [22]. The "blocking effect" decreases with the increase of background NaCl Concentration, which is attributed to the reduced blocking effect caused by compression of electrical double layer surrounding the surface of barite particles [23]. When 0.5M NaCl was added to the feed solution, negligible breakthrough of $BaSO_4$ particles was observed even after 30 PV of fluid passing through the column.

The effect of ionic strength on the transport of colloidal particles through porous sand media has been widely studied and can be explained by the classical DLVO theory [24-26]. However, elevated salt concentration used in this study not only reduced the electrostatic interactions, but also increased the size of $BaSO_4$ particles. The increased particle size results in greater tendency of particle-collector collisions, while the reduced electrostatic repulsion leads to greater fraction of the collisions resulting in attachment.

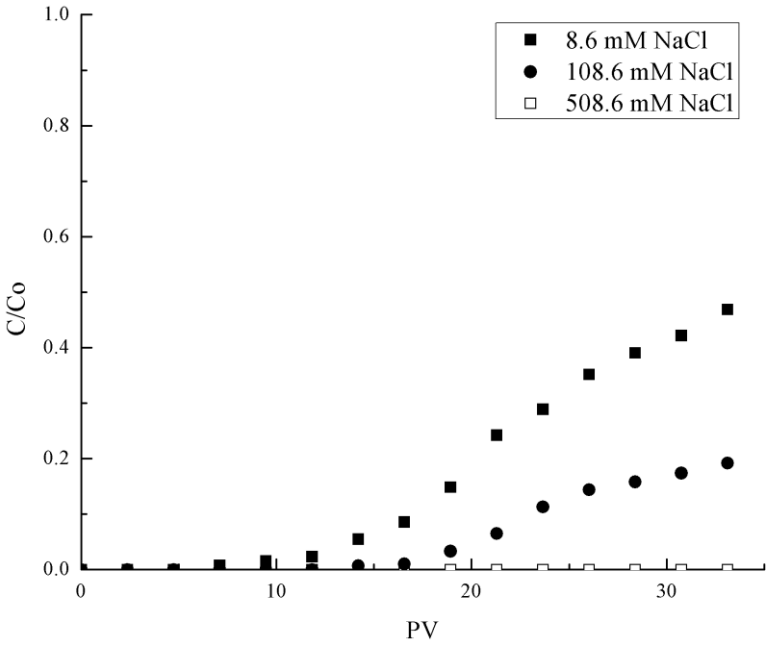

Figure 8.4 Impact of ionic strength on $BaSO_4$ transport through proppant media

8.3.3 Impact of antiscalants on $BaSO_4$ particles transport through proppant sand media

Although the selected antiscalants could not inhibit $BaSO_4$ precipitation under the experimental conditions used in this study, it is important to evaluate the transport of antiscalant-modified barite particles through proppant sand media in order to understand the anti-deposition function of antiscalants and fate of barite particles when antiscalants are added to hydraulic fracturing fluid.

The effect of selected antiscalants on transport of barite particles through proppant sand media was compared at 0.5M background NaCl concentration and pH 7. As shown in Figure 8.5, both polymeric antiscalants (i.e., PMA and SPPCA) can significantly improve mobility of barite particles at high ionic strength. However, the presence of EG did not yield any measurable barite in the effluent throughout the experiment, suggesting that EG that is commonly employed as

antiscalant in shale gas extraction had no impact on mobility of $BaSO_4$ through the proppant pack. The lack of mobility of bare and EG-modified barite particles suggests that these particles are most like retained at the tail-end of the proppant pack during flowback period, which may potentially cause significant reduction in well productivity.

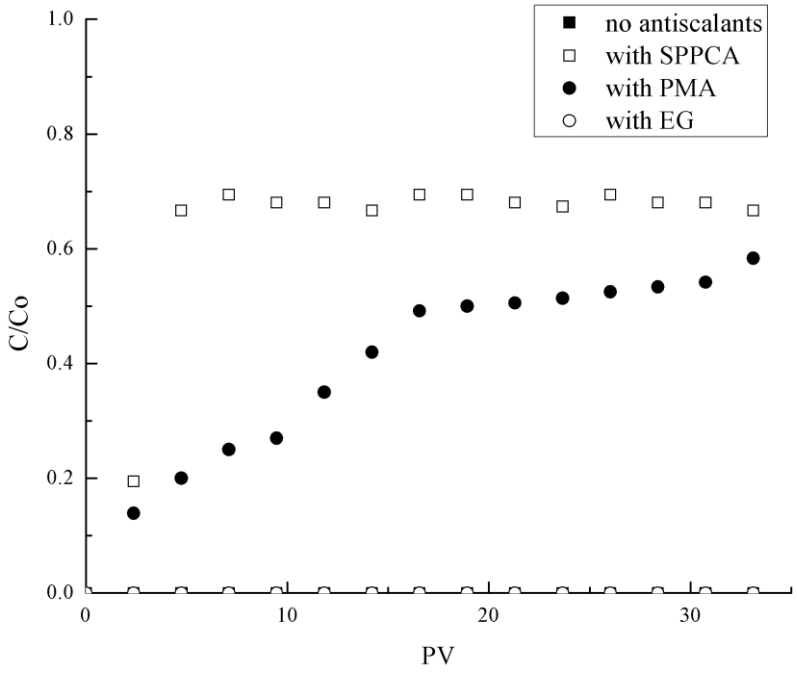

Figure 8.5 Impact of SPPCA and PMA on $BaSO_4$ transport through proppant column at pH 7 and high background NaCl concentration of 508.6 mM

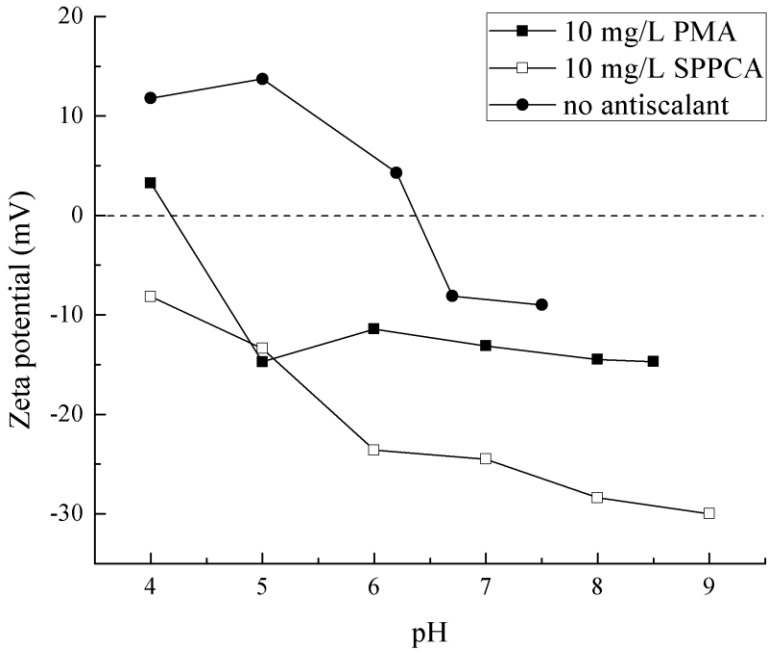

Figure 8.6 Zeta potential of $BaSO_4$ particles formed in the presence of PMA and SPPCA.

Zeta potential of barite particles was measured to determine the impact of polymeric antiscalants on the surface charge of barite particles. As illustrated in Figure 8.6, presence of both SPPCA and PMA resulted in the shift of point of zero charge of freshly precipitated $BaSO_4$ towards lower pH. Because the surface of silica that is most commonly used as proppant is negatively charged at pH above 3 [27], particles with greater negative surface charge will exhibit greater mobility because of particle-collector and particle-particle electrostatic repulsion interaction. Electrostatic interaction between particle and collector and between barite particles was calculated using classic DLVO theory with the assumption of sphere-plate geometry [28]. Zeta potential of silica particles was calculated for NaCl concentration of 0.5M using Graham's equation, assuming a constant surface charge density[24, 27-29]. These calculations revealed that all electrostatic energy barriers in the presence of 508.6mM NaCl are zero for all pH conditions (pH=4.0-8.5) evaluated in this study. This finding is consistent with previous studies that the

electrostatic repulsion is essentially screened for IS>0.3M [22, 24]. While the variation in the surface charge properties may be beneficial to prevent the deposition of barite particles in porous sand media for relatively dilute solutions (e.g., groundwater), it is not an important factor for the conditions that are prevalent for for unconventional gas extraction from deep formations.

As the electrostatic interactions are screened at high salt concentrations that are typical for deep formation brines, the enhanced mobility observed for polymer-modified barite particles suggests the existence of steric repulsion that remains strong even at high ionic strength [24]. Accordingly, the monomeric EG that is too small to provide steric repulsion has no impact on barite mobility through proppant sand media at high background NaCl concentration [30]. The results in Figure 8.5 also indicate that SPPCA is more effective at enhancing the mobility of barite particles through proppant media than PMA, which can be attributed to the greater steric repulsion induced by SPPCA with higher molecular weight [24].

Mobility of barite particles formed in the presence of PMA and SPPCA is very dependent on the solution pH. As can be seen in Figure 8.7, mobility of barite particles increases with pH for both polymeric antiscalants tested in this study. The change is particularly dramatic in the case of PMA where no breakthrough of barite particles was observed at pH 4 and rapid breakthrough was observed at pH 8.5 (Fig. 8.7b). The increase in pH can result in deprotonation of polyelectrolytes, which affects the electrostatic properties and potentially the conformation of polymer itself [13, 31].

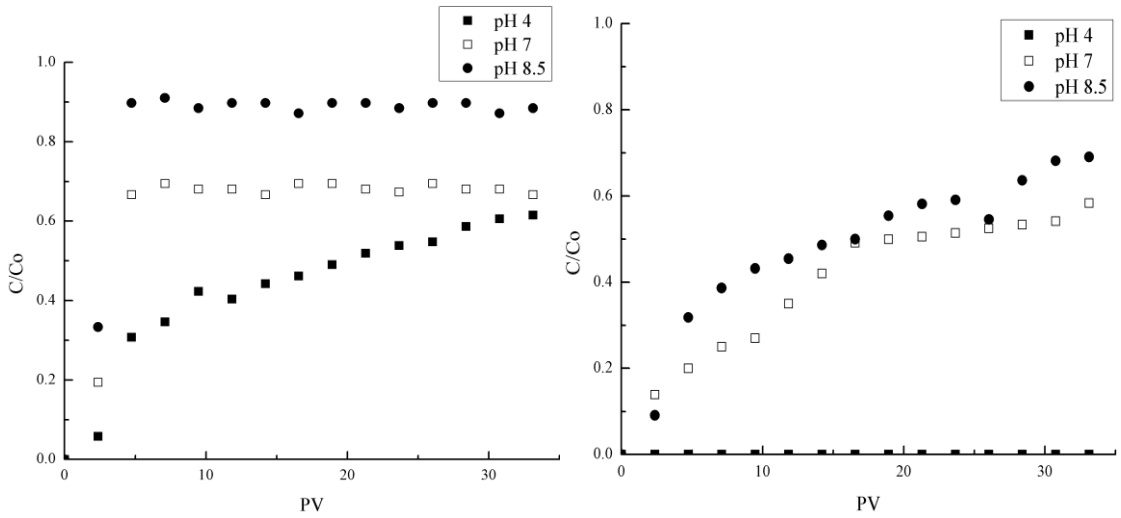

Figure 8.7 Breakthrough of (a) SPPCA and (b) PMA modified $BaSO_4$ particles as a function of pH at background NaCl concentration of 508.6mM.

Because the electrostatic repulsion has minimal influence on barite deposition at high ionic strength evaluated in this study, the difference in the mobility of polymer-modified $BaSO_4$ at various pH levels is likely due to the conformation of the polymers. It was reported previously that conformational transition of polymer was attributed to the turning of polymer charge with pH [32]. For highly charged polymers, extended-coil conformation occurs due to electrostatic repulsion between the charged units, while the polymer chain generally collapses into a compact coil at reduced charge density [32, 33]. Deprotonation of the carboxyl group of carboxylic polymeric antiscalants at higher pH can increase the charge density of the polymer, which results in the extended-coil conformation. The increase in thickness of the polymer "brush" layer can in turn result in greater particle-collector and particle-particle steric repulsion, which in turn reduces the retention of barite particles by the proppant media [30].

8.4 CONCLUSIONS

The impact of antiscalants on the formation of barite scales and the transport of barite particles through proppant pack was evaluated in this study. Antiscalants that are generally used as threshold inhibitors are unlikely to prevent formation of barite particles because of supersaturation levels that are typical for unconventional gas extraction. When sulfate-rich fluid is used for hydraulic fracturing, formation of barite particles is inevitable and these particles will travel through the proppant pack during the flowback period. While the antiscalants are incapable of inhibiting barite formation, they can reduce the size and alter the morphology of barite particles.

The mobility of barite particles through saturated porous proppant pack is important to estimate the potential for well plugging by barite scales. This study evaluated the transport of $BaSO_4$ particles formed at various conditions to elucidate the role of antiscalants in controling $BaSO_4$ transport in the subsurface and the fate of barite particles when sulfate-rich hydraulic fracturing fluid is used. The breakthrough experiments revealed that the retention of bare $BaSO_4$ particles in proppant pack at high background NaCl concentration (508.6 mM) is significant because of their large size and screened electrostatic repulsion. Ethylene glycol, which is often used in shale gas extraction to control scaling in the subsurface, has limited impact on the mobility of barite particles through proppant pack at high ionic strength (I=0.5M). Therefore, in the absence of antiscalants or in the presence of commonly used ethylene glycol, $BaSO_4$ particles that are formed in the subsurface are most likely to be retained by the tail-end section of the proppant pack along the shale fractures, which is detrimental to gas well productivity.

On the other hand, polymeric antiscalants, such as PMA and SPPCA, can mitigate the retention of $BaSO_4$ particles in proppant sands even at high background NaCl concentration by

limiting the particle size and inducing stronger steric repulsion. The mobility of polymer-modified barite particles increases with pH, which is likely due to the extended-coil conformation of polymer. The enhanced mobility of polymer-modified $BaSO_4$ particles is beneficial to reduce the damage of well productivity.

9.0 SUMMARY, CONCLUSIONS AND FUTURE WORK

9.1 SUMMARY AND CONCLUSIONS

Unconventional natural gas extraction from Marcellus Shale produces large quantities of wastewater (i.e., flowback and produced water), which raises significant environmental concerns about wastewater management. Due to the lack of Class II UIC wells in Pennsylvania, flowback water is commonly reused for hydraulic fracturing. As only 10-30% of the injection fluid is recovered during the flowback period, it is necessary to supplement this impaired water for hydraulic fracturing of subsequent wells. As abundant AMD is present in the vicinity of planned shale gas wells, it can serve as a make-up water source to reduce the need for fresh water utilization and the cost of water transport.

The overall objective of this study was to demonstrate the feasibility of using AMD for flowback water reuse. Specific objectives of this work were to: (1) conduct bench-scale experiments to examine the kinetics and equilibrium of chemical reactions that may occur when flowback water and AMD are mixed; (2) evaluate the feasibility of membrane microfiltration for the removal of suspended solids generated after mixing flowback water and AMD; (3) demonstrate the feasibility of the proposed co-treatment process of flowback water and AMD in a pilot-scale system; and (4) evaluate the fate of barite that may form in the subsurface when sulfate is present in the fracturing fluid with specific emphasis on the impact of antiscalant on the formation and transport of barite in the unconventional gas wells.

9.1.1 Utilization of abandoned mine drainage for Marcellus Shale flowback water reuse

Marcellus Shale flowback water, characterized by high concentrations of total dissolved solids, radioactive elements and organic matter, is generally reused for hydraulic fracturing in Pennsylvania. Abandoned mine drainage (AMD), a wastewater source that is often located near permitted shale gas well sites, can serve as a make-up water for flowback water reuse.

Both laboratory and pilot-scale studies revealed that sulfate concentration can be controlled below 100 mg/L by adjusting the mixing ratio between flowback water and AMD. Celestite precipitation is very slow and should not be considered for the control of sulfate in the finished water. Pilot-scale study demonstrated that coagulation/flocculation is an effective process to assist in the removal of suspended solids after flowback water and AMD are mixed. Fe^{3+} contained in the AMD can serve as a coagulant to enhance the removal of suspended solids, during which Fe^{2+} is co-precipitated and the total iron is reduced to a desirable level.

Barite particles generated in the proposed co-treatment process incorporate over 99% of radium present in the flowback water through coprecipitation reactions, which creates a management problem for the radioactive solid waste. This study demonstrated that sludge recycling can be used to increase the size of barite particles formed by mixing flowback water and AMD so that they can be used as weighting agent in drilling mud. This alternative management approach for Ra-enriched barite waste can be used to offset

the treatment cost, promote flowback water reuse, reduce environmental impacts of AMD and reduce pressure on fresh water sources. In addition, this approach can be used in the centralized wastewater treatment plants that employ sulfate precipitation for flowback water treatment.

9.1.2 Feasibility of membrane microfiltration to assist reuse of Marcellus Shale flowback water

Feasibility of using polymeric microfiltration membranes to assist in the reuse of flowback water was evaluated in this study. Severe membrane fouling was observed for two out of three flowback water samples evaluated in this study. This study revealed that the presence of iron-based sub-micron colloidal particles that may be present in the early flowback water is the main reason for rapid decline of permeate flux. Stability of these sub-micron colloidal particles in the flowback water at high ionic strength is attributed to organic coating on the particle surface.

Bench-scale cross-flow filtration with ceramic microfiltration membranes was evaluated for direct filtration of Marcellus Shale flowback water that does not contain submicron particles. This study revealed that strength of the aggregated particulate matter in the flowback water is a key factor that leads to severe permeate flux decline during cross-flow filtration.

Therefore, it is necessary to assess the presence of submicron particles and evaluate the floc strength of the particles in the flowback water when considering microfiltration for flowback water treatment.

9.1.3 Impact of antiscalants on the fate of barite in the shale gas wells

The impact of antiscalants on the formation of barite particles and their transport through the proppant pack was evaluated using bench-scale experiments combined with modeling efforts. Antiscalants that are generally used as threshold inhibitors cannot prevent formation of barite particles in the subsurface because of high barite supersaturation that is typical for shale gas extraction. However, the presence of antiscalants can alter the morphology and limit the size of barite particles at high ionic strength.

This study revealed that the mobility of barite particles formed in the absence of antiscalants through the proppant pack at high ionic strength (508.6 mM) was very low because of large size of barite particles and screened electrostatic repulsion. Ethylene glycol that is a common scale inhibitor used in shale gas extraction has virtually no impact on the mobility of barite particles through the proppant pack.

On the other hand, polymeric antiscalants, such as PMA and SPPCA, can effectively reduce the retention of barite particles in the proppant pack even at high background NaCl concentration by limiting the particle size and inducing stronger steric repulsion. The mobility of polymer-modified barite particles increases with pH, which is likely due to the extended-coil conformation of polymer.

9.2 KEY CONTRIBUTIONS

This study demonstrated the feasibility of using AMD as a make-up water source for flowback water reuse with emphasis on elucidating the scientific and engineering aspects of the co-treatment of flowback water and AMD.

The specific contributions of this dissertation are summarized as follows:

- Overview of the challenges and concerns associated with the co-treatment of flowback water and AMD.
- Critical review of the current and future management approaches for Marcellus Shale flowback water.
- Understanding of barium sulfate precipitation kinetics and equilibrium when flowback water and AMD are mixed based on both laboratory and pilot-scale studies.
- Pilot-scale demonstration of the co-treatment of flowback water and AMD with emphasis on meeting the prerequisite finished water quality.
- Proposed and validated a new approach for the reuse of Ra-enriched barite generated by mixing flowback water and AMD.
- Evaluated feasibility of membrane microfiltration to separate the solids in the flowback water or those formed by mixing flowback water and AMD and provided scientific evidence of the membrane fouling mechanisms.
- Investigated the fate of barite that may form in the subsurface with emphasis on the impact of antiscalants on its formation and transport through the proppant pack.

9.3 FUTURE WORK

Several promising directions for future work to broaden the findings of this study related to co-treatment of flowback water and AMD and application of membrane microfiltration for flowback water reuse include:

- Fundamental understanding of the source and fate of sub-micron colloidal particles that caused severe microfiltration membrane fouling
- Development of optimization the pre-treatment process to mitigate the fouling of microfiltration membranes
- Development of a predictive model for the size of barium sulfate particles that form during the co-treatment of flowback water and AMD based on the fundamental understanding of the particle growth under relevant process conditions
- Further understanding of fundamental interactions between polymeric antiscalants and barium sulfate particles to fully understand the anti-scaling mechanisms.

The presence of submicron particles in flowback water is a key concern when considering membrane microfiltration for solids removal from flowback water. This study found that the stable colloidal particles might exist in early flowback water and mainly consist of iron oxide (Chapter 5). It would be very important to understand the source and fate of submicron colloids in flowback water. The composition of the

colloidal particles contained in flowback water generated at different days can be analyzed using SEM/EDX analysis and correlated with the corresponding flowback water quality. In addition, it is important to track the dissolved iron concentration in the flowback water to identify whether the presence of submicron particles is because of iron hydroxide precipitation.

Possible pretreatment of the flowback water to minimize membrane fouling may involve coagulation/flocculation and/or oxidation to mitigate the membrane fouling caused by submicron particles. This study found that oxidation with hydrogen peroxide could destabilize the colloidal particles in flowback water, which effectively mitigated membrane fouling. Other oxidants like free chlorine, chlorine dioxide or ozone may be even more effective in accomplishing this goal. Alternatively, coagulation/flocculation as a pre-treatment process for the mitigation of membrane fouling is worth evaluating. Chapter 5 indicated that the charge neutralization is not effective in destabilizing colloidal particles that are presents in flowback water because of the organic coatings on the colloid surfaces. Therefore, sweep flocculation may be an effective mechanism to control these sub-micron colloidal particles. Chapter 6 demonstrated that the floc strength of the particulate matter in flowback water can significantly affect the performance of membrane filtration. Therefore, it will be necessary to optimize the coagulation process to yield more stable flocs. A potential work may include evaluation of the impact of pH, type and dosage of antiscalants, and shear conditions using the system that combines coagulation/flocculation and microfiltration.

It would be very useful to develop a predictive model for the size of barite particles generated in the proposed co-treatment of flowback water and AMD. The pilot-

scale test conducted in this study demonstrated that sludge recycling can be used to grow barium sulfate particles to a larger size and enable the use of Ra-enriched barite as a weighting agent in drilling mud formulation. A predictive model for the size of barium sulfate particles as a function of operational parameters (e.g., saturation index, mixing speed, TSS, ionic strength and so forth) could be used to guide the design and operation of the full-scale treatment systems. Such model would have ramification for other treatment process that involve precipitation reactions (e.g., softening).

The effect of antiscalants on the inhibition of barium sulfate formation has been widely studied, but the exact anti-scaling mechanisms are still not well understood. To advance the understanding of anti-scaling mechanisms of polymeric antiscalants, it will be helpful to evaluate the interaction between antiscalants and barium sulfate particles. Future work could focus on the adsorption of selected of antiscalants as a function of pH and temperature using classical adsorption experiments with freshly and aged barite crystals to provide insight into thermodynamics of the adsorption process and establish the extent of physical or chemical adsorption processes in an effort to explain the differences in barite nucleation and crystal growth. These experiments could also guide the development of new antiscalants that are particularly suitable barium sulfate and sulfates in general.

APPENDIX A

Supporting Information for Chapter 7

A.1 Bench-scale beaker test

Bench-scale beaker tests were conducted to evaluate the reaction rate as a function of saturation index ($SI = \log \frac{\text{Ion Activity Product}}{K_{sp}}$), using various flowback water and AMD samples collected previously as well as synthetic $BaCl_2$ and Na_2SO_4 solution. The characteristics of flowback water and AMD samples used for these bench-scale tests are listed in Table A1. The experimental conditions for the bench-scale tests were designed to assess the sulfate reaction rate as a function of saturation index and are listed in Table A2. The saturation index was calculated with PHREEQC software with the Pitzer database.

Table A1. Characteristics of the flowback water and AMD used for beaker tests

	Flowback Water			AMD			
	A	B	C	1	2	3	4
Na^{+}(mg/L)	27,946	14,913	81,442	281	104	145	1,899
Ca^{2+}(mg/L)	15,021	2,973	32,901	353	76	77	50
Mg^{2+}(mg/L)	1,720	531	3,513	53	49	38	104
Ba^{2+}(mg/L)	236	850	6,256	-	-	0	-
Sr^{2+}(mg/L)	1,799	874	11,910	-	1.5	0.7	-
Cl^{-}(mg/L)	104,300	35,380	188,728	101	71	252	-
SO_4(mg/L)				696	709	309	560
pH	6.43	7.38	3.86	5.97	6.14	6.12	2.82

Table A2. Experimental conditions for the bench-scale beaker tests

Description	SI for BaSO4
20% FB A+80% AMD1	2.58
20% FB B+80% AMD2	3.61
40% FB B+60% AMD2	3.56
50% FB B+50% AMD2	3.46
10% FB B+90% AMD3	3.23
20% FB B+80% AMD3	3.26
25% FB B+75% AMD3	3.25
70% FB B+30% AMD3	2.89
10% FB C+90% AMD4	3.71
2mM $BaCl_2$+2mM Na_2SO_4	4.17
4mM BaCl2+4mM Na_2SO_4	4.65
5mM BaCl2+5mM Na_2SO_4	4.81

BIBLIOGRAPHY

Chapter 1

1 He, C.; Zhang, T.; Vidic, R. D., Use of abandoned mine drainage for the development of unconventional gas resources. *Disruptive Science and Technology* (2013), *1*(4), 169-176.

2 Vidic, R. D.; Brantley, S. L.; Vandenbossche, J. M.; Yoxtheimer, D.; Abad, J. D., Impact of shale gas development on regional water quality. Science (2013), 340(6134).

3 U.S. Energy Information Administration, Annual Energy Outlook. (2013), DOE/EIA-0383.

4 King, G. E., Thirty years of gas shale fracturing: What have we learned? SPE Annual Technical Conference and Exhibition (2010), SPE-133456-MS.

5 Arthur, J. D.; Bohm, B.; Layne, M., Hydraulic fracturing considerations for natural gas wells of the Marcellus Shale. Groundwater Protection Council Annual Forum (2008).

6 de Witt Jr, W. Principal oil and gas plays in the Appalachian Basin (Province 131); 1993.

7 Milici, R. C.; Swezey, C., Assessment of appalachian basin oil and gas resources: Devonian shale-middle and upper paleozoic total petroleum system. U.S. Geological Survey. (2006), Open-file Report Series, 2006-1237.

8 Gregory, K. B.; Vidic, R. D.; Dzombak, D. A., Water management challenges associated with the production of shale gas by hydraulic fracturing. Elements (2011), 7(3), 181-186.

9 Barbot, E.; Vidic, N. S.; Gregory, K. B.; Vidic, R. D., Spatial and temporal correlation of water quality parameters of produced waters from Devonian-age shale following hydraulic fracturing. Environmental Science & Technology (2013), 47(6), 2562-2569.

10 PA DEP, Wastewater treatment requrements. (2010), 25 PA Code 95.

11 U.S. Geological Survey, Pennsylvania. (1999), FS-039–99.

12 Gray, N. F. Environmental impact and remediation of acid mine drainage: a management problem. Environmental Geology (1997), 30(1-2), 62-71.

13. Kondash, A. J.; Warner, N. R.; Lahav, O.; Vengosh, A., Radium and barium removal through blending hydraulic fracturing fluids with acid mine drainage. Environmental Science & Technology (2013), 48(2), 1334-1342.

Chapter 2

1 U.S. Department Of Energy, Modern Shale Gas Development in the United States: A Primer. (2009).

2 U.S. Energy Information Administration, Annual Energy Outlook. (2013), DOE/EIA-0383.

3 Gregory, K. B.; Vidic, R. D.; Dzombak, D. A., Water management challenges associated with the production of shale gas by hydraulic fracturing. *Elements* (2011), *7*(3), 181-186.

4 Vidic, R. D.; Brantley, S. L.; Vandenbossche, J. M.; Yoxtheimer, D.; Abad, J. D., Impact of shale gas development on regional water quality. *Science* (2013), *340*(6134).

5 Soeder, D. J., Porosity and permeability of eastern Devonian gas shale. *SPE Formation Evaluation* (1988), *3*(01), 116-124.

6 Ameri, S.; Aminian, K.; Miller, J.; Doricich, D.; Yost, A., A systematic approach for economic development of the devonian shale gas resources. SPE Eastern Regional Meeting. (1985).

7 Kidder, M.; Palmgren, T.; Ovalle, A.; Kapila, M., Treatment options for reuse of frac flowback and produced water from shale. *World oil* (2011), *232*(7).

8 Barbot, E.; Vidic, N. S.; Gregory, K. B.; Vidic, R. D., Spatial and temporal correlation of water quality parameters of produced waters from Devonian-age shale following hydraulic fracturing. *Environmental Science & Technology* (2013), *47*(6), 2562-2569.

9 Miller, D. J.; Huang, X.; Li, H.; Kasemset, S.; Lee, A.; Agnihotri, D.; Hayes, T.; Paul, D. R.; Freeman, B. D., Fouling-resistant membranes for the treatment of flowback water from hydraulic shale fracturing: a pilot study. *Journal of Membrane Science* (2013), *437*, 265-275.

10 Arthur, J. D.; Bohm, B.; Layne, M., Hydraulic fracturing considerations for natural gas wells of the Marcellus Shale. Groundwater Protection Council Annual Forum (2008).

11 Kargbo, D. M.; Wilhelm, R. G.; Campbell, D. J., Natural gas plays in the Marcellus shale: Challenges and potential opportunities. *Environmental Science & Technology* (2010), *44*(15), 5679-5684.

12 Johnson, D. B., Chemical and microbiological characteristics of mineral spoils and drainage waters at abandoned coal and metal mines. *Water, Air and Soil Pollution: Focus* (2003), *3*(1), 47-66.

13 Gray, N., Acid mine drainage composition and the implications for its impact on lotic systems. *Water Research* (1998), *32*(7), 2122-2134.

14 U.S. Environmental Protection Agency, Acid Mine Drinage Prediction. (2004), EPA530-R-94-036.

15 Singer, P. C.; Stumm, W., Acidic mine drainage: the rate-determining step. *Science* (1970), *167*(3921), 1121-1123.

16 Moses, C. O.; Herman, J. S., Pyrite oxidation at circumneutral pH. *Geochimica et Cosmochimica Acta* (1991), *55*(2), 471-482.

17 Evangelou, V., *Pyrite oxidation and its control*. CRC Press, Boca Raton, FL, (1995).

18 U.S. Geological Survey, Pennsylvania. (1999), FS-039–99.

19 Berghorn, G. H.; Hunzeker, G. R., Passive Treatment Alternatives for Remediating Abandoned ‐ Mine Drainage. *Remediation Journal* (2001), *11*(3), 111-127.

20 Cravotta, C. A., Dissolved metals and associated constituents in abandoned coal-mine discharges, Pennsylvania, USA. Part 1: Constituent quantities and correlations. *Applied Geochemistry* (2008), *23*(2), 166-202.

21 Tam, K.; Tiu, C., Role of ionic species and valency on the steady shear behavior of partially hydrolyzed polyacrylamide solutions. *Colloid and Polymer Science* (1990), *268*(10), 911-920.

22 Kamel, A.; Shah, S. N., Effects of salinity and temperature on drag reduction characteristics of polymers in straight circular pipes. *Journal of Petroleum Science and Engineering* (2009), *67*(1), 23-33.

23 Paktinat, J.; O'Neil, B. J.; Aften, C. W.; Hurd, M. D., Critical evaluation of high brine tolerant additives used in shale slickwater fracs. SPE Production and Operations Symposium. (2011), SPE-141356-MS.

24 Rassenfoss, S., From flowback to fracturing: Water recycling grows in the Marcellus shale. *Journal of Petroleum Technology* (2011), *63*(7), 48-51.

25 Phillips, L. E.; Lappin-Scott, H. M., Enrichment and characterisation of sulfate-reducing bacteria from sandstone rock cores from the UK Continental shelf. *FEMS microbiology reviews* (1997), *20*(3-4), 415-423.

26 Cord-Ruwisch, R.; Kleinitz, W.; Widdel, F., Sulfate-reducing bacteria and their activities in oil production. *Journal of Petroleum Technology* (1987), *39*(01), 97-106.

27 Baldi, F.; Pepi, M.; Burrini, D.; Kniewald, G.; Scali, D.; Lanciotti, E., Dissolution of Barium from Barite in Sewage Sludges and Cultures of Desulfovibrio desulfuricans. *Applied and Environmental Microbiology* (1996), *62*(7), 2398-2404.

28 Phillips, E. J.; Landa, E. R.; Kraemer, T.; Zielinski, R., Sulfate-reducing bacteria release barium and radium from naturally occurring radioactive material in oil-field barite. *Geomicrobiology Journal* (2001), *18*(2), 167-182.

29 Langmuir, D.; Riese, A. C., The thermodynamic properties of radium. *Geochimica et Cosmochimica Acta* (1985), *49*(7), 1593-1601.

30 Silva, J.; Matis, H.; Kostedt IV, W.; Watkins, V., Produced water pretreatment for water recovery and salt production. Research Partnership for Secure Energy for America, Final Report. (2012), 08122-36.

31 Doerner, H.; Hoskins, W. M., Co-precipitation of radium and barium sulfates. *Journal of the American Chemical Society* (1925), *47*(3), 662-675.

32 Code of Federal Regulations, Standards for water withdrawls. In 2012; Vol. C.F.R. § 806.23.

33 PA DEP, White paper: Utilization of mine influenced water for natural gas extraction activities. (2013).

34 Jones, F.; Oliviera, A.; Parkinson, G.; Rohl, A.; Stanley, A.; Upson, T., The effect of calcium ions on the precipitation of barium sulphate 1: Calcium ions in the absence of organic additives. *Journal of Crystal Growth* (2004), *262*(1), 572-580.

35 He, C.; Wang, X.; Liu, W.; Barbot, E.; Vidic, R. D., Microfiltration in recycling of Marcellus Shale flowback water: Solids removal and potential fouling of polymeric microfiltration membranes. *Journal of Membrane Science* (2014), *462*, 88-95.

36 Zheng, X., Optimization of treatment options to enable the use of abandoned mine drainage (AMD) for hydraulic fracturing in Marcellus Shale. Master Thesis, University of Pittsburgh. (2013).

Chapter 3

1 U.S. Energy Information Administration, Drilling Sideways: A review of horizontal well technology and its domestic application. (1993), DOE/EIA-TR-0565.

2 King, G. E., Thirty years of gas shale fracturing: What have we learned? *SPE Annual Technical Conference and Exhibition* (2010), SPE-133456-MS.

3 Arthur, J. D.; Bohm, B.; Layne, M., Hydraulic fracturing considerations for natural gas wells of the Marcellus Shale. Groundwater Protection Council Annual Forum (2008).

4 Milici, R. C.; Swezey, C., Assessment of appalachian basin oil and gas resources: Devonian shale-middle and upper paleozoic total petroleum system. U.S. Geological Survey. (2006), Open-file Report Series, 2006-1237.

5 U.S. Energy Information Administration, Annual Energy Outlook. (2013), DOE/EIA-0383.

6 Gregory, K. B.; Vidic, R. D.; Dzombak, D. A., Water management challenges associated with the production of shale gas by hydraulic fracturing. *Elements* (2011), *7*(3), 181-186.

7 Vidic, R. D.; Brantley, S. L.; Vandenbossche, J. M.; Yoxtheimer, D.; Abad, J. D., Impact of shale gas development on regional water quality. *Science* (2013), *340*(6134).

8 He, C.; Zhang, T.; Vidic, R. D., Use of abandoned mine drainage for the development of unconventional gas resources. *Disruptive Science and Technology* (2013), *1*(4), 169-176.

9 He, C.; Li, M.; Liu, W.; Barbot, E.; Vidic, R., Kinetics and Equilibrium of Barium and Strontium Sulfate Formation in Marcellus Shale Flowback Water. *Journal of Environmental Engineering* (2014), *140*(5), B4014001.

10 Kidder, M.; Palmgren, T.; Ovalle, A.; Kapila, M., Treatment options for reuse of frac flowback and produced water from shale. *World oil* (2011), *232*(7).

11 Barbot, E.; Vidic, N. S.; Gregory, K. B.; Vidic, R. D., Spatial and temporal correlation of water quality parameters of produced waters from Devonian-age shale following hydraulic fracturing. *Environmental Science & Technology* (2013), *47*(6), 2562-2569.

12 Nicot, J.-P.; Scanlon, B. R., Water use for shale-gas production in Texas, US. *Environmental science & technology* (2012), *46*(6), 3580-3586.

13 Ferrar, K. J.; Michanowicz, D. R.; Christen, C. L.; Mulcahy, N.; Malone, S. L.; Sharma, R. K., Assessment of effluent contaminants from three facilities discharging Marcellus Shale wastewater to surface waters in Pennsylvania. *Environmental Science & Technology* (2013), *47*(7), 3472-3481.

14 Wilson, J. M.; VanBriesen, J. M., Oil and gas produced water management and surface drinking water sources in Pennsylvania. *Environmental Practice* (2012), *14*(04), 288-300.

15 Warner, N. R.; Christie, C. A.; Jackson, R. B.; Vengosh, A., Impacts of shale gas wastewater disposal on water quality in western Pennsylvania. *Environmental Science & Technology* (2013), *47*(20), 11849-11857.

16 PA DEP, Wastewater treatment requrements. (2010), 25 PA Code 95.

17 Kuijvenhoven, C. S., P.; Padmasiri, S.; Fedotov, V.; Hassing, T.; Hagemeijer, P.; Meyer, C., Treatment of water from fracturing operations for unconventional gas production. Shale Gas Water Management Conference. (2011).

18 Vidic, R. D. H., T.D.; Hughes, S. , Techno-economic assessment of water management solutions: Assessing the economics of technologies, and emerging solutions for shale gas water management. Marcellus Initiative Conference, Pittsburgh, PA. (2011).

19 Silva, J.; Matis, H.; Kostedt IV, W.; Watkins, V., Produced water pretreatment for water recovery and salt production. Research Partnership for Secure Energy for America, Final Report. (2012), 08122-36.

20 Langmuir, D.; Riese, A. C., The thermodynamic properties of radium. *Geochimica et Cosmochimica Acta* (1985), *49*(7), 1593-1601.

21 Sturchio, N.; Banner, J.; Binz, C.; Heraty, L.; Musgrove, M., Radium geochemistry of ground waters in Paleozoic carbonate aquifers, midcontinent, USA. *Applied Geochemistry* (2001), *16*(1), 109-122.

22 Zhang, T.; Gregory, K.; Hammack, R. W.; Vidic, R. D., Co-precipitation of radium with barium and strontium sulfate and its impact on the fate of radium during treatment of produced water from unconventional gas extraction. *Environmental Science & Technology* (2014), *48*(8), 4596-4603.

23 Akovali, Y., Nuclear data sheets for A= 226. *Nuclear Data Sheets* (1996), *77*(2), 433-470.

24 Rowan, E.; Engle, M.; Kirby, C.; Kraemer, T., Radium content of oil-and gas-field produced waters in the Northern Appalachian basin (USA)—Summary and discussion of data. US Geological Survey Scientific Investigations Report. (2011), 2011-5135.

25 Laul, J., Natural radionuclides in groundwaters. *Journal of Radioanalytical and Nuclear Chemistry* (1992), *156*(2), 235-242.

26 Ames, L. L.; McGarrah, J. E.; Walker, B. A., Sorption of trace constituents from aqueous solutions onto secondary minerals. II. Radium. *Clays and Clay Minerals* (1983), *31*(5), 335-342.

27 U.S. Environmental Protection Agency, EPA facts about radium. (2002).

28 Smith, K. P.; Arnish, J. J.; Williams, G. P.; Blunt, D. L., Assessment of the disposal of radioactive petroleum industry waste in nonhazardous landfills using risk-based modeling. *Environmental Science & Technology* (2003), *37*(10), 2060-2066.

29 Agency for Toxic Substances and Disease Registry, Toxicological profile for radium. (1990), CAS # 7440-14-4.

30 Resnikoff, M.; Alexandrova, E.; Travers, J., Radioactivity in marcellus shale. (2010), Report prepared for Residents of for the Preservation of Lowman and Chemung (RFPLC).

31 Rassenfoss, S., From flowback to fracturing: Water recycling grows in the Marcellus shale. *Journal of Petroleum Technology* (2011), *63*(7), 48-51.

32 Curtright, A. E.; Giglio, K., *Coal mine drainage for Marcellus Shale natural gas extraction*. Rand Corporation, Santa Monica, CA, (2012).

33 PA DEP, White paper: Utilization of mine influenced water for natural gas extraction activities. (2013).

34 Cravotta, C. A., Dissolved metals and associated constituents in abandoned coal-mine discharges, Pennsylvania, USA. Part 1: Constituent quantities and correlations. *Applied Geochemistry* (2008), *23*(2), 166-202.

35 He, C.; Wang, X.; Liu, W.; Barbot, E.; Vidic, R. D., Microfiltration in recycling of Marcellus Shale flowback water: Solids removal and potential fouling of polymeric microfiltration membranes. *Journal of Membrane Science* (2014), *462*, 88-95.

36 Zheng, X., Optimization of treatment options to enable the use of abandoned mine drainage (AMD) for hydraulic fracturing in Marcellus Shale. Master Thesis, University of Pittsburgh. (2013).

37 Gordon, L.; Rowley, K., Coprecipitation of radium with barium sulfate. *Analytical Chemistry* (1957), *29*(1), 34-37.

38 http://www.tenorm.com/regs2.htm - States

39 PA DEP, Final guidance document on radioactivity monitoring at solid waste processing and disposal facilities. (2004), 250-3100-001.

40 Yoshida, Y.; Yoshikawa, H.; Nakanishi, T., Partition coefficients of Ra and Ba in calcite. *Geochemical Journal* (2008), *42*(3), 295-304.

Chapter 4

1 King, G. E., Thirty years of gas shale fracturing: What have we learned? *SPE Annual Technical Conference and Exhibition* (2010), SPE-133456-MS.

2 Reinicke, A.; Rybacki, E.; Stanchits, S.; Huenges, E.; Dresen, G., Hydraulic fracturing stimulation techniques and formation damage mechanisms—Implications from laboratory testing of tight sandstone–proppant systems. *Chemie der Erde-Geochemistry* (2010), *70*, 107-117.

3 He, C.; Zhang, T.; Vidic, R. D., Use of abandoned mine drainage for the development of unconventional gas resources. *Disruptive Science and Technology* (2013), *1*(4), 169-176.

4 Engelder, T.; Lash, G. G., Marcellus Shale play‘ s vast resource potential creating stir in Appalachia. *The American Oil & Gas Reporter* (2008), *51*(6), 76-87.

5 Milici, R. C.; Swezey, C., Assessment of appalachian basin oil and gas resources: Devonian shale-middle and upper paleozoic total petroleum system. U.S. Geological Survey. (2006), Open-file Report Series, 2006-1237.

6 Gaudlip, A.; Paugh, L.; Hayes, T., Marcellus shale water management challenges in Pennsylvania, SPE Shale Gas Production Conference, Fort Worth, TA. (2008), SPE-119898-MS.

7 Kidder, M.; Palmgren, T.; Ovalle, A.; Kapila, M., Treatment options for reuse of frac flowback and produced water from shale. *World oil* (2011), *232*(7).

8 Barbot, E.; Vidic, N. S.; Gregory, K. B.; Vidic, R. D., Spatial and temporal correlation of water quality parameters of produced waters from Devonian-age shale following hydraulic fracturing. *Environmental Science & Technology* (2013), *47*(6), 2562-2569.

9 Vidic, R. D.; Brantley, S. L.; Vandenbossche, J. M.; Yoxtheimer, D.; Abad, J. D., Impact of shale gas development on regional water quality. *Science* (2013), *340*(6134).

10 Arthur, J. D.; Bohm, B.; Layne, M., Hydraulic fracturing considerations for natural gas wells of the Marcellus Shale. Groundwater Protection Council Annual Forum (2008).

11 U.S. Environmental Protection Agency, Acid Mine Drinage Prediction. (2004), EPA530-R-94-036.

12 Gray, N., Acid mine drainage composition and the implications for its impact on lotic systems. *Water Research* (1998), *32*(7), 2122-2134.

13 Cravotta, C. A., Dissolved metals and associated constituents in abandoned coal-mine discharges, Pennsylvania, USA. Part 1: Constituent quantities and correlations. *Applied Geochemistry* (2008), *23*(2), 166-202.

14 He, C.; Zhang, T.; Zheng, X.; Li, Y.; Vidic, R. D., Management of Marcellus Shale Produced Water in Pennsylvania: A Review of Current Strategies and Perspectives. *Energy Technology* (2014), *2*(12), 968-976.

15 He, C.; Wang, X.; Liu, W.; Barbot, E.; Vidic, R. D., Microfiltration in recycling of Marcellus Shale flowback water: Solids removal and potential fouling of polymeric microfiltration membranes. *Journal of Membrane Science* (2014), *462*, 88-95.

16 Kondash, A. J.; Warner, N. R.; Lahav, O.; Vengosh, A., Radium and barium removal through blending hydraulic fracturing fluids with acid mine drainage. *Environmental Science & Technology* (2013), *48*(2), 1334-1342.

17 He, C.; Li, M.; Liu, W.; Barbot, E.; Vidic, R., Kinetics and Equilibrium of Barium and Strontium Sulfate Formation in Marcellus Shale Flowback Water. *Journal of Environmental Engineering* (2014), *140*(5), B4014001.

18 Risthaus, P.; Bosbach, D.; Becker, U.; Putnis, A., Barite scale formation and dissolution at high ionic strength studied with atomic force microscopy. *Colloids and Surfaces A: Physicochemical and Engineering Aspects* (2001), *191*(3), 201-214.

19 Nancollas, G.; Purdie, N., The kinetics of crystal growth. *Q. Rev. Chem. Soc.* (1964), *18*(1), 1-20.

20 Gardner, G.; Nancollas, G., Crystal growth in aqueous solution at elevated temperatures. Barium sulfate growth kinetics. *The Journal of Physical Chemistry* (1983), *87*(23), 4699-4703.

21 van der Leeden, M. C.; Kashchiev, D.; Van Rosmalen, G. M., Precipitation of barium sulfate: Induction time and the effect of an additive on nucleation and growth. *Journal of Colloid and Interface Science* (1992), *152*(2), 338-350.

22 Davies, C.; Jones, A., The precipitation of silver chloride from aqueous solutions. Part 2: Kinetics of growth of seed crystals. *Transactions of the Faraday Society* (1955), *51*, 812-817.

23 Reddy, M. M.; Nancollas, G. H., The crystallization of calcium carbonate: I. Isotopic exchange and kinetics. *Journal of Colloid and Interface Science* (1971), *36*(2), 166-172.

24 Jones, F.; Oliviera, A.; Parkinson, G.; Rohl, A.; Stanley, A.; Upson, T., The effect of calcium ions on the precipitation of barium sulphate 1: Calcium ions in the absence of organic additives. *Journal of Crystal Growth* (2004), *262*(1), 572-580.

Chapter 5

1 U.S. Energy Information Administration, World shale gas resources: an initial assessment of 14 regions outside the United States. (2011).

2 Milici, R. C.; Swezey, C., Assessment of appalachian basin oil and gas resources: Devonian shale-middle and upper paleozoic total petroleum system. U.S. Geological Survey. (2006), Open-file Report Series, 2006-1237.

3 Engelder, T.; Lash, G. G., Marcellus Shale play‘ s vast resource potential creating stir in Appalachia. *The American Oil & Gas Reporter* (2008), *51*(6), 76-87.

4 King, G. E., Thirty years of gas shale fracturing: What have we learned? *SPE Annual Technical Conference and Exhibition* (2010), SPE-133456-MS.

5 Reinicke, A.; Rybacki, E.; Stanchits, S.; Huenges, E.; Dresen, G., Hydraulic fracturing stimulation techniques and formation damage mechanisms—Implications from laboratory testing of tight sandstone–proppant systems. *Chemie der Erde-Geochemistry* (2010), *70*, 107-117.

6 Economides, M. J.; Watters, L. T.; Dunn-Norman, S., *Petroleum well construction*. John Wiley Sons, West Sussex, UK, (1998).

7 Gaudlip, A.; Paugh, L.; Hayes, T., Marcellus shale water management challenges in Pennsylvania, SPE Shale Gas Production Conference, Fort Worth, TA. (2008), SPE-119898-MS.

8 Kidder, M.; Palmgren, T.; Ovalle, A.; Kapila, M., Treatment options for reuse of frac flowback and produced water from shale. *World oil* (2011), *232*(7).

9 U.S. Department Of Energy, Modern Shale Gas Development in the United States: A Primer. (2009).

10 Vidic, R. D.; Brantley, S. L.; Vandenbossche, J. M.; Yoxtheimer, D.; Abad, J. D., Impact of shale gas development on regional water quality. *Science* (2013), *340*(6134).

11 Kargbo, D. M.; Wilhelm, R. G.; Campbell, D. J., Natural gas plays in the Marcellus shale: Challenges and potential opportunities. *Environmental Science & Technology* (2010), *44*(15), 5679-5684.

12 Arthur, J. D.; Bohm, B.; Layne, M., Hydraulic fracturing considerations for natural gas wells of the Marcellus Shale. Groundwater Protection Council Annual Forum (2008).

13 He, C.; Zhang, T.; Vidic, R. D., Use of abandoned mine drainage for the development of unconventional gas resources. *Disruptive Science and Technology* (2013), *1*(4), 169-176.

14 Akcil, A.; Koldas, S., Acid Mine Drainage (AMD): causes, treatment and case studies. *Journal of Cleaner Production* (2006), *14*(12), 1139-1145.

15 Jiang, Q.; Rentschler, J.; Perrone, R.; Liu, K., Application of ceramic membrane and ion-exchange for the treatment of the flowback water from Marcellus shale gas production. *Journal of Membrane Science* (2013), *431*, 55-61.

16 Howe, K. J.; Clark, M. M., Fouling of microfiltration and ultrafiltration membranes by natural waters. *Environmental Science & Technology* (2002), *36*(16), 3571-3576.

17 Singh, G.; Song, L., Impact of feed water acidification with weak and strong acids on colloidal silica fouling in ultrafiltration membrane processes. *Water Research* (2008), *42*(3), 707-713.

18 Hotze, E. M.; Phenrat, T.; Lowry, G. V., Nanoparticle aggregation: Challenges to understanding transport and reactivity in the environment. *Journal of Environmental Quality* (2010), *39*(6), 1909-1924.

19 Jermann, D.; Pronk, W.; Boller, M., Mutual influences between natural organic matter and inorganic particles and their combined effect on ultrafiltration membrane fouling. *Environmental Science & Technology* (2008), *42*(24), 9129-9136.

20 Cheng, Y.; Yin, L.; Lin, S.; Wiesner, M.; Bernhardt, E.; Liu, J., Toxicity reduction of polymer-stabilized silver nanoparticles by sunlight. *The Journal of Physical Chemistry C* (2011), *115*(11), 4425-4432.

21 Barbot, E.; Vidic, N. S.; Gregory, K. B.; Vidic, R. D., Spatial and temporal correlation of water quality parameters of produced waters from Devonian-age shale following hydraulic fracturing. *Environmental Science & Technology* (2013), *47*(6), 2562-2569.

22 Ho, C.-C.; Zydney, A. L., A combined pore blockage and cake filtration model for protein fouling during microfiltration. *Journal of Colloid and Interface Science* (2000), *232*(2), 389-399.

23 Jones, F.; Oliviera, A.; Parkinson, G.; Rohl, A.; Stanley, A.; Upson, T., The effect of calcium cations on the precipitation of barium sulfate 2: Calcium ions in the presence of organic additives. *Journal of Crystal Growth* (2004), *270*(3), 593-603.

24 Schäfer, A.; Schwicker, U.; Fischer, M.; Fane, A. G.; Waite, T., Microfiltration of colloids and natural organic matter. *Journal of Membrane Science* (2000), *171*(2), 151-172.

25 Faibish, R. S.; Elimelech, M.; Cohen, Y., Effect of interparticle electrostatic double layer interactions on permeate flux decline in crossflow membrane filtration of colloidal suspensions: an experimental investigation. *Journal of Colloid and Interface Science* (1998), *204*(1), 77-86.

26 Koo, C. H.; Mohammad, A. W.; Talib, M. Z. M., Review of the effect of selected physicochemical factors on membrane fouling propensity based on fouling indices. *Desalination* (2012), *287*, 167-177.

27 Yiantsios, S.; Karabelas, A., The effect of colloid stability on membrane fouling. *Desalination* (1998), *118*(1), 143-152.

28 Park, C.; Kim, H.; Hong, S.; Choi, S.-I., Variation and prediction of membrane fouling index under various feed water characteristics. *Journal of Membrane Science* (2006), *284*(1), 248-254.

29 Huynh, K. A.; Chen, K. L., Aggregation kinetics of citrate and polyvinylpyrrolidone coated silver nanoparticles in monovalent and divalent electrolyte solutions. *Environmental Science & Technology* (2011), *45*(13), 5564-5571.

30 Saleh, N.; Kim, H.-J.; Phenrat, T.; Matyjaszewski, K.; Tilton, R. D.; Lowry, G. V., Ionic Strength and Composition Affect the Mobility of Surface-Modified Fe0 Nanoparticles in Water-Saturated Sand Columns. *Environmental Science & Technology* (2008), *42*(9), 3349-3355.

31 Pincus, P., Colloid stabilization with grafted polyelectrolytes. *Macromolecules* (1991), *24*(10), 2912-2919.

32 Edwards, P. J.; Tracy, L. L.; Wilson, W. K., Chloride concentration gradients in tank-stored hydraulic fracturing fluids following flowback. U.S. Department of Agriculture. (2011), NRS-14.

33 Paktinat, J.; O'Neil, B. J.; Aften, C. W.; Hurd, M. D., Critical evaluation of high brine tolerant additives used in shale slickwater fracs. SPE Production and Operations Symposium. (2011), SPE-141356-MS.

34 U.S. Environmental Protection Agency, Proceedings of the technical workshops for the hydraulic fracturing study: Chemical and analytical methods. (2011).

Chapter 6

1 Bibby, K. J.; Brantley, S. L.; Reible, D. D.; Linden, K. G.; Mouser, P. J.; Gregory, K. B.; Ellis, B. R.; Vidic, R. D., Suggested reporting parameters for investigations of wastewater from unconventional shale gas extraction. *Environmental Science & Technology* (2013), *47*(23), 13220-13221.

2 He, C.; Zhang, T.; Zheng, X.; Li, Y.; Vidic, R. D., Management of Marcellus Shale Produced Water in Pennsylvania: A Review of Current Strategies and Perspectives. *Energy Technology* (2014), *2*(12), 968-976.

3 He, C.; Zhang, T.; Vidic, R. D., Use of abandoned mine drainage for the development of unconventional gas resources. *Disruptive Science and Technology* (2013), *1*(4), 169-176.

4 He, C.; Li, M.; Liu, W.; Barbot, E.; Vidic, R., Kinetics and Equilibrium of Barium and Strontium Sulfate Formation in Marcellus Shale Flowback Water. *Journal of Environmental Engineering* (2014), *140*(5), B4014001.

5 Zhang, T.; Gregory, K.; Hammack, R. W.; Vidic, R. D., Co-precipitation of radium with barium and strontium sulfate and its impact on the fate of radium during treatment of produced water from unconventional gas extraction. *Environmental Science & Technology* (2014), *48*(8), 4596-4603.

6 Ferrar, K. J.; Michanowicz, D. R.; Christen, C. L.; Mulcahy, N.; Malone, S. L.; Sharma, R. K., Assessment of effluent contaminants from three facilities discharging Marcellus Shale wastewater to surface waters in Pennsylvania. *Environmental Science & Technology* (2013), *47*(7), 3472-3481.

7 Wilson, J. M.; VanBriesen, J. M., Oil and gas produced water management and surface drinking water sources in Pennsylvania. *Environmental Practice* (2012), *14*(04), 288-300.

8 Shaffer, D. L.; Arias Chavez, L. H.; Ben-Sasson, M.; Romero-Vargas Castrillón, S.; Yip, N. Y.; Elimelech, M., Desalination and reuse of high-salinity shale gas produced water: drivers, technologies, and future directions. *Environmental Science & Technology* (2013), *47*(17), 9569-9583.

9 Vidic, R. D.; Brantley, S. L.; Vandenbossche, J. M.; Yoxtheimer, D.; Abad, J. D., Impact of shale gas development on regional water quality. *Science* (2013), *340*(6134).

10 He, C.; Wang, X.; Liu, W.; Barbot, E.; Vidic, R. D., Microfiltration in recycling of Marcellus Shale flowback water: Solids removal and potential fouling of polymeric microfiltration membranes. *Journal of Membrane Science* (2014), *462*, 88-95.

11 Miller, D. J.; Kasemset, S.; Wang, L.; Paul, D. R.; Freeman, B. D., Constant flux crossflow filtration evaluation of surface-modified fouling-resistant membranes. *Journal of Membrane Science* (2014), *452*, 171-183.

12 Tarabara, V. V.; Koyuncu, I.; Wiesner, M. R., Effect of hydrodynamics and solution ionic strength on permeate flux in cross-flow filtration: direct experimental observation of filter cake cross-sections. *Journal of Membrane Science* (2004), *241*(1), 65-78.

13 Yu, W.; Liu, T.; Gregory, J.; Campos, L.; Li, G.; Qu, J., Influence of flocs breakage process on submerged ultrafiltration membrane fouling. *Journal of Membrane Science* (2011), *385*, 194-199.

14 Bendick, J.; Modise, C.; Miller, C.; Neufeld, R.; Vidic, R., Application of cross-flow microfiltration for the treatment of combined sewer overflow wastewater. *Journal of Environmental Engineering* (2004), *130*(12), 1442-1449.

15 Li, M.; Zhao, Y.; Zhou, S.; Xing, W.; Wong, F.-S., Resistance analysis for ceramic membrane microfiltration of raw soy sauce. *Journal of Membrane Science* (2007), *299*(1), 122-129.

16 Shin, H.-S.; Kang, S.-T., Characteristics and fates of soluble microbial products in ceramic membrane bioreactor at various sludge retention times. *Water Research* (2003), *37*(1), 121-127.

17 Van der Bruggen, B.; Vandecasteele, C.; Van Gestel, T.; Doyen, W.; Leysen, R., A review of pressure ‐ driven membrane processes in wastewater treatment and drinking water production. *Environmental Progress* (2003), *22*(1), 46-56.

18 Lin, Y.; De Vries, K.; Burggraaf, A., Thermal stability and its improvement of the alumina membrane top-layers prepared by sol-gel methods. *Journal of Materials Science* (1991), *26*(3), 715-720.

19 de Wit, P.; Kappert, E. J.; Lohaus, T.; Wessling, M.; Nijmeijer, A.; Benes, N. E., Highly permeable and mechanically robust silicon carbide hollow fiber membranes. *Journal of Membrane Science* (2015), *475*, 480-487.

20 Barbot, E.; Moustier, S.; Bottero, J.-Y.; Moulin, P., Coagulation and ultrafiltration: Understanding of the key parameters of the hybrid process. *Journal of Membrane Science* (2008), *325*(2), 520-527.

21 Hofs, B.; Ogier, J.; Vries, D.; Beerendonk, E. F.; Cornelissen, E. R., Comparison of ceramic and polymeric membrane permeability and fouling using surface water. *Separation and Purification Technology* (2011), *79*(3), 365-374.

22 Huisman, I. H.; Trägårdh, G.; Trägårdh, C.; Pihlajamäki, A., Determining the zeta-potential of ceramic microfiltration membranes using the electroviscous effect. *Journal of Membrane Science* (1998), *147*(2), 187-194.

23 Hermia, J., Constant pressure blocking filtration law application to powder-law non-Newtonian fluid. *Transactions of the Institution of Chemical Engineers* (1982), *60*, 183-187.

24 Hwang, K.-J.; Lin, T.-T., Effect of morphology of polymeric membrane on the performance of cross-flow microfiltration. *Journal of Membrane Science* (2002), *199*(1), 41-52.

25 Mourouzidis-Mourouzis, S.; Karabelas, A., Whey protein fouling of large pore-size ceramic microfiltration membranes at small cross-flow velocity. *Journal of Membrane Science* (2008), *323*(1), 17-27.

26 Jegatheesan, V.; Phong, D.; Shu, L.; Aim, R. B., Performance of ceramic micro-and ultrafiltration membranes treating limed and partially clarified sugar cane juice. *Journal of Membrane Science* (2009), *327*(1), 69-77.

27 Ho, C.-C.; Zydney, A. L., A combined pore blockage and cake filtration model for protein fouling during microfiltration. *Journal of Colloid and Interface Science* (2000), *232*(2), 389-399.

28 Parker, D. S.; Kaufman, W. J.; Jenkins, D., Floc breakup in turbulent flocculation processes. *Journal of the Sanitary Engineering Division* (1972), *98*(1), 79-99.

29 Kang, S.-T.; Subramani, A.; Hoek, E. M.; Deshusses, M. A.; Matsumoto, M. R., Direct observation of biofouling in cross-flow microfiltration: Mechanisms of deposition and release. *Journal of Membrane Science* (2004), *244*(1), 151-165.

30 Tombácz, E.; Csanaky, C.; Illés, E., Polydisperse fractal aggregate formation in clay mineral and iron oxide suspensions, pH and ionic strength dependence. *Colloid and Polymer Science* (2001), *279*(5), 484-492.

31 Bagga, A.; Chellam, S.; Clifford, D. A., Evaluation of iron chemical coagulation and electrocoagulation pretreatment for surface water microfiltration. *Journal of Membrane Science* (2008), *309*(1), 82-93.

32 Simonič, M.; Vnučec, D., Coagulation and UF treatment of pulp and paper mill wastewater in comparison. *Central European Journal of Chemistry* (2012), *10*(1), 127-136.

33 Zhang, X.; Fan, L.; Roddick, F. A., Feedwater coagulation to mitigate the fouling of a ceramic MF membrane caused by soluble algal organic matter. *Separation and Purification Technology* (2014), *133*, 221-226.

34 Lee, S.-J.; Dilaver, M.; Park, P.-K.; Kim, J.-H., Comparative analysis of fouling characteristics of ceramic and polymeric microfiltration membranes using filtration models. *Journal of Membrane Science* (2013), *432*, 97-105.

35 Yuan, W.; Kocic, A.; Zydney, A. L., Analysis of humic acid fouling during microfiltration using a pore blockage–cake filtration model. *Journal of Membrane Science* (2002), *198*(1), 51-62.

36 Jarvis, P.; Jefferson, B.; Gregory, J.; Parsons, S. A., A review of floc strength and breakage. *Water Research* (2005), *39*(14), 3121-3137.

37 Wang, J.; Guan, J.; Santiwong, S.; Waite, T. D., Characterization of floc size and structure under different monomer and polymer coagulants on microfiltration membrane fouling. *Journal of Membrane Science* (2008), *321*(2), 132-138.

38 Ladner, D. A.; Vardon, D. R.; Clark, M. M., Effects of shear on microfiltration and ultrafiltration fouling by marine bloom-forming algae. *Journal of Membrane Science* (2010), *356*(1), 33-43.

39 Kim, J.-S.; Lee, C.-H.; Chang, I.-S., Effect of pump shear on the performance of a crossflow membrane bioreactor. *Water Research* (2001), *35*(9), 2137-2144.

Chapter 7

1 Engelder, T.; Lash, G. G., Marcellus Shale play‘ s vast resource potential creating stir in Appalachia. *The American Oil & Gas Reporter* (2008), *51*(6), 76-87.

2 Milici, R. C.; Swezey, C., Assessment of appalachian basin oil and gas resources: Devonian shale-middle and upper paleozoic total petroleum system. U.S. Geological Survey. (2006), Open-file Report Series, 2006-1237.

3 Kinnaman, T. C., The economic impact of shale gas extraction: A review of existing studies. *Ecological Economics* (2011), *70*(7), 1243-1249.

4 Gregory, K. B.; Vidic, R. D.; Dzombak, D. A., Water management challenges associated with the production of shale gas by hydraulic fracturing. *Elements* (2011), *7*(3), 181-186.

5 Kargbo, D. M.; Wilhelm, R. G.; Campbell, D. J., Natural gas plays in the Marcellus shale: Challenges and potential opportunities. *Environmental Science & Technology* (2010), *44*(15), 5679-5684.

6 Rowan, E.; Engle, M.; Kirby, C.; Kraemer, T., Radium content of oil-and gas-field produced waters in the Northern Appalachian basin (USA)—Summary and discussion of data. US Geological Survey Scientific Investigations Report. (2011), 2011-5135.

7 U.S. Department Of Energy, Modern Shale Gas Development in the United States: A Primer. (2009).

8 He, C.; Wang, X.; Liu, W.; Barbot, E.; Vidic, R. D., Microfiltration in recycling of Marcellus Shale flowback water: Solids removal and potential fouling of polymeric microfiltration membranes. *Journal of Membrane Science* (2014), *462*, 88-95.

9 Johnson, D. B., Chemical and microbiological characteristics of mineral spoils and drainage waters at abandoned coal and metal mines. *Water, Air and Soil Pollution: Focus* (2003), *3*(1), 47-66.

10 Gray, N., Acid mine drainage composition and the implications for its impact on lotic systems. *Water Research* (1998), *32*(7), 2122-2134.

11 Kondash, A. J.; Warner, N. R.; Lahav, O.; Vengosh, A., Radium and barium removal through blending hydraulic fracturing fluids with acid mine drainage. *Environmental Science & Technology* (2013), *48*(2), 1334-1342.

12 He, C.; Zhang, T.; Vidic, R. D., Use of abandoned mine drainage for the development of unconventional gas resources. *Disruptive Science and Technology* (2013), *1*(4), 169-176.

13 Zhang, T.; Gregory, K.; Hammack, R. W.; Vidic, R. D., Co-precipitation of radium with barium and strontium sulfate and its impact on the fate of radium during treatment of produced water from unconventional gas extraction. *Environmental Science & Technology* (2014), *48*(8), 4596-4603.

14 He, C.; Li, M.; Liu, W.; Barbot, E.; Vidic, R., Kinetics and Equilibrium of Barium and Strontium Sulfate Formation in Marcellus Shale Flowback Water. *Journal of Environmental Engineering* (2014), *140*(5), B4014001.

15 He, C.; Zhang, T.; Zheng, X.; Li, Y.; Vidic, R. D., Management of Marcellus Shale Produced Water in Pennsylvania: A Review of Current Strategies and Perspectives. *Energy Technology* (2014), *2*(12), 968-976.

16 PA DEP, Final guidance document on radioactivity monitoring at solid waste processing and disposal facilities. (2004), 250-3100-001.

17 API, Specification for drilling fluids materials, API Specification 13A. (2010).

18 Kucher, M.; Babic, D.; Kind, M., Precipitation of barium sulfate: experimental investigation about the influence of supersaturation and free lattice ion ratio on particle formation. *Chemical Engineering and Processing: Process Intensification* (2006), *45*(10), 900-907.

19 Wong, D.; Jaworski, Z.; Nienow, A., Effect of ion excess on particle size and morphology during barium sulphate precipitation: an experimental study. *Chemical Engineering Science* (2001), *56*(3), 727-734.

20 Barbot, E.; Vidic, N. S.; Gregory, K. B.; Vidic, R. D., Spatial and temporal correlation of water quality parameters of produced waters from Devonian-age shale following hydraulic fracturing. *Environmental Science & Technology* (2013), *47*(6), 2562-2569.

21 Cravotta Iii, C. A., Dissolved metals and associated constituents in abandoned coal-mine discharges, Pennsylvania, USA. Part 2: Geochemical controls on constituent concentrations. *Applied Geochemistry* (2008), *23*(2), 203-226.

22 Cravotta, C. A., Dissolved metals and associated constituents in abandoned coal-mine discharges, Pennsylvania, USA. Part 1: Constituent quantities and correlations. *Applied Geochemistry* (2008), *23*(2), 166-202.

23 Wei, X.; Viadero, R. C., Synthesis of magnetite nanoparticles with ferric iron recovered from acid mine drainage: Implications for environmental engineering. *Colloids and Surfaces A: Physicochemical and Engineering Aspects* (2007), *294*(1), 280-286.

24 Druschel, G. K.; Baker, B. J.; Gihring, T. M.; Banfield, J. F., Acid mine drainage biogeochemistry at Iron Mountain, California. *Geochemical Transactions* (2004), *5*(2), 13-32.

25 Ott, A. N., Estimating iron and aluminum content of acid mine discharge from a north-central Pennsylvania coal field by use of acidity titration curves, Water-Resources Investigations Report. (1986), 84-4335.

26 Cornell, R. M.; Giovanoli, R.; Schneider, W., Review of the hydrolysis of iron (III) and the crystallization of amorphous iron (III) hydroxide hydrate. *Journal of Chemical Technology and Biotechnology* (1989), *46*(2), 115-134.

27 Tang, C. Y.; Fu, Q. S.; Robertson, A.; Criddle, C. S.; Leckie, J. O., Use of reverse osmosis membranes to remove perfluorooctane sulfonate (PFOS) from semiconductor wastewater. *Environmental science & technology* (2006), *40*(23), 7343-7349.

28 Nancollas, G.; Purdie, N., The kinetics of crystal growth. *Q. Rev. Chem. Soc.* (1964), *18*(1), 1-20.

29 Salama, E.-S.; Kim, J. R.; Ji, M.-K.; Cho, D.-W.; Abou-Shanab, R. A.; Kabra, A. N.; Jeon, B.-H., Application of acid mine drainage for coagulation/flocculation of microalgal biomass. *Bioresource Technology* (2015), *186*, 232-237.

30 Sun, Y.; Xiong, X.; Zhou, G.; Li, C.; Guan, X., Removal of arsenate from water by coagulation with in situ formed versus pre-formed Fe (III). *Separation and Purification Technology* (2013), *115*, 198-204.

31 Zheng, X., Optimization of treatment options to enable the use of abandoned mine drainage (AMD) for hydraulic fracturing in Marcellus Shale. Master Thesis, University of Pittsburgh. (2013).

32 Singer, P. C.; Stumm, W., Acidic mine drainage: the rate-determining step. *Science* (1970), *167*(3921), 1121-1123.

33 Tronc, E.; Belleville, P.; Jolivet, J. P.; Livage, J., Transformation of ferric hydroxide into spinel by iron (II) adsorption. *Langmuir* (1992), *8*(1), 313-319.

34 Demopoulos, G., Aqueous precipitation and crystallization for the production of particulate solids with desired properties. *Hydrometallurgy* (2009), *96*(3), 199-214.

35 Nason, J. A.; Lawler, D. F., Particle size distribution dynamics during precipitative softening: Constant solution composition. *Water Research* (2008), *42*(14), 3667-3676.

36 Davies, C.; Jones, A., The precipitation of silver chloride from aqueous solutions. Part 2.—Kinetics of growth of seed crystals. *Transactions of the Faraday Society* (1955), *51*, 812-817.

37 Sánchez-Pastor, N.; Pina, C.; Fernández-Díaz, L., Relationships between crystal morphology and composition in the (Ba, Sr) SO 4–H 2 O solid solution–aqueous solution system. *Chemical geology* (2006), *225*(3), 266-277.

38 McIntire, W., Trace element partition coefficients—a review of theory and applications to geology. *Geochimica et Cosmochimica Acta* (1963), *27*(12), 1209-1264.

39 Klute, A., *Methods of soil analysis. Part 1. Physical and mineralogical methods*. American Society of Agronomy, Inc., Madison, WI, (1986).

Chapter 8

1 Vidic, R. D.; Brantley, S. L.; Vandenbossche, J. M.; Yoxtheimer, D.; Abad, J. D., Impact of shale gas development on regional water quality. *Science* (2013), *340*(6134).

2 He, C.; Zhang, T.; Vidic, R. D., Use of abandoned mine drainage for the development of unconventional gas resources. *Disruptive Science and Technology* (2013), *1*(4), 169-176.

3 He, C.; Zhang, T.; Zheng, X.; Li, Y.; Vidic, R. D., Management of Marcellus Shale Produced Water in Pennsylvania: A Review of Current Strategies and Perspectives. *Energy Technology* (2014), *2*(12), 968-976.

4 Barbot, E.; Vidic, N. S.; Gregory, K. B.; Vidic, R. D., Spatial and temporal correlation of water quality parameters of produced waters from Devonian-age shale following hydraulic fracturing. *Environmental Science & Technology* (2013), *47*(6), 2562-2569.

5 Dunn, K.; Yen, T. F., Dissolution of Barium Sulfate Scale Deposits by Chelating Agents. *Environmental Science & Technology* (1999), *33*(16), 2821-2824.

6 Antony, A.; Low, J. H.; Gray, S.; Childress, A. E.; Le-Clech, P.; Leslie, G., Scale formation and control in high pressure membrane water treatment systems: A review. *Journal of Membrane Science* (2011), *383*(1–2), 1-16.

7 Li, H.; Hsieh, M.-K.; Chien, S.-H.; Monnell, J. D.; Dzombak, D. A.; Vidic, R. D., Control of mineral scale deposition in cooling systems using secondary-treated municipal wastewater. *water research* (2011), *45*(2), 748-760.

8 Jones, F.; Oliveira, A.; Rohl, A. L.; Parkinson, G. M.; Ogden, M. I.; Reyhani, M. M., Investigation into the effect of phosphonate inhibitors on barium sulfate precipitation. *Journal of Crystal Growth* (2002), *237–239, Part 1*(0), 424-429.

9 Greenlee, L. F.; Testa, F.; Lawler, D. F.; Freeman, B. D.; Moulin, P., The effect of antiscalant addition on calcium carbonate precipitation for a simplified synthetic brackish water reverse osmosis concentrate. *Water research* (2010), *44*(9), 2957-2969.

10 Xiao, J.; Kan, A.; Tomson, M., Prediction of BaSO4 precipitation in the presence and absence of a polymeric inhibitor: Phosphino-polycarboxylic acid. *Langmuir* (2001), *17*(15), 4668-4673.

11 Mavredaki, E.; Neville, A.; Sorbie, K. S., Initial stages of barium sulfate formation at surfaces in the presence of inhibitors. *Crystal Growth & Design* (2011), *11*(11), 4751-4758.

12 Johnson, P. R.; Sun, N.; Elimelech, M., Colloid transport in geochemically heterogeneous porous media: Modeling and measurements. *Environmental Science & Technology* (1996), *30*(11), 3284-3293.

13 van der Leeden, M. C., *The Role of Polyelectrolytes in Barium Sulphate Precipitation*. Delft University, (1991).

14 van der Leeden, M. C.; Kashchiev, D.; Van Rosmalen, G. M., Precipitation of barium sulfate: Induction time and the effect of an additive on nucleation and growth. *Journal of Colloid and Interface Science* (1992), *152*(2), 338-350.

15 Shaw, S. S.; Sorbie, K.; Boak, L. S., The Effects of Barium Sulfate Saturation Ratio, Calcium, and Magnesium on the Inhibition Efficiency: Part II Polymeric Scale Inhibitors. *SPE Production & Operations* (2012), *27*(04), 390-403.

16 Gregory, K. B.; Vidic, R. D.; Dzombak, D. A., Water management challenges associated with the production of shale gas by hydraulic fracturing. *Elements* (2011), *7*(3), 181-186.

17 Risthaus, P.; Bosbach, D.; Becker, U.; Putnis, A., Barite scale formation and dissolution at high ionic strength studied with atomic force microscopy. *Colloids and Surfaces A: Physicochemical and Engineering Aspects* (2001), *191*(3), 201-214.

18 Benton, W. J.; Collins, I. R.; Grimsey, I. M.; Parkinson, G. M.; Rodger, S. A., Nucleation, growth and inhibition of barium sulfate-controlled modification with organic and inorganic additives. *Faraday Discuss.* (1993), *95*, 281-297.

19 Uchida, M.; Sue, A.; Yoshioka, T.; Okuwaki, A., Morphology of barium sulfate synthesized with barium (II)–aminocarboxylate chelating precursors. *CrystEngComm* (2001), *3*(5), 21-26.

20 Yao, K.-M.; Habibian, M. T.; O'Melia, C. R., Water and waste water filtration. Concepts and applications. *Environmental Science & Technology* (1971), *5*(11), 1105-1112.

21 Tufenkji, N.; Elimelech, M., Correlation equation for predicting single-collector efficiency in physicochemical filtration in saturated porous media. *Environmental Science & Technology* (2004), *38*(2), 529-536.

22 Redman, J. A.; Walker, S. L.; Elimelech, M., Bacterial adhesion and transport in porous media: Role of the secondary energy minimum. *Environmental Science & Technology* (2004), *38*(6), 1777-1785.

23 Johnson, P. R.; Elimelech, M., Dynamics of colloid deposition in porous media: Blocking based on random sequential adsorption. *Langmuir* (1995), *11*(3), 801-812.

24 Saleh, N.; Kim, H.-J.; Phenrat, T.; Matyjaszewski, K.; Tilton, R. D.; Lowry, G. V., Ionic Strength and Composition Affect the Mobility of Surface-Modified Fe0 Nanoparticles in Water-Saturated Sand Columns. *Environmental Science & Technology* (2008), *42*(9), 3349-3355.

25 Liu, D.; Johnson, P. R.; Elimelech, M., Colloid Deposition Dynamics in Flow-Through Porous Media: Role of Electrolyte Concentration. *Environmental Science & Technology* (1995), *29*(12), 2963-2973.

26 Bradford, S. A.; Torkzaban, S.; Walker, S. L., Coupling of physical and chemical mechanisms of colloid straining in saturated porous media. *Water Research* (2007), *41*(13), 3012-3024.

27 Solovitch, N.; Labille, J. r. m.; Rose, J. r. m.; Chaurand, P.; Borschneck, D.; Wiesner, M. R.; Bottero, J.-Y., Concurrent aggregation and deposition of TiO2 nanoparticles in a sandy porous media. *Environmental Science & Technology* (2010), *44*(13), 4897-4902.

28 Hiemenz, P. C.; Rajagopalan, R., *Principles of Colloid and Surface Chemistry, revised and expanded*. CRC press, (1997) Vol. 14.

29 Johnson, P. R., A comparison of streaming and microelectrophoresis methods for obtaining the ζ potential of granular porous media surfaces. *Journal of Colloid and Interface Science* (1999), *209*(1), 264-267.

30 Hotze, E. M.; Phenrat, T.; Lowry, G. V., Nanoparticle aggregation: Challenges to understanding transport and reactivity in the environment. *Journal of Environmental Quality* (2010), *39*(6), 1909-1924.

31 Wan, K.-W.; Malgesini, B.; Verpilio, I.; Ferruti, P.; Griffiths, P. C.; Paul, A.; Hann, A. C.; Duncan, R., Poly(amidoamine) Salt Form: Effect on pH-Dependent Membrane Activity and Polymer Conformation in Solution. *Biomacromolecules* (2004), *5*(3), 1102-1109.

32 Kirwan, L. J.; Papastavrou, G.; Borkovec, M.; Behrens, S. H., Imaging the coil-to-globule conformational transition of a weak polyelectrolyte by tuning the polyelectrolyte charge density. *Nano letters* (2004), *4*(1), 149-152.

33 Yu, X.; Somasundaran, P., Role of polymer conformation in interparticle-bridging dominated flocculation. *Journal of Colloid and Interface Science* (1996), *177*(2), 283-287.